# ALADIN

# NEWSLETTER 32

*January-July 2007*

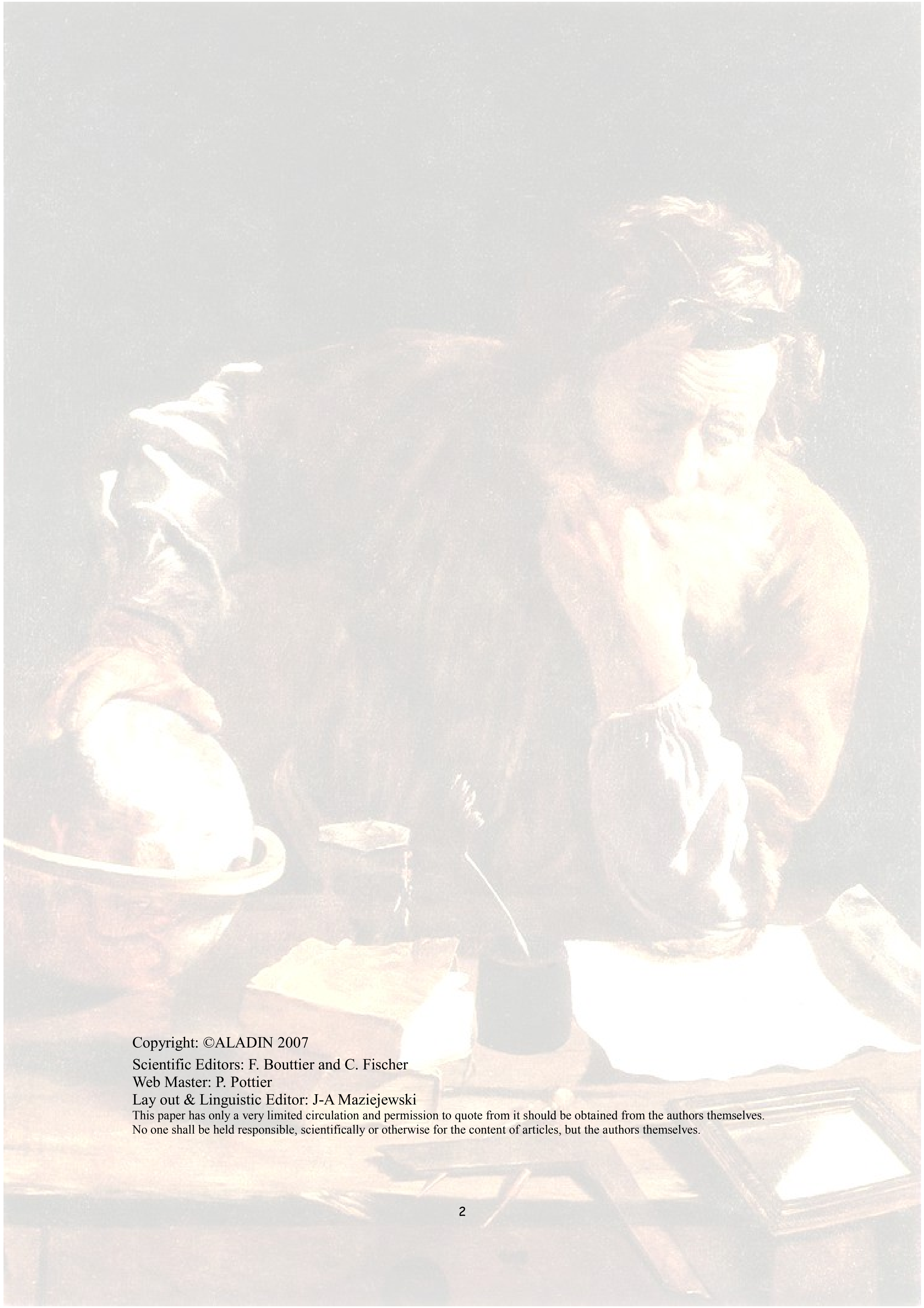



Scientific Editors: F. Bouttier and C. Fischer
Web Master: P. Pottier
Lay out & Linguistic Editor: J-A Maziejewski

**CONTENT**

# 1. EDITORIAL

## 1.1. Foreword

**A patchwork summary, by Claude Fischer**

Dear readers, the last 6 months have been marked by several encouraging meetings at the level of both the Aladin/Hirlam community and the wider NWP world. As years pass by, the size and density of the Aladin (+ Hirlam) workshops have gone increasing. Thus, in Oslo, innovation and development have been the major themes for presentations. I expect the quality and the volume of R&D to continue to increase in future, and the whole process might require further adaptations.

These would encompass project management for partner countries, more multi-lateral initiatives for fundings (possibly not always with Météo-France, for instance), more flexible availability for coordination meetings (especially, the possibility to meet via modern video-conference systems). I would also like here to stress the excellence of the Norrkoeping SRNWP workshop on data assimilation, which has been very appreciated by the Aladin attendees.

In a previous foreword, to newsletter 29, I had the opportunity to focus on the almost inevitable existence of differing opinions, contradictions and tensions within such a huge and complex project like the whole of Harmonie will be. As most of you, I would wish them never to happen or to be quickly removed. My only point here can be, quite modestly, that we will have to live with them as long as the reasons for collaboration clearly outweigh the risks and "waste of energy". We also need to remain careful on our communication and mutual understanding, since most of us are not professionals in public relation techniques.

In terms of R&D, I welcome the fact that both NWP systems AROME and Alaro find their way towards concrete realization. The steady progress for assimilation of radar data, a topic for regular coordination with Hirlam, also should end as a major component for our future D.A. systems. Progress made with assimilation techniques (FGAT, wavelet functions, SL of the adjoint hydrostatic model) and satellite observations (surface emissivities over land, the more regular use of radiances in the Hungarian and Moroccan systems) also are encouraging and must be carried on. We also seem to be in a slow but steady progress as far as R&D and operations for the Surfex surface scheme are concerned. Eventually, while "fine-scale" aspects of dynamics remain well mastered by our community (NH, BBC, coupling diagnostics, filtering), we might remain puzzled by the extraordinary difficulty to reach a breakthrough in the field of very high resolution lateral boundary coupling.

As final word, let me wish you a pleasant reading of the present newsletter, prepared for all editorial matters and with his usual care and precision by Jean A. Maziejewski, our "Sekretarski" in chief.

C. Fischer, Météo-France

## 1.2. EVENTS

### ALADIN/HIRLAM WORKSHOP, OSLO, NORWAY 23d-26th April 2007

La photo

### Training Course on ALARO-0, Radostovice, Czech Republic, 26-30 March 2007

N. Pristov

Twenty seven people from twelve countries attended one week Training Course on ALARO-0 organized by the ALADIN PM, the WGL for Physics of RC LACE and the Czech Local Organising Committee.

The 17 lectures, the 9 exercise hours and the 6 working group sessions on the documentation and other related issues were prepared to improve the basis of the scientific maintenance and networking.

Lectures were focus on the components of the ALARO-0:

- the governing equations set,
- the  horizontal diffusion (SLHD),
- turbulent diffusion (a pseudo-prognostic TKE scheme),
- radiation,
- the microphysical processes (more sophisticated and efficient parameterization including new prognostic variables - cloud liquid and solid water, rain, snow – all treated through the use of the PDF-based sedimentation method)
- a unified and coherent solution for the treatment of moist processes under the 3MT approach (cascading call of different parameterizations, prognostic convective updrafts and

downdrafts, convective and resolved processes treated in a spirit of common handling of the water vapour resource, with downdrafts having their closure separated from the one of the updrafts).

The last two lectures (on ALARO-0 implementation, an overview of training with discussion and plans) were of the debriefing type.

The level of the lectures was correctly chosen, the interest for the promising aspects of 3MT was the most appraised part. The quality of the preparatory work on the documentation was recognised by all participants and it contributed to a balanced shape between upstream science, algorithmics and their code concretizations. The exercises were judged difficult but nevertheless stimulating and well targeted, at least for people already familiar with parameterization issues. ALARO-0 experiences (porting, case studies) at services were presented during the evening WG sessions where  the main focus of interest was obviously the excellent cost-efficiency ratio of ALARO-0-minus-3MT.

Far more information can be found at the following address: http://www.rclace.eu/?page=99




## 1.3. ANNOUNCEMENTS

- EWGLAM/SRNWP/CSSI: Dubrovnik – Croatia, $8^{th}$ -$11^{th}$ October 2007

To contact the organizers (Alica Bajic, Stjepan Ivatek-Sahdan), please use this e-mail address: ewglam07@cirus.dhz.hr

visit the web site: http://meteo.hr/EWGLAM07/

- AAA surface workshop: Budapest (Hungarian Meteorological Service), 2-14/11/2007

Teachers: Jean-Francois Mahfouf (Meteo France), Francois Bouyssel (Meteo France) (boloni.g@met.hu).

## 1.4. GOSSIP

- The printable version of the Proceedings of the 28th EWGLAM Meeting is ready. You can download it from the SRNWP-webpage at:

  http://srnwp.cscs.ch/Annual_Meetings/2006/entrypage2006.htm
- Congratulations to Martina Tudor who successfully defended her PhD thesis.
- Judit and Marian are happy to announce their marriage on the $18^{th}$ of August 2007.

# 2. OPERATIONS

## 2.1. INTRODUCTION

(F. Bouttier, Météo-France)

Many operational changes have happened at the Aladin partner's institutes as explained in the per-country sections below. In Météo-France, the major change has been the supercomputer switch on May 9th, from the Fujitsu VPP5000 machines to the NEC SX-8R machines. The operational machine 'sumo' now takes care of all the normal ARPEGE and ALADIN production in Toulouse.

## 2.2. CYCLES

(F. Bouttier, Météo-France)

The operational cycle used in Météo-France from March to June 2007 (thus, on both Fujitsu and NEC machines) is cy31t1_op1. One important mod in cy31t1_op1 was a bugfix to the LACONE routine, in order to circumvent peculiarities of the NEC floating point arithmetic. A parallel test suite in MF has been running in June and July, based on cy32t0 (a the time of writing the test suite cycle is not fully stable and still undergoing debugging). cy32t2 was near completion in June 2007.

The next planned cycle in MF is cy32t3 which will feature some technical cleaning and Arome model upgrades.

A phone conference about software evolution took place between MF and ECMWF on 13 June 2007. At ECMWF, IFS cycle cy32r2 went into operations in June (upgrades of RRTM, simplified physics, subgrid orography scheme, ozone chemistry, three 4D-Var outer loops, assimilation of MetOp/IASI and MetOp/ASCAT), the summer e-suite was cy32r3 (upgrades of convection, hydrology, TEMP bias correction, changes to satellite data assimilation: COSMIC GPS-RO, microwave Aqua/AMSR-E, TRMM/TMI, DMSP-F16/SSMI-S, NOAA/SBUV ozone). Further planned changes regard quality control, semi-Lagrangian, microphysics, more Metop data. Karim Yessad is planning some substantial code cleaning.

Thus, this autumn's big challenge will be the production of a joint cy33. Merging of the partners' modifications remains an essential ALADIN cooperation group activity; much work has already been done on merging ALARO mods into the mainstream cycles, and this will continue.

## 2.3. Transversal informations

(F. Bouttier, Météo-France)

The evolution of the SRNWP European-wide cooperation has been a hot topic, with four themes: renewal of the SRNWP itself (the "SRNWP programme"), and three workpackages (interoperability, European mulitmodel EPS, verification). Support has been sought from EUMETNET who agreed on the SRNWP programme and issued a call for proposals on the interoperability workpackage. Funding has been decided, new the challenge is to find volunteers to manage and execute the contract, while keeping in touch with all four European consortia (ALADIN, HIRLAM, COSMO and Met Office). If this works, it may insert our ALADIN consortium activities into a broader European SRNWP framework that does not only R&D, but also operational activities.

## 2.4. Changes in the Operational Version of ARPEGE

(F. Bouttier, Météo-France)

A new Web page contains a (nearly up to date) summary of the ARPEGE and ALADIN-France configurations: http://www.cnrm.meteo.fr/gmap/

The notable ARPEGE change between January and June 2007, apart from the switch to NEC summarized, is the cy31t1 suite that went into operations on 26 February 2007. It features improvements to the soil ice melting that adresses weaknesses in springtime T2m raised by our helpful ALADIN partners, as well as many technical changes to prepare for the NEC switch and for the next test suite (with a lot of new satellite data). Several physics (and SLHD diffusion) changes that were developed for the 31t1 suite have been postponed for a future suite, because the time constraint imposed by the NEC switch would not allow for a safe testing of these changes.

Other ARPEGE operational changes have included changes to the production times linked to differences in technical behaviour between the NEC and Fujitsu machines, and use of the new Meteosat-9 satellite (atmospheric motion winds and SEVIRI radiances) since Eumetsat discontinued production from the older Meteosat-8.

In August 2007, the cy32t0 parallel test suite has reached a satisfactory, stable state, with assimilation of important new satellite data (GPS radio-occultation, DMSP-F14/SSMI, MetOp AMSU, MHS, HIRS and ASCAT), use of the new 1/12 SST analyses from NESDIS, microphysics improvements. Problems with the HIRS screening algorithm are being investigated, which may lead to some fixes before this test suite can be implemented into operations.

Substantial experimentation has started on the higher-resolution ARPEGE configuration (T538c2.4L60 i.e. 15km resolution over much of Europe), which is due for operational implementation before end 2007.

## 2.5. ALGERIA

### 2.5.1. ALADIN/Algérie operational version (m.benamara@meteo.dz)

- **Summary:**

The current Aladin/Algérie version is operational since September 09, 2006. It was implemented on the old Météo France's computer and is now running on the new one, until the Algerian meteorological service receives its own computer.

This operational version is run twice a day at 00 and at 12UTC and special connections to Météo France's computers (Cougar and Tori) are allowed to the Algerian scientists who are in charge of ALADIN/Algérie at Algiers. The compressed outputs (in grib format) are then downloaded from "Cougar" via internet and are plotted in a format best suited to the forecasters. A web page with restricted access was set up with a daily update of the ALADIN/Algérie fields.

The ALADIN outputs are integrated in the forecasting system at the national forecasting centre at Algiers, as recommended in the last MoU.

Besides, some derived fields are computed using the model outputs and the wam model (Max Planck institute of Hamburg, Germany) is forced with Aladin 10m winds.

- **Status:**

ALADIN/Algérie is coupled with the global model ARPEGE every 3 hours, its horizontal resolution is 12km and the time step of the model is 415.385s. The frequency of the output files is 3 hours and the forecast range is up to 48h.

The ALADIN/Algérie model is, at the moment, run in dynamical adaptation. The current cycle of ALADIN/Algérie is the same as the one of ALADIN/France, it passed to 31t1 since February 13, 2007.

- **Integrated Domain:**

The ALADIN/Algérie domain extends from 18.55°N to 46.45°N and from 10.7°W to 17.2° E. The number of points is: 300x300 for the processing and 280x280 for the post processing.

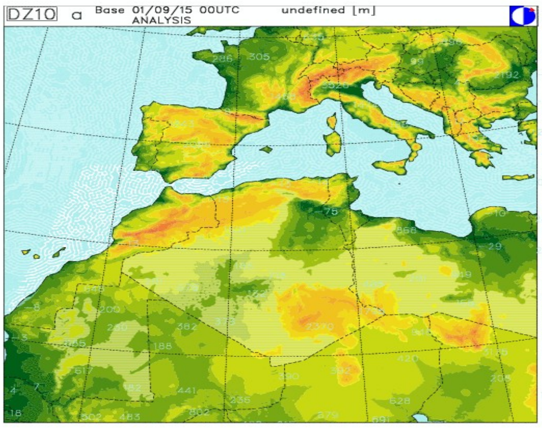


Fig.1: ALADIN/Algérie integrated domain

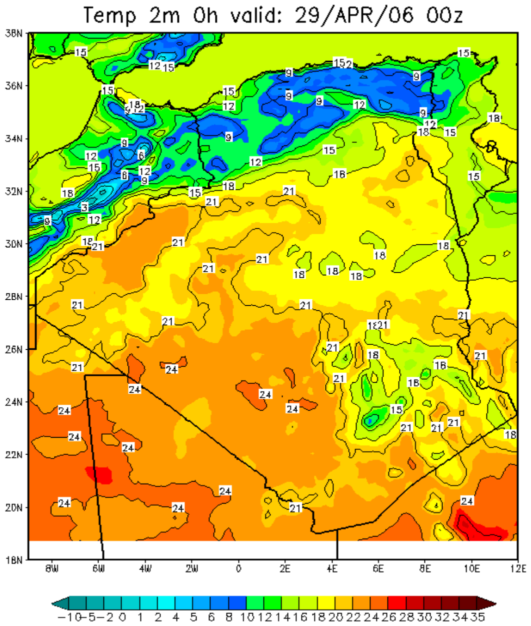


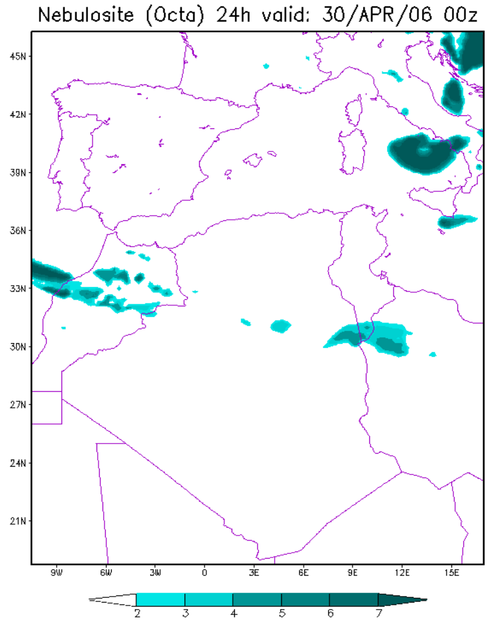


Fig.2 and 3: Examples of ALADIN/Algérie outputs

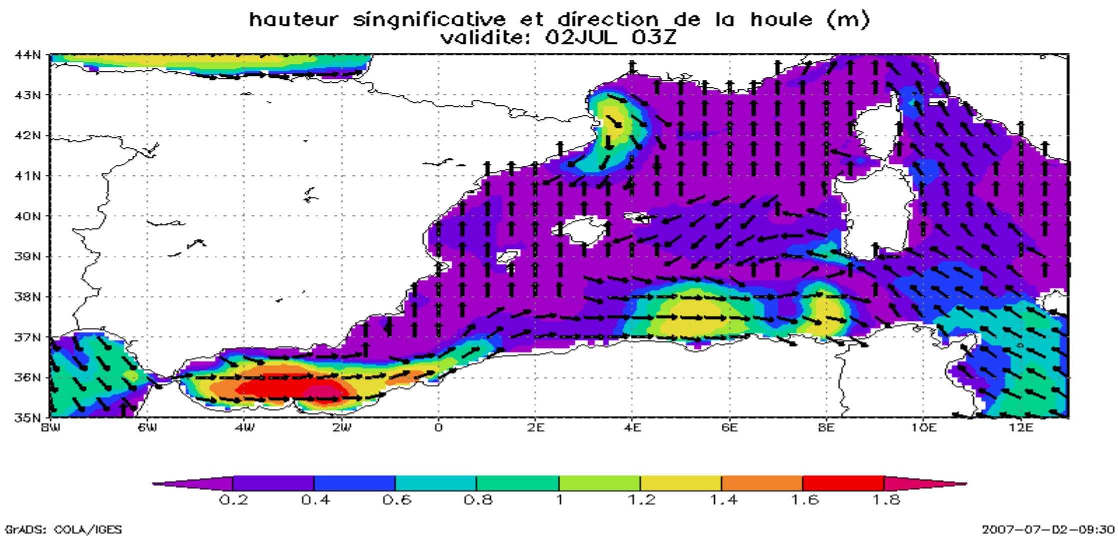


Fig.4: WAM model output (swell hight and direction)

## ❑ Derived fields:

In addition to the traditional fields, as MSLP, geopotential and temperature at different levels, some derived fields are computed, using the model outputs, to help the forecasters in their daily forecasts for some parameters related to "severe weather". Some of these derived fields are presented hereafter.

- **Latent instability index**

Some stability indices, as latent instability index, were developed to be used by ETA model and then were adapted to ALADIN/Algérie. The latent instability index is computed for the following layers: 1000/850hPa, 850/700hPa and 700/500hPa.

This index (W.S Harley, 1992) is based on the dry and saturated equivalent potential temperature and it expresses the instability degree of the layer. The instability is stronger as the index is negative.

- **Presentation of the index**

**Clat** (c1/c2) = 1.e5 x [1. / Tseb (c1/c2)] x [Pts (c1/c2) – Pte (c1/c2)] / (c1 – c2)

c1 – c2: thickness of the layer considered
Tseb average equivalent potential temperature
Tseb (c1/c2) = (pte (c1) + pts (c2)) / 2.
Pte (c1) = tetae (equivalent potential temperature)
Pts (c2) = tetase (saturated equivalent potential temperature)

Pte = Tp + 1.555 x (1000. / pres) x Es
Pts = Tp + 1.555 x (1000. / pres) x Esd

pres: pressure at the considered level
Tp : potential temperature
Es : vapour tension

Esd : saturated vapour tension

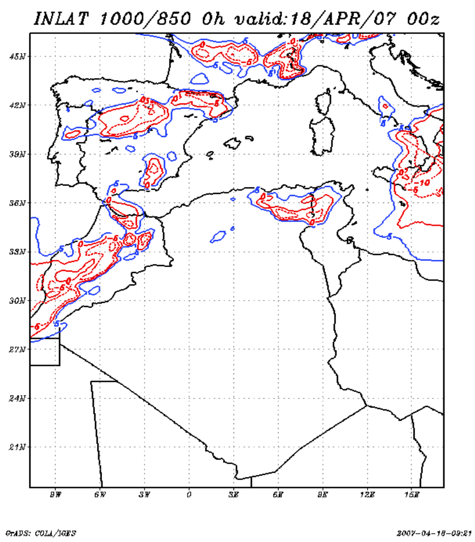

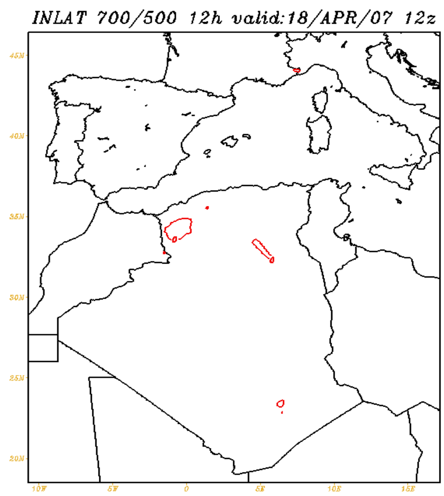


**Fig. .5 and 6**: Latent instability at the layers: 1000/850 and 700/500 hPa

- **K index**

It measures the probability of the storms development.

- **Presentation of the index:**

KI = (T850 – T500) + TD850 – (T700 – TD700)

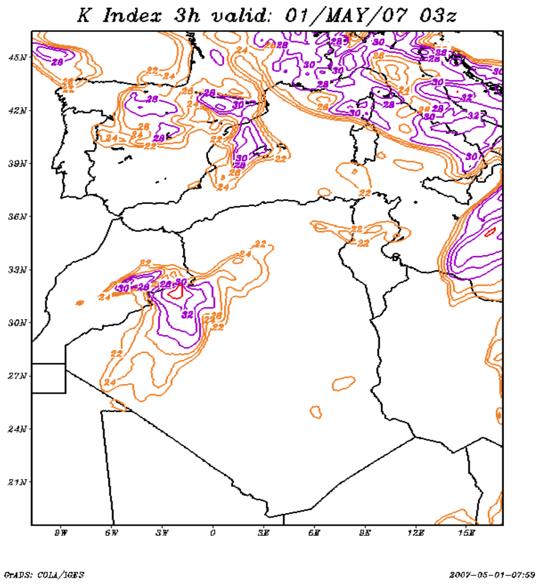


**Fig.7**: K index field

## ❑ The isentropic potential vorticity

The potential vorticity field is computed on the isentropics 315 and 330 °K.

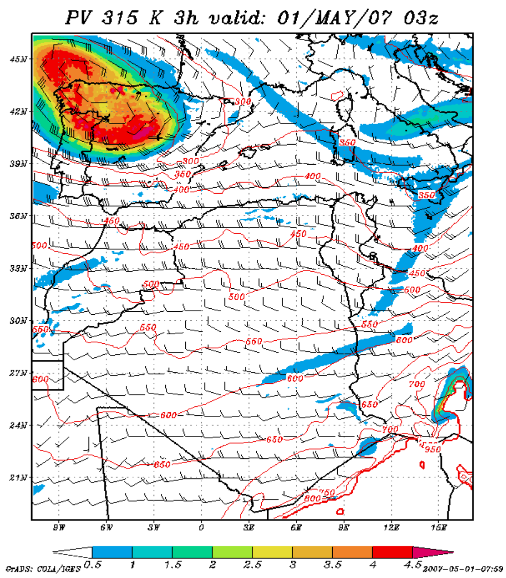


**Fig. 8**: Potential vorticity 315 °K

**2.5.2. Verification of ALADIN/Algérie (k.bouchouicha@meteo.dz)**


**Abstract**

This article has two purposes. The first one is to describe the methods which are under use at the forecasting centre of Algiers, for the verification of ALADIN/Algérie model, and the second one is to discuss the results concerning some meteorological parameters, in order to have a better idea about the behaviour of the model, using both analysis and observations. In this way, it will be possible to evaluate how well the model is able to forecast the main meteorological parameters, such as precipitations, 2 m temperature and 10 m wind, to underline some indices which can help forecasters who are the main users of the model outputs.


❑ **Introduction**

One of the most important aspects of numerical weather prediction is the verification of the model outputs. The methods witch are used for the verification of ALADIN/Algérie outputs in this article are the ones which are under use in many countries of the ALADIN Consortia and the main objective of this work is to learn about verification, in particular to know which way is better to extract the most important information from the ALADIN/Algérie outputs, taking into account the results of the verification.

The forecaster can use the data verification results to evaluate the model tendency (where and when the model tends to over or under forecast), in order to have a better idea about the quality of the model outputs which can help him to improve the forecasts of some meteorological parameters.

The verification system which is used is in two parts:

- Part One:

The scores which are computed for the surface parameters, at synoptic stations, are the following ones: BIAS, RMSE and MAE for the parameters: 2m temperature, 10m wind direction and speed and MSLP.

Standard verification scores as BIAS and POD, based on the contingency table, are also computed for the verification of precipitations and cloud cover.

- Part Two:

The following model outputs: Geopotentiel, temperature, humidity and wind components are controlled against the analysis at various levels (1000hPa to 100hPa) plus MSLP, and the computed scores are: BIAS, RMSE and CA (Correlation Anomaly).

❑ **Part one: Using the observations:**

☑ **Datasets**

Data used in the frame of this study are the ones collected from synoptic stations every three hours, during the period extending from September 1 to November 30, 2006. For this part, a subset of 40 professional stations among the 76 of the Algerian network are used, as shown in Figure 1.

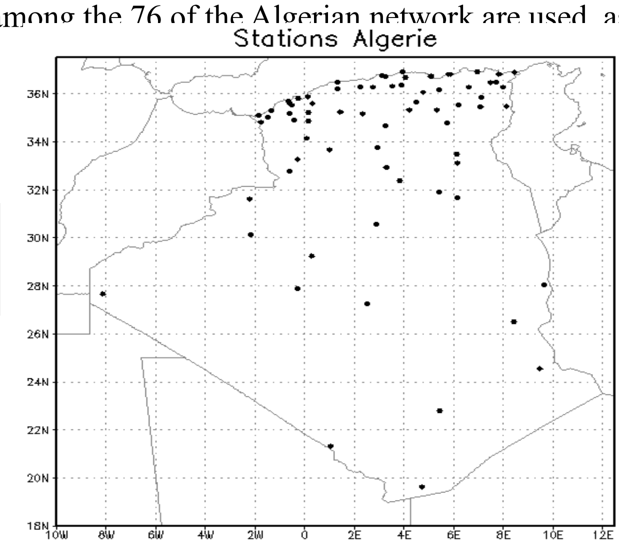


Fig 1: Location of the Algerian synoptical stations

☑ **Basic procedures:**

➢ Categorical forecasts

Contingency table can be used as outcome (yes or no) for a given event or forecast, e.g, rain event. The number of correct forecasts for a specific event is given by A and the number of observed events but not forecasted, is given by B. The number of forecasts which can not be verified is represented by C and the number of events which are neither forecasted nor observed is represented by D.

| Contingency Table | | | | | |
|---|---|---|---|---|---|
| Forecasted | | Observed | | | |
| | | Yes | No | ∑ Fc |
| | Yes | A | B | A+B |
| | No | C | D | C+D |
| | ∑ obs | A+C | B+D | Total |

The computed scores from this table are:

Probability Of Detection (POD): It is the number of rainy events (observed and forecasted) divided by the total number of forecasted events. The best possible score is 1, the worst is 0.

$$POD = \frac{A}{A+B}$$

False Alarm Ratio (FAR): It is the number of false alarms (unverified rainy events) divided by the total number of rainy observed events. The best possible score is 0, the worst is 1.

$$FAR = \frac{C}{A+C}$$

The POD and the FAR are often used together in the verification of the precipitations.

Bias: It indicates whether the forecasts are under estimated or over estimated.

$$BIAS = \frac{A+C}{A+B}$$

➢ Continuous Variables

Concerning these variables, some other scores, as the following ones, are computed:

*Mean Error (ME) or Bias:* indicates the average tendency of the model's error.

$$ME(BIAS) = \frac{1}{N}\sum_{i=1}^{N}(f_i - o_i)$$

Where N= number of cases; $f_i$ the *ith* forecast and $o_i$ the *ith* observation.

*Mean Absolute Error (MAE):* It is the average of the absolute model's error, if the MAE is equal to zero, the forecast is perfect and the value increases proportionally with the discrepancies between forecast and observation; it describes the typical magnitude for the forecast error.

$$MAE = \frac{1}{N}\sum_{i=1}^{N} |f_i - o_i|$$

*Root Mean Square Error (RMSE):* It measures the amplitude of the forecast error.

$$RMSE = \sqrt{\frac{1}{N}\left[\sum_{i=1}^{N} (f_i - o_i)^2\right]}$$

*Correlation coefficient (R):* It describes the relationship between the forecast and the observation. R measures the strength and the direction of a linear relationship between two variables.

The value of R varies between -1 and 1. The + and – signs are used for positive linear correlations and negative linear correlations, respectively.

$$R = \frac{\sum_{i=1}^{N} \left[(f_i - \bar{f})(o_i - \bar{o})\right]}{\sqrt{\sum_{i=1}^{N} (f_i - \bar{f})^2}\sqrt{\sum_{i=1}^{N} (o_i - \bar{o})^2}}$$

☑ **Presentation of the results:**

The scores (BIAS, MAE, RMSE and R) are computed using the model outputs (forecast range:12h and 30h) and synoptic surface observations over ALADIN/Algérie domain and are plotted as diagrams by range and time evolution. Monthly averages of these scores are also computed.

The selected period is: September to November 2006 and the model outputs are every three hours.

Direct comparisons between the previous forecasts and the observations are done for the following parameters: 2m temperature plus MSLP, and the selected stations are:

- DAR-EL-BEIDA north of Algeria (Lat: 36 41N , Long: 03 13E )
- TAMANRASSET south of Algeria (Lat: 22 49N , long: 05 27E )

The results are presented in Figures 2 and 3.

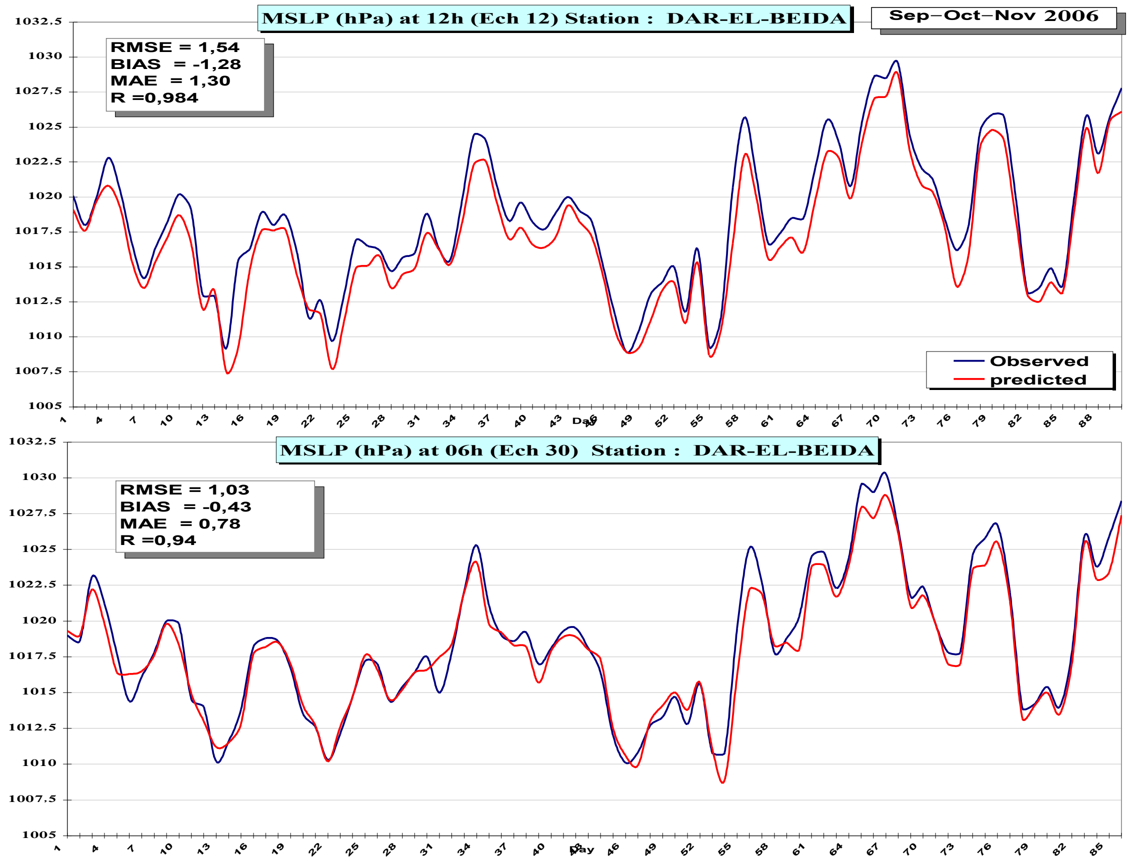


Fig 2 : RMSE and BIAS for MSPL at DAR-EL-BEIDA

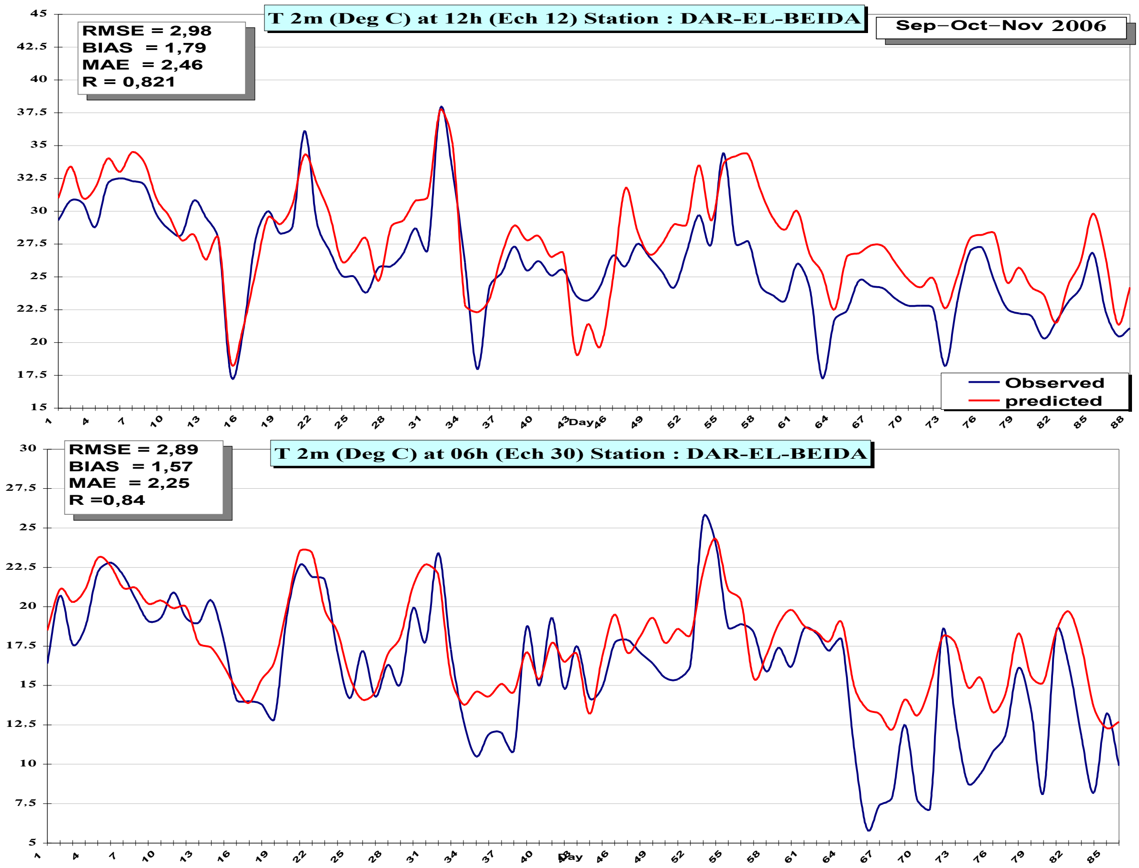


Fig 3 : RMSE and BIAS for 2m Temperature at DAR-EL-BEIDA

### ☑ Discussion:

a) MSLP: the RMSE increases with the time-step (from 0.6 to 1.5 hPa); the bias presents a large amplitude (from ±0.2 to ±0.5 hPa) during the first 12 hours and decreases with respect to the time-step.

b) TEMPERATURE: the RMSE increases from 0.7 to 3.5 degrees, and it seems that the bias is too large at 30 hours forecast range (about ±1.5 degrees).

## ❑ Part two : Using the Analysis

### ☑ Datasets

The data used here are as follows: model outputs grided data every 12 hours from September 1 to November 30 2006, and the corresponding analysis over all the ALADIN/Algérie domain.

- Methodology:

The same methods described previously are used here in addition to the following one:

*Anomaly correlation (AC):* it is defined as the correlation between the predicted and analyzed anomalies of the variables. The anomalies are deviations from the mean climatological values. The following expression is used to compute the anomaly correlation.

$$AC = \frac{\sum_{N,M}\left[(P_{N,M} - \bar{C}_{N,M})(A_{N,M} - \bar{C}_{N,M})\right]}{\left[\sum_{N,M}(P_{N,M} - \bar{C}_{N,M})^2 \sum_{N,M}(A_{N,M} - \bar{C}_{N,M})^2\right]^{\frac{1}{2}}}$$

$C$ represents the climatologically average of the variable given for each grid point
$P$ represents the forecast; A represents the analysis of the model
N, M grid point. (N*M) the number of grid points

### ☑ Results:

a) MSLP: the following diagrams shows the time evolution of the mean scores (AC and RMSE) over the Algerian domain for the Mean Sea Level Pressure during the following months: September, October, November and December 2006.

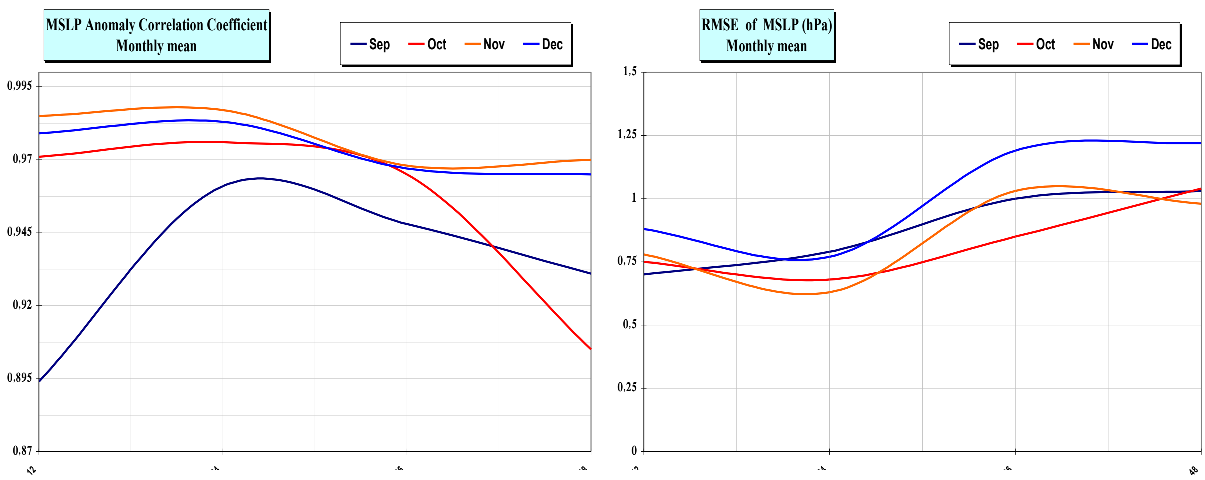


Fig. 4: Time evolution (12, 24, 36 and 48 hours) of the mean scores AC and RMSE for MSLP

b) Geopotentiel

Time evolution of the mean scores (AC, RMSE)

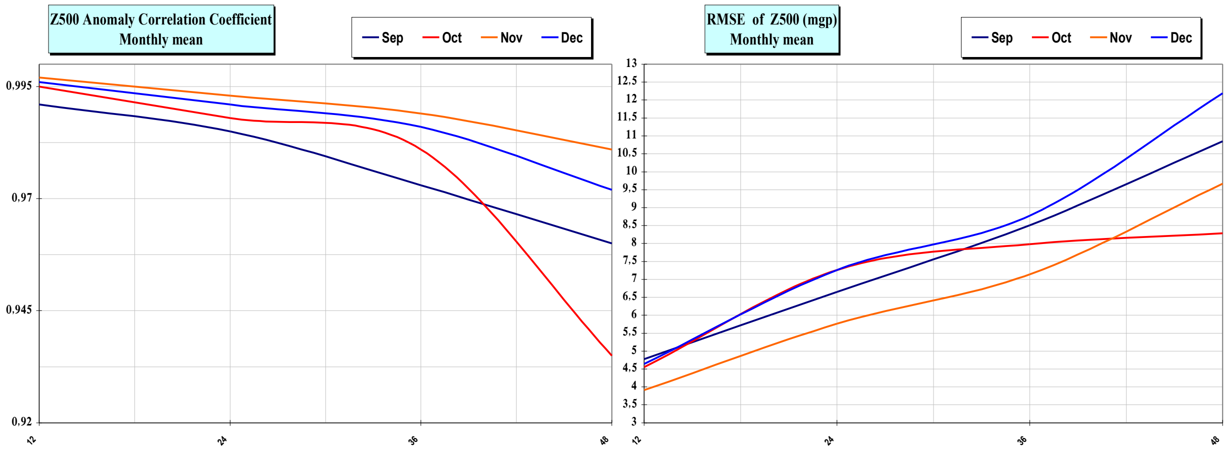


Fig. 5: Time evolution (12, 24, 36 and 48 hours) of the mean scores AC and RMSE for 500hPa

c) Temperature

Spatial evolution of the RMSE and time evolution of AC

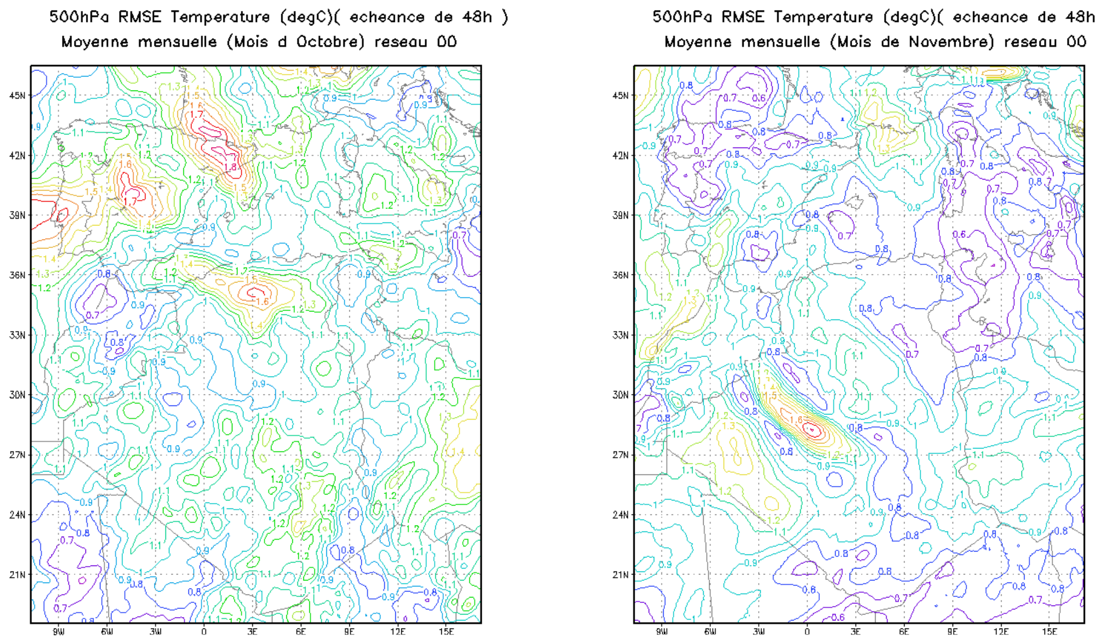


Fig 6: 500 hPa RMSE Temperature for October 2006 at 48 hours forecast range

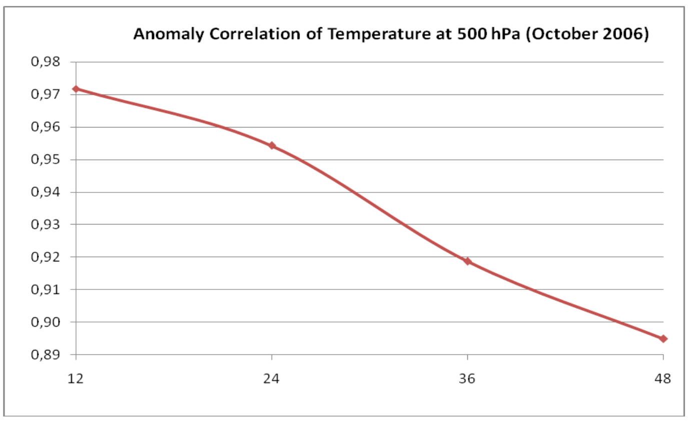


Fig 7: Anomaly Correlation of Temperature at 500 hPa (October 2006)

☑ **Discussion:**

**MSLP**

- The RMSE increases with time-step (from 0.6 to 1.2 hPa) for all the months (Sep, Oct, Nov, Dec).
- The AC is higher than 0.96 for November and December, and became lower than 0.91 after 36 hours forecast for all the months, except for September.

**Geopotentiel**

- RMSE increases from 4 to 12 mgp with time-step for all the months (Sep, Oct, Nov, Dec) at 500 hPa.
- AC is higher than 0.98 during the first 36 hours forecast and decreases with respect to the time-step increasing for all the months, except for October were the AC reached a value of 0.93 at 48 hours forecast.

**Temperature**

- RMSE greater than 1.5 Degrees at 48h forecast for October and November at 500 hPa.
- Reduction of the AC after 12 hours forecast.

❑ **General conclusion**

The analysis of the previous results showed that the behavior of ALADIN/Algérie model is too good because of the acceptable results which are given by the computed scores.

In case of 2 meters temperature, the model error is sometimes greater than five (05) degrees at some stations. This can be explained by an appreciable difference between the altitudes of the nearest grid point and the station.

The second step of the verification is to evaluate the appreciations of the forecasters concerning the daily use of ALADIN/Algérie outputs, in order to point out which parameters are well forecasted by the model and the ones which are not.

## 2.6. AUSTRIA

wang@zamg.ac.at

In the first half of 2007, there were several changes in the ALADIN-AUSTRIA operational suite at ZAMG:

- · New computer system NEC SX8R with 16 CPUs (32 Gflops/CPU, 128 GB RAM, 4.4 TB storage) has been installed, and the ALADIN-AUSTRIA is now running on this new computer system operationally.
- · ALADIN-AUSTRIA runs 4 times per day: 00, 06 12 and 18UTC, where 00 and 12 UTC run are up to 72 hours; 06 and 18 UTC run up to 60 hours.
- · ALADIN-LAEF has been put into pre-operational status. Details see the contribution of Alexander Kann etc. in this newsletter.

## 2.7. BELGIUM

## 2.8. BULGARIA

## 2.9. CROATIA

Martina Tudor and Stjepan Ivatek-Šahdan

### 2.9.1. Summary

The operational suite runs on SGI Altix using only 16 out of 24 processors. The other 8 processors are reserved for research. This set-up will continue until the licence for the queueing software for additional 8 processors is purchased.

The primary transfer of LBC files is done through internet. The backup for the transfer of the LBC files is ecgate.

A version of Alaro0, ported to Viking, is continuously maintained, when any improvements become available. It provides the second operational 72 hour forecast on the same domain and resolution (8km) and on the same number of levels in the vertical as the reference (first) Aladin 72 hour forecast obtained with AL29T2mxl. Both are run twice a day, for 00 and 12 UTC starting from ARPEGE analyses with DFI.

The old SGI machine (Mrcina) was permanently stopped since the electric power could not support all the machines in the systems room and the cooling for the systems room when temperatures exceeded 30°C. It is still used for research due to difficulties in porting some research tools on the new SGI Altix. Several researchers are awaiting for some colder weather for the machine to be switched on.

### 2.9.2. Operational suite

- **Status**

The status did not change significantly since the last newsletter report.

AL32T1 is ported.

Internet address with some of the ALADIN products, like total precipitation and 10 m wind: http://prognoza.hr/aladin_prognoza_e.html .

- **Plans**

Switch to AL32T1 in operational suite after some extended testing.

A single large high resolution dynamical adaptation domain is created. Although it requires far more CPU-time than the 6 small domains, the largest problem remaining is the storage of the output files.

## 2.10. CZECH REPUBLIC

Radmila Brozkova

### 2.10.1. Main changes in the operational applications

There was one quite important change in the operational application of ALADIN/CE: a pioneering evolution toward the application of ALARO-0 (yet without the 3MT scheme) in the beginning of 2007. It was an important step toward the prognostic character of the physics. Indeed, there is for example the first NWP application with a prognostic TKE among the IFS/ARPEGE/ALADIN galaxy.

➢ **ALARO-0 without 3MT**

This configuration got operational on 30th January 2007. The development was based still on the cycle CY29T2, with the following content:

1. Improvements in radiation scheme;
2. Novelties in water cycle computing environment;
3. Condensation and microphysics scheme;
4. Introduction of pseudo-prognostic turbulent kinetic energy scheme and some re-tunings;
5. Use of prognostic snow density and albedo (following ARPEGE);
6. Use of recent climate profiles of ozone (following ARPEGE);
7. Optimization of computation of semi-Lagrangian interpolation weights.

The major package of novelties in the model physics represents the result of the ALARO effort, where many ALADIN people took part. It follows the plan established in 2005 at ALADIN workshop in Bratislava. The content of the present e-suite thus encompasses the so-called ALARO-0 version, yet without the 3MT scheme treating the deep moist convection and without other three smaller issues (better aerosol description, improved radiative gaseous transmission functions, vertical transport of liquid and solid cloud water by the vertical diffusion scheme, where some more study is needed). Another important point is that the interface between the parameterizations and dynamical core follows on the equations described in Catry et al., 2007.

☑ **Radiation scheme**

Here we have several ingredients. There is a new saturation cloud model, which improves optical properties of clouds in solar and thermal band. Documentation exists and a publication is under preparation. As far as the thermal band computations are concerned, these are based on the net exchange rate formalism. In the e-suite we have now better tuning of the statistical estimation of the secondary exchange terms. Finally, a simplified version of the Voigt effect parameterization was included, following Geleyn et al., 2005. As the last improvement the recent climate profiles of ozone were introduced, following the work in ARPEGE of Y. Bouteloup.

☑ **Water cycle computing environment**

We have introduced coherent corrections of negative humidity and water species. When a negative value is detected, it is set to zero but the difference is counted in the budget as a flux divergence and there is associated pumping of water vapor. These corrections are introduced before the call to parameterizations to account for negative values that may occur within the advection. In the computations of cloudiness and shallow convection we use now the total water content (water vapor plus condensed liquid and solid cloud water).

### ☑ Condensation and microphysics

There is a new scheme to compute the condensates entering the microphysical scheme. The condensation-evaporation process depends on the presence of cloudiness. This one is diagnosed by an algorithm close to the current operational Xu-Randal scheme (ACNEBN) but with a constraint to reach equilibrium with respect to total water content and critical humidity profile. The mesh-size is also taken into account (it is not assumed that the cloud occupies the whole grid-box). Cloudiness computed this way is used in microphysics (in order to account for the influence of cloud and/or precipitation coverage on the intensity of microphysical effects), while the cloudiness used for the radiation scheme remains the one computed by ACNEBN. The microphysical scheme itself has prognostic treatment of four water species: liquid and solid cloud water, rain and snow. The sedimentation is solved by a statistical approach (a publication is under preparation). In addition, there is a parameterization of Wegener-Bergeron-Findeisen process and a diagnostic type of a graupel effect parameterization. There exists some documentation, except (still) for the condensation part.

### ☑ Turbulence

We have introduced the so-called pseudo-prognostic TKE (Turbulent Kinetic Energy) scheme. TKE is a prognostic variable, while the vertical exchange coefficients are still computed using the results of a diagnostic computation (ACCOEFK) to set the equilibrium position of the prognostic part of the scheme (some documentation is available).

Besides, there is retuning of mixing under stable conditions and also a small retuning of mixing length in the free atmosphere, following the work done in ARPEGE (F. Bouyssel, E. Bazile). We have used the rewriting of ACDIFUS routine to move VZIUSTAR0 coefficient to namelist. Also, the vertical diffusion scheme (ACDIFUS) uses so called “moist conservative” variables for diffusion of dry static energy and water vapor (following P. Marquet and L. Gerard).

### ☑ Soil scheme

We have followed ARPEGE and introduced the use of prognostic albedo and snow density. This became possible with the so-called TOPO30 version of climate files, which is in use since 23/01/2006.

### ☑ Technicalities

We introduced optimized routine ELASCAW computing weights of semi-Lagrangian interpolators. It is faster and results are bit-identical.

Before getting operational, this package was tested quite a long time in an e-suite, for both summer and winter periods. The results could be summarised as follows:

Geopotential and relative humidity scores with respect to TEMP observations are improved in both summer and winter tests. Temperature scores are improved as well, except a warm bias nearby the tropopause level. In winter it is negligible, in summer it is a bit more pronounced; it is linked to the convection. Wind scores are mostly neutral, with a small improvement at the top of boundary layer.

Screen level scores in winter show less pronounced diurnal cycle compared to the operational version and cold bias in the night is little bit improved. In summer the diurnal cycle is not modified. For both periods there is a small worsening of the surface pressure bias.

The most important change brought by this e-suite is in the pattern of precipitation fields (see Figure 1). These are smoother; the exaggerated spots are mostly suppressed. The precipitations occur also on the crest of mountains while before the shadow effect was too strong. The scores (contingency tables and ETS) show a small improvement. The amount of cloudiness is comparable with that of the operational version.

- **ALADIN/Afghanistan**

A special configuration of the ALADIN model was prepared to serve the mission of Czech Army in Afghanistan. It got resolution close to 10km and is coupled with ARPEGE. Because of a very complex terrain the blending technique results were superior to the dynamical adaptation mode. Due to absence of any surface observation data no surface analysis was envisaged and thus the model runs in a pure blending mode. The application was moved to the ALARO-0 (without 3MT) shortly after the main suite.

## 2.11. FRANCE

(F. Bouttier, bouttier@meteo.fr)

The ALADIN-France configuration is documented in a summary under the web page http://www.cnrm.meteo.fr/gmap/

ALADIN-France inherits from all ARPEGE changes, which have been listed in section 2.11 of this newsletter, with the addition of

- a new balance equation for the ALADIN 3D-Var (non-linear omega, as developed and documented by ECMWF) is included in the current cy32t0 test suite.
- assimilation of 10m wind observations from SYNOP and automated surface stations over land.
- the microphysics change (also in ARPEGE) is expected to alleviate spurious wind circulations in ALADIN, linked to excessive evaporation of precipitation.

As advertised earlier, an ALADIN 3D-Var assimilation runs over the Southwestern Indian Ocean, which covers Madagascar and some French islands there, this application is primarily used for tropical cyclone forecasting.

The new NEC machine used for the ARPEGE and ALADIN-France operational production features:

- 2 machines (one for research, one for operation) of 16 nodes, each node contain 8 vector processing elements
- the NEC is about 4 times faster than the previous VPP system
- each NEC machine has a front-end (TX7 machine) which is used for everything except actual number crunching, in particular the TX7 takes care of compiling, file retrieval and archiving, so that users are ***strongly*** encouraged to split their jobs accordingly.
- very large memory, and many disk systems...
- ...so that NEC users should study the new NEC user documentation in order to work efficiently.

## 2.12. HUNGARY

(kullmann.l@met.hu)

There were only small changes in the operational version of the ALADIN/HU model during the first half of 2007:

- Improving AMDAR data preprocessing (reading in netcdf format).
- New bias correction file was calculated for ATOVS data.
- MSG/GEOWIND and SHIP data are used operationally.
- Tuning of turbulent mixing length computation.

### 2.12.1. The main characteristics of the recent operational suite:

- ALADIN cycle: cy30t1
- Horizontal resolution: 8 km
- Vertical levels: 49
- Grid: linear
- Data assimilation: 3d-var with 6h cycling
- Observations: SYNOP (geopotential), TEMP (temperature, wind components, humidity, geopotential), AMDAR (temperature, wind components), ATOVS:AMSU-A and AMSU-B radiances, MSG/GEOWIND (AMV).
- Production is performed 4 times per day: 0 UTC (+54h), 6 UTC (+48h), 12 UTC (+48h), 18 UTC (+36h).

### 2.12.2. Parallel suites during the period:

- BACKUP: We run a backup suite on the IBM (p655) machine. The same 3d-var system is used as for the operational but production is performed only at 0 and 12 UTC. For the backup we use cy28t3.
- Dynamical adaptation as a reference to 3d-var system at same vertical and horizontal resolution (cy28t3 is used).
- ALADIN 3d-var using ensemble B matrix (based on cy30t1).

## 2.13. MOROCCO

## 2.14. POLAND

*Marek Jezczynski zijerczy@cyf-kr.edu.pl*

In November 2006 some changes to ALADIN operational suite was introduced: forecast range was enhanced up to 54 hours and coupling frequency was increased from 6 to 3 hours. The changes were followed by porting all operational stuff to new machine: ALTIX 3700, accompanied with change of model version to AL29T2mxl ( great thanks to Stjepan Ivatek-Sahdan for his help ! ).

After exchange of machine and model environment, during first two months, operational runs quite frequently suffered because of technical problems with new hardware and also hung-up's of operational system and PBS queue system.

To react quicker for some potential threats to operational production the model environment is now being monitored every 15 minutes with especially prepared simple piece of software which diagnose a threat and signalize its occurrence.

Current operational suite:

- domain: 2270 x 2270 km
- grid size: 169 x 169 x 31 ( without extension zone )
- timestep: 600 sec.
- range: 54 hours
- coupling: ARPEGE, 3-hour frequency
- runs: 2/day

## 2.15. PORTUGAL

Maria Monteiro, Manuel Lopes, Nuno Lopes, João Rio, João Ferreira (for further information: maria.monteiro@meteo.pt)

### 2.15.1. Introduction

On the first half of 2007 no many changes have taken place on the Portuguese NWP operational systems. Main reason has been due to the acquisition of a HPC platform and so the focus put on the preparation and planning of the new computer facilities for the development of NWP activities. However, some changes have taken place since the last time a Portuguese contribution was payed to the newsletter: the dissemination of ALADIN/Portugal products to INM for forecasting purposes, the integration of ALADIN/Portugal predicted fields on the PEPS system, the upgrade of objective verification procedures in order to have the time consistency check of the basic model fields, in a time window of 3 months, using skill scores ALADIN *vs*. ECMWF and finally the inclusion of an operational wind dynamical adaptation scheme for three different geographical regions of Portugal. Now, an historical archive of ALADIN/Portugal operational outputs exists and it contains GRIB data information from 2005 to 2007. The CANARI version AL12 was validated over an area of Portugal and adjacent Atlantic Ocean where coastal analysis have shown erroneous meteorological information and therefore ODB is being installed in order to allow the local usage of a more recent CANARI cycle. Training is still a priority inside the team. Finally, the organization of François Bouttier visit to Portugal was prepared in cooperation with the Évora University, in order to allow the presentation of the AROME model to the Portuguese meteorological community early this year.

### 2.15.2. Operational version

ALADIN/Portugal operational model runs CY28T03 since 6th of June 2006 on the DecAlpha cluster ES40 2/667. Parallel runs are performed with changes that have just taken place on some *namelists* in order to keep historical files available to run the wind dynamical adaptation. Parallel post-processing is being made under the Debian based PaiPix Linux distribution on a AMD dual core processors PC in order to disseminate ALADIN/Portugal products to the PEPS project.

### 2.15.3. Time consistency check of ALADIN/Portugal operational system performance

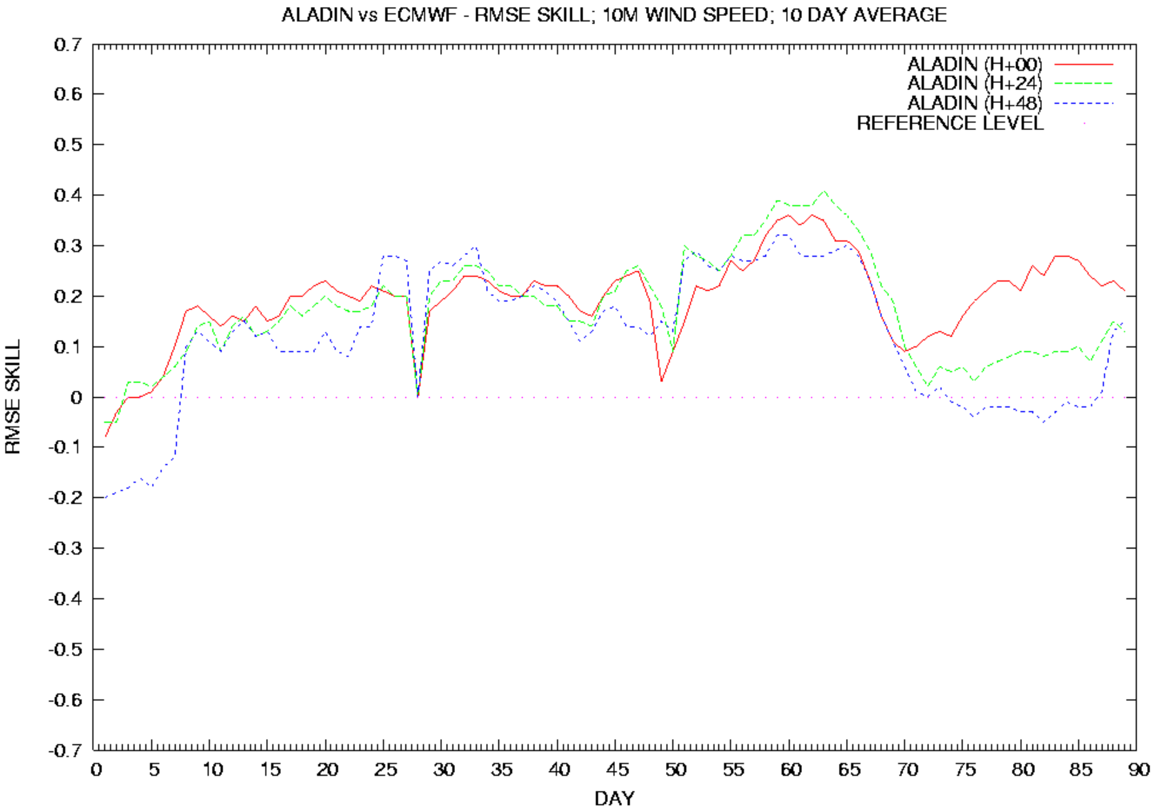


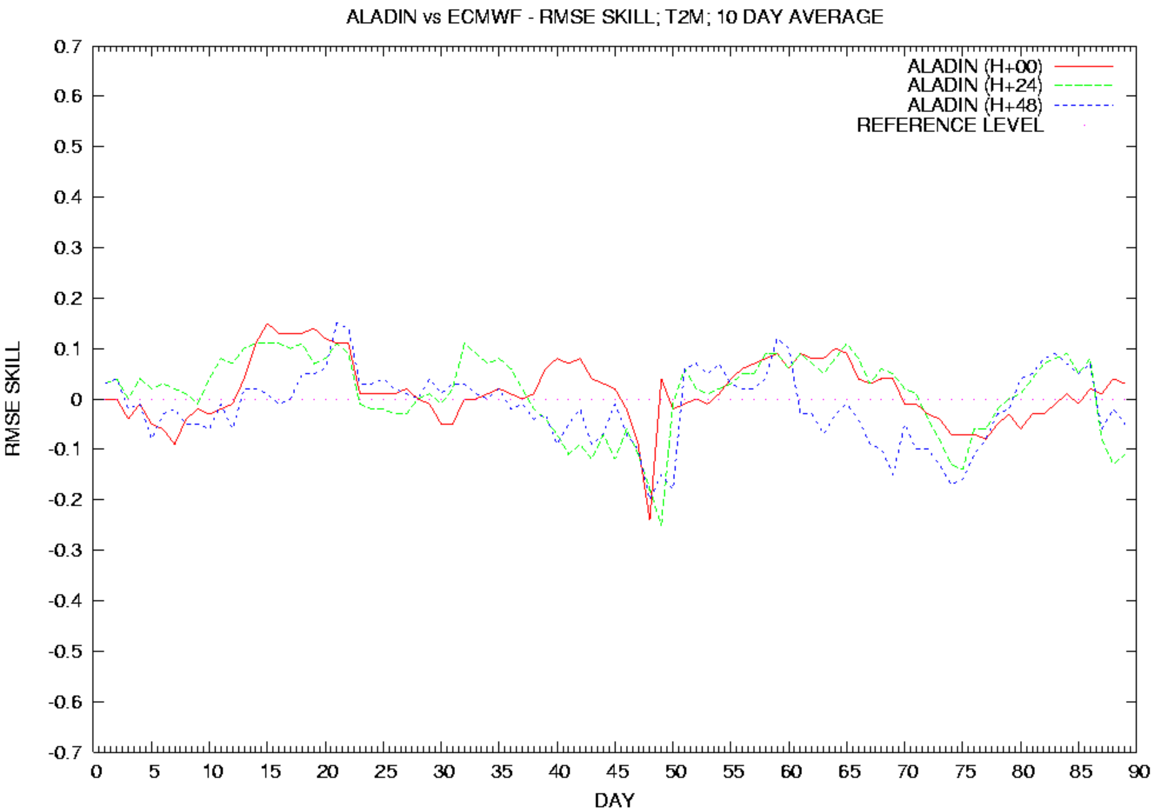


Time consistency check is a reliable way to control the model performance when boundary constraints to your operational model – like the changes on the initial and boundary conditions due to an cycle upgrade of its system, or the computer platform migration of its system – are changed.

Some appropriate scores, the RMSE SKILL's scores, are evaluated operationally and a performance control of our model basic outputs is being built to avoid the miss usage of ALADIN/Portugal products by forecasters and other end-products clients. Besides RMSE skills scores, series of RMSE and BIAS of ALADIN/Portugal are also updated on a daily basis for 3 months backward time window.

### 2.15.4. Wind dynamical adaptation

The genesis to build an operational wind dynamical adaptation system based on ALADIN/Portugal was an informal cooperation research project started on demand of Portuguese wind power supply companies to the University of Lisbon: ALADIN/Portugal wind dynamical adaptation was tested against MM5 (Lisbon University) as possible forcing fields to the management models of wind power supply stations. Taking into account the preliminary conclusions, that there was an increased value over direct wind output fields although depended on the synoptic situations, an operational system was setup in order to evaluate its added value also for other purposes and in particular, for forest fire prevention.

After the 4th of July 2007, the Portuguese team started the operational run of the dynamical adaptation procedure of ALADIN/Portugal, on a PaiPix Linux distribution PC. The used cycle is CY29T02 with the initial and boundary conditions being produced by ALADIN/Portugal CY28T03, our main operational cycle. The principal characteristics of the dynamical adaptation are:

- 3 domains over mainland, covering the northern, the center and the southern parts of the mainland Portugal;
- approximately 3 km in horizontal resolution;
- 2 runs, for 00 UTC and 12 UTC;
- 48 hours forecast with 3 hours outputs;
- post-processing for the u- and v-components of the horizontal wind at 10 meters.

The figures below show an example of the wind field derived from dynamical adaptation for each one of the 3 referred domains.

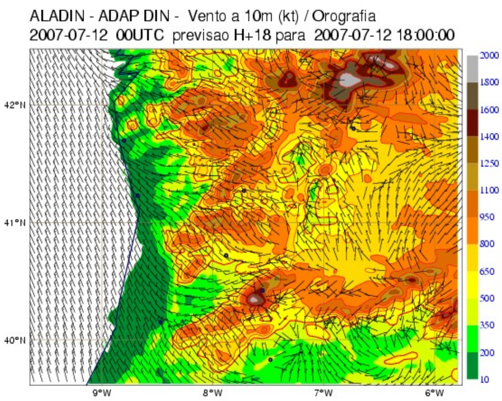


**Fig. 1** – H+18 forecast of the 10m wind field for the North domain, run 00 UTC of 12th July 2007.

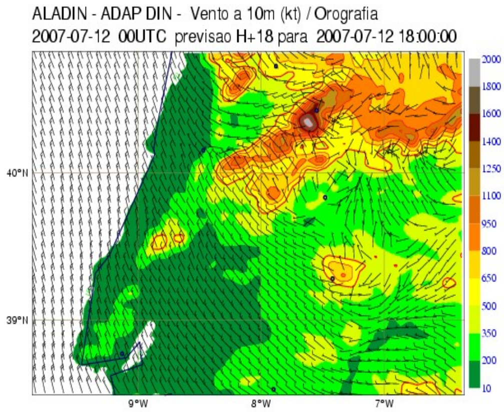


**Fig. 2** – Forecast H+18 of the horizontal wind field at 10 meters for the Center domain, run 00 UTC of 12th July 2007.

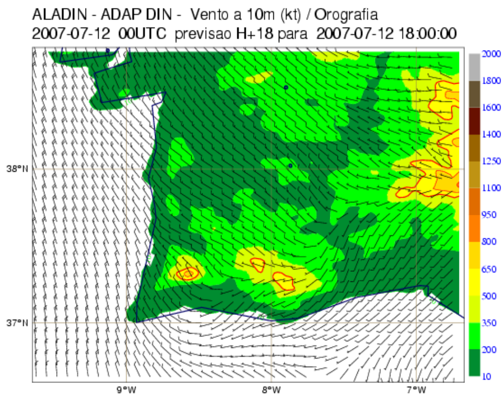


**Fig. 3** – Forecast H+18 of the horizontal wind field at 10 meters for the South domain, run 00 UTC of 12th July 2007.

## 2.16. ROMANIA

doina.banciu@meteo.inmh.ro, simona_ecaterina_stefanescu@yahoo.com

- The operational suite - still based still on the cy28t3, with no modificationsof of the model set-up or the integration domain.

  The main modifications of the operational suite carried out since last report concern:
  - Extension of the forecast range for the 00 run up to 78h and of the 12 run up to 66 h
  - Introduction of two additional runs for 06 and 18 up to 48 forecast range.

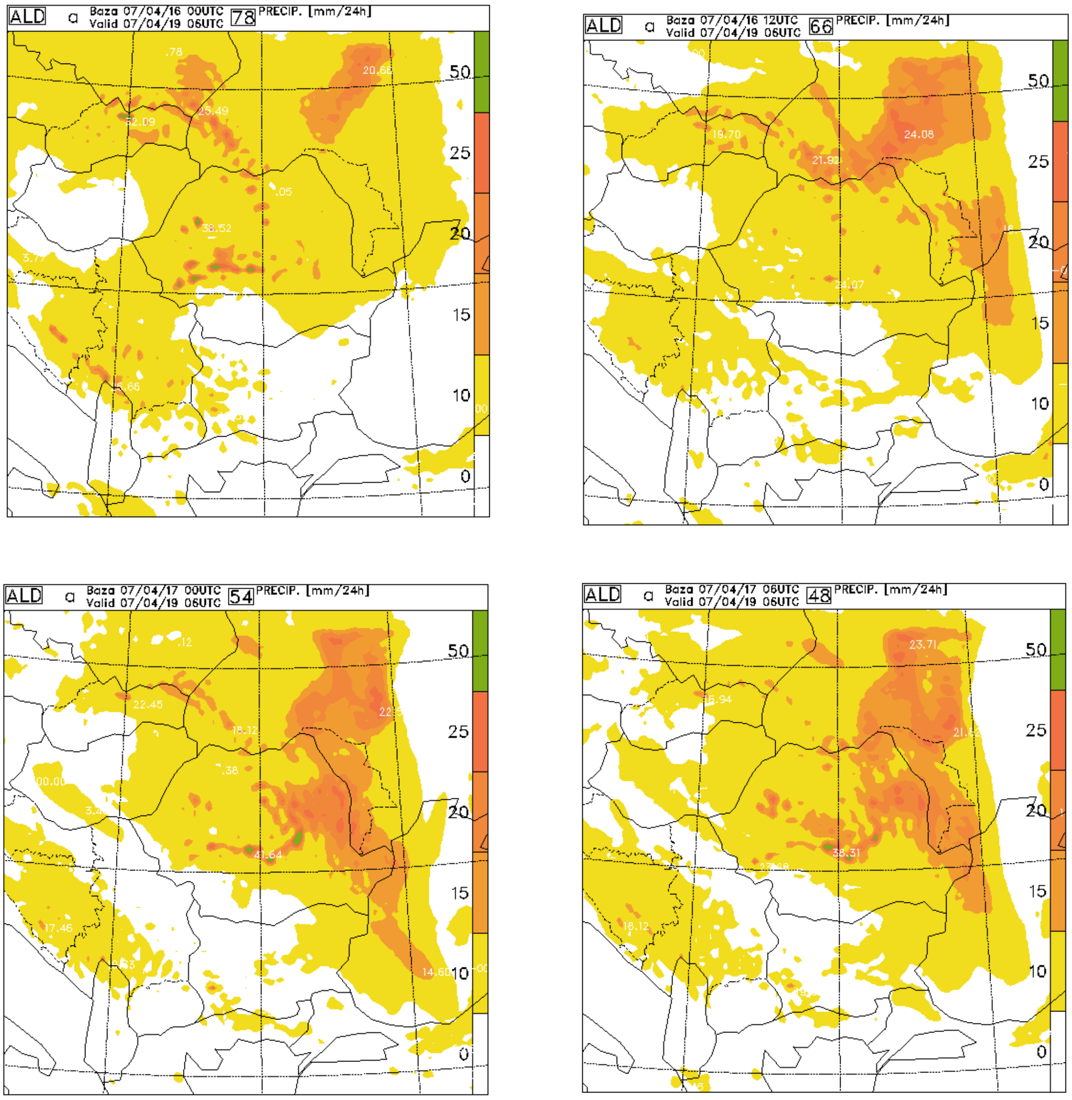

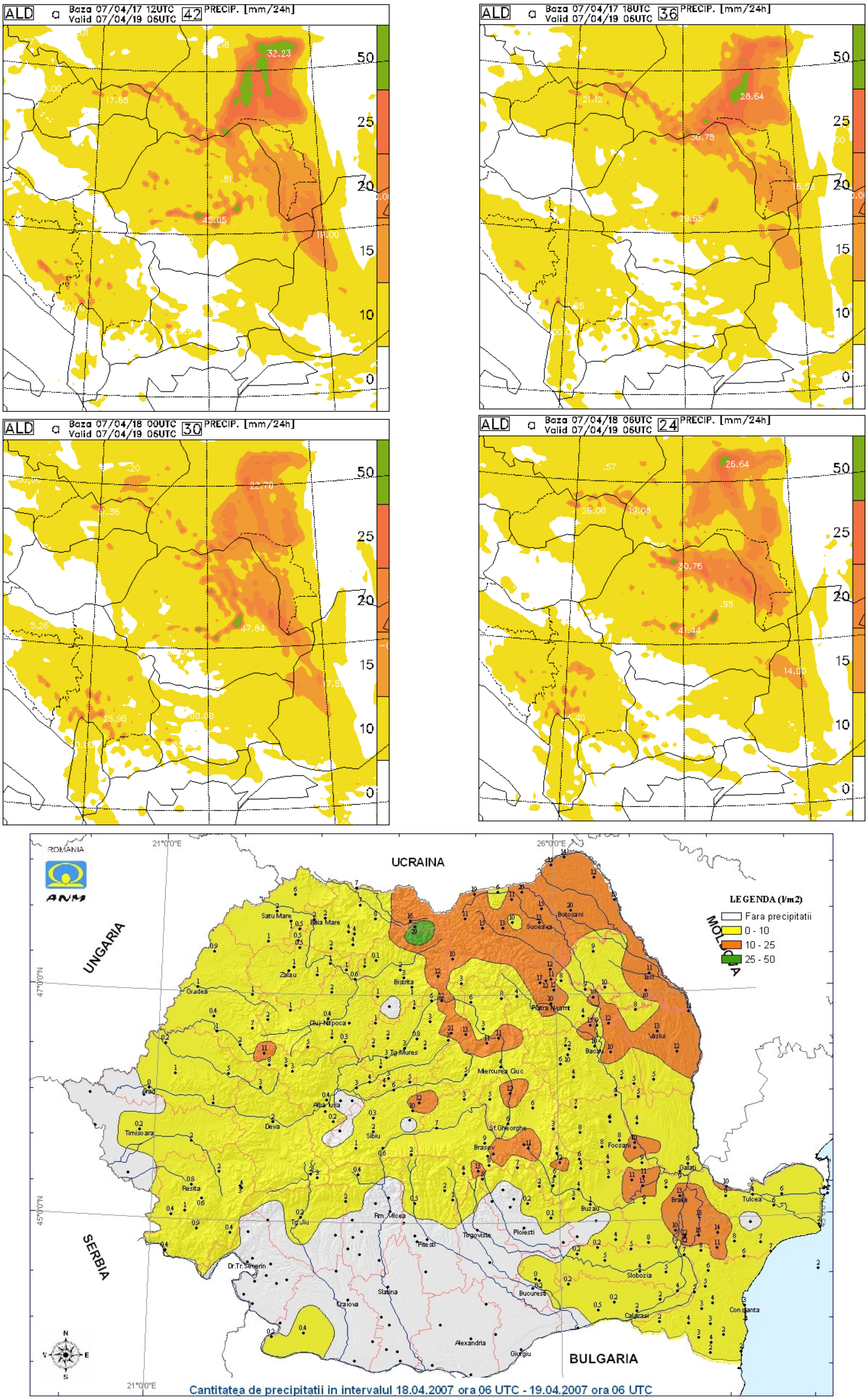


**Fig.1**Updated information available due to the 4 runs: the 24h accumulated precipitations forecasted by different runs valid at 19 April 2007 06 UTC compared with the observed 24h accumulated precipitations valid at 19 April 2007 06 UTC

The Aladin products for 06 and 18 UTC runs have been added on the intranet web page, together with the development of other new ones.

- **Tests related to Arpege coupling files produced on NEC at Meteo-France**

The new climatic files and coupling files produced on NEC have been tested in order to investigate their compatibility with the Aladin operational suite in Romania.

Differences between the operational run and the runs with NEC climatic (test1) or coupling files (test 2) have been computed for surface fields (mean sea level pressure, 2m temperature and relative humidity, 10m wind components) and upper air fields (geopotential, temperature, relative humidity and wind components at 500 hPa pressure level). For the first test, these differences were not significant at the initial time and also during the 24h forecast. For the second test, some numerical differences were found, but with no significant meteorological importance (figure 2).

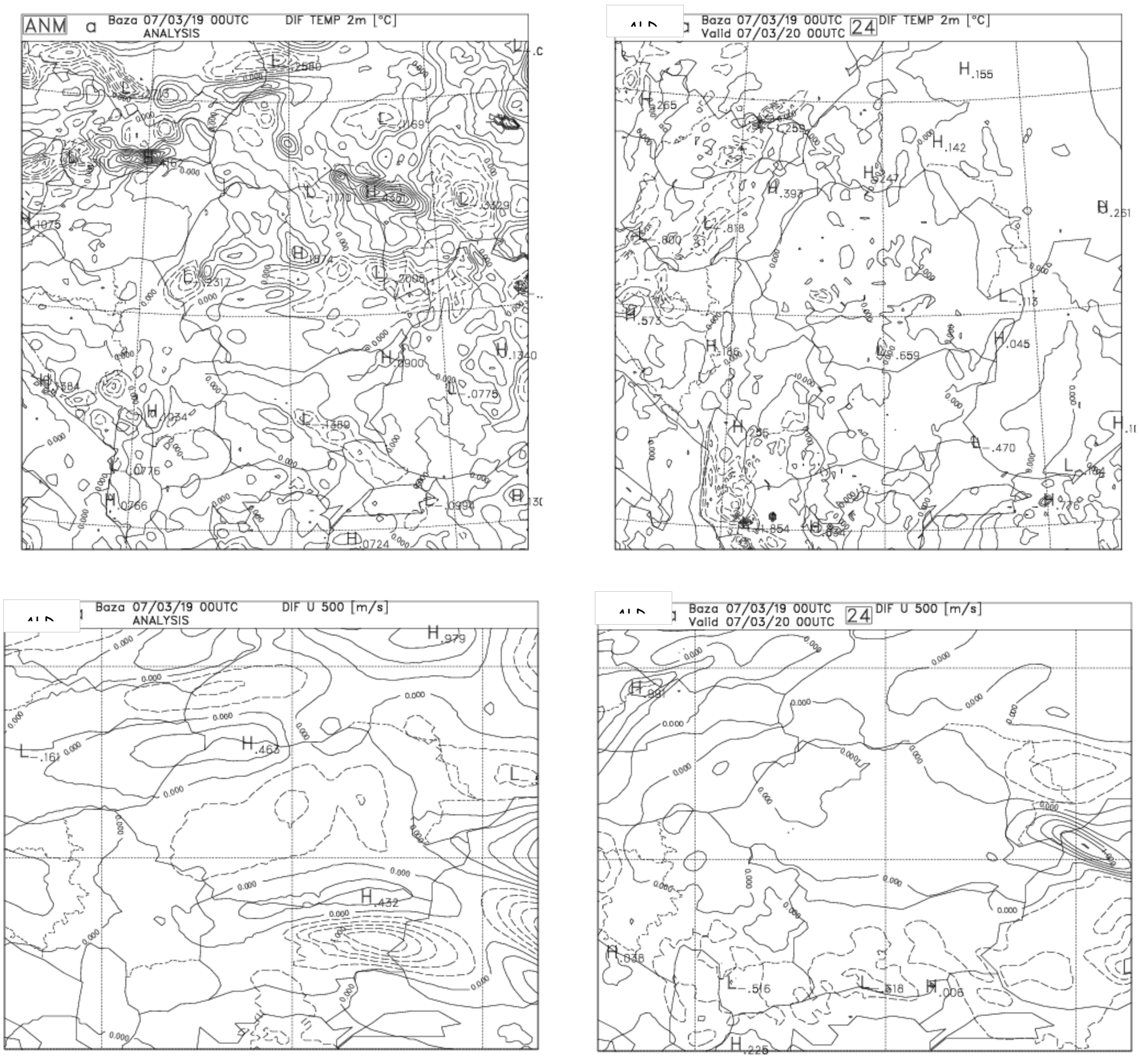


Fig.2 Differences in the 2m temperature field at initial time (top left panel) and 24h forecast (top right panel) and in the zonal wind component at 500 hPa level at the initial time (bottom left panel) and 24h forecast (bottom right panel).

- **Development of Aladin / hydrological model interface**

In order to couple the hydrological model with Aladin data, the Aladin output frequency has been changed to 1h (for the moment for the 06 UTC run only). Also, operational procedures for post-processing and GRIB coding of new parameters (for example short and long wave radiative fluxes) have been developed.

- **Implementation of cy32t1**

The last export version of the Aladin model was implemented and partially validated on different platform (SUN E4500, Linux Cluster, SGI). An ALARO e-suite is foreseen for this autumn.

## 2.17. SLOVAKIA

## 2.18. SLOVENIA

(more details neva.pristov@rzs-hm.si)

The main characteristics of the operational suite has remained unchanged. The novelty was the backup solution for downloading the coupling files from ecgate server at ECMWF. It has been used on one occasion so far. In the parallel suite, ALARO-0 without 3MT is running. The main improvements can be seen in precipitation pattern.

A very large domain was set up (512x512 points) which will serve as a benchmarking domain for AROME. As a consequence of some testing with this large domain, it was discovered that with a high number of processors, AROME takes an awful long time for reading of the initial surface file. ALADIN and AROME performance was tested on several clusters with the latest Intel processors. Performance of dual and quad core was compared. The results obtained with quad core show approx. 25% degradation when small number of cores is used, but getting to just few percent of degradation with a bigger number of cores.

Gmkpack and Intel 9.0 compiler were used for porting the export cycle cy32t1. ALADIN with ALARO configuration and AROME work smoothly with only a few modifications in the code, further validations is still ongoing. It was found that grib packing does not work with unoptimized code. c927 is running on one processor, but there are some problems on more processors which have still to be diagnosed. We have also started preparations of an environment for data assimilation with ODB. At the moment, BATOR seems to work, but there are still unresolved issues with MANDALAY and c701.

A gl tool was installed (developed by Ulf Andrae, SMHI) for the conversion of different file formats. This tool is most handy for the conversion of lfi files to grib format.

## 2.19. TUNISIA

## 2.20. HIRLAM

# 3. RSEARCH & DEVELOPMENTS

## 3.1. ALGERIA

## 3.2. AUSTRIA

## 3.3. BELGIUM

## 3.4. BULGARIA

## 3.5. CROATIA

The research on EPS, coupling of physics to dynamics, air-sea interaction, NH dynamics and SLHD in high resolution has continued.

## 3.6. CZECH REPUBLIC

*Radmila Brozkova*

One of the main effort was the porting and validation of the export cycle CY32T1. This cycle was validated with respect to the operational version based on the cycle CY29T2. Some bugs were still found in the CANARI surface and also in the physics. These fixes were put to a patch, which was distributed to other teams by the RC LACE WGL on physics, Neva Pristov.

Now the cycle is ready for a regular e-suite.

- **Data assimilation**

Here the work continues mainly in collaboration within RC LACE, namely with Hungarian Meteorological Service. Besides the CANARI surface data assimilation, there are preparations for a 3DVAR (Alena Trojakova). New background statistics were computed for the resolution of 43 levels and enhanced model physics. At the first stage a test of the assimilation of TEMP, SEVIRI and SYNOP data is envisaged.

As it regards the 4DVAR tools, a substantial effort was put to development of the TL/AD code of the semi-Lagrangian scheme in ALADIN (Filip Vana)

.

- **Dynamics**

Once more, the most important work is made here on behalf of RC LACE. There are several topics which were touched: coupling issues (Filip Vana and Jan Masek, visitor from Slovakia), interpolation operators to be used in SLHD (Jan Masek). Recently, a check for the non-hydrostatic dynamics interface to physics as it regards the governing equations of Catry et al. (2007) is performed (Petra Smolikova).

- **Physics**

Recent major development was happening in the physics, due to the prognostic enhancement of the schemes. In March, CHMI hosted the ALARO training course in Radostovice. Here also, RC LACE structure was essential for the organisation of the training course as well as for the following developments.

Concerning the moist physics, some weaknesses of the first microphysics version were corrected, namely in the computation of evaporation/melting and in the geometry of clouds. The problem of possible unification of cloudiness computation was addressed by Joao Rio (visitor from

Portugal). The effort continued on the debugging and validation of the 3MT scheme, helped by a short visit of Luc Gerard from Belgium. However the essential step forward was due to the upgrade of the DDH diagnostics toward new prognostic variables and associated fluxes. This important piece of work was accomplished by Tomislav Kovacic (visitor from Croatia). Work on 3MT is progressing well and accelerated thanks to new DDH. It will continue with a stay of Doina Banciu (Romania) in August. A possible refinement of the statistical sedimentation scheme is now being analysed by Martin Janousek.

Another piece of work, this time rather analytical, was made by Ivan Bastak (visitor from Slovakia) on the p-TKE concept and the CBR scheme. This study is also still continuing.

The so called new gravity wave drag scheme is still not completely compensating the enveloppe orography effect. A study of a possible improvement of the scheme is performed by Tomas Kral (c.f. his master thesis).

Development work important for the implementation of SURFEX is planned for the second half of a year.

- **Ensemble forecast**

CHMI has became a member of the GLAMEPS project. A study was done recently on the singular vector configuration (Richard Mladek, on a visit at HMS, Budapest).

- **New forecast products**

Thanks to the availability of new prognostic fields in the physics, it became possible to satisfy various user demands. It concerns environmental applications (chemical module camx), aviation meteorology applications (TKE based outputs), etc.

**References**


www.rclace.eu


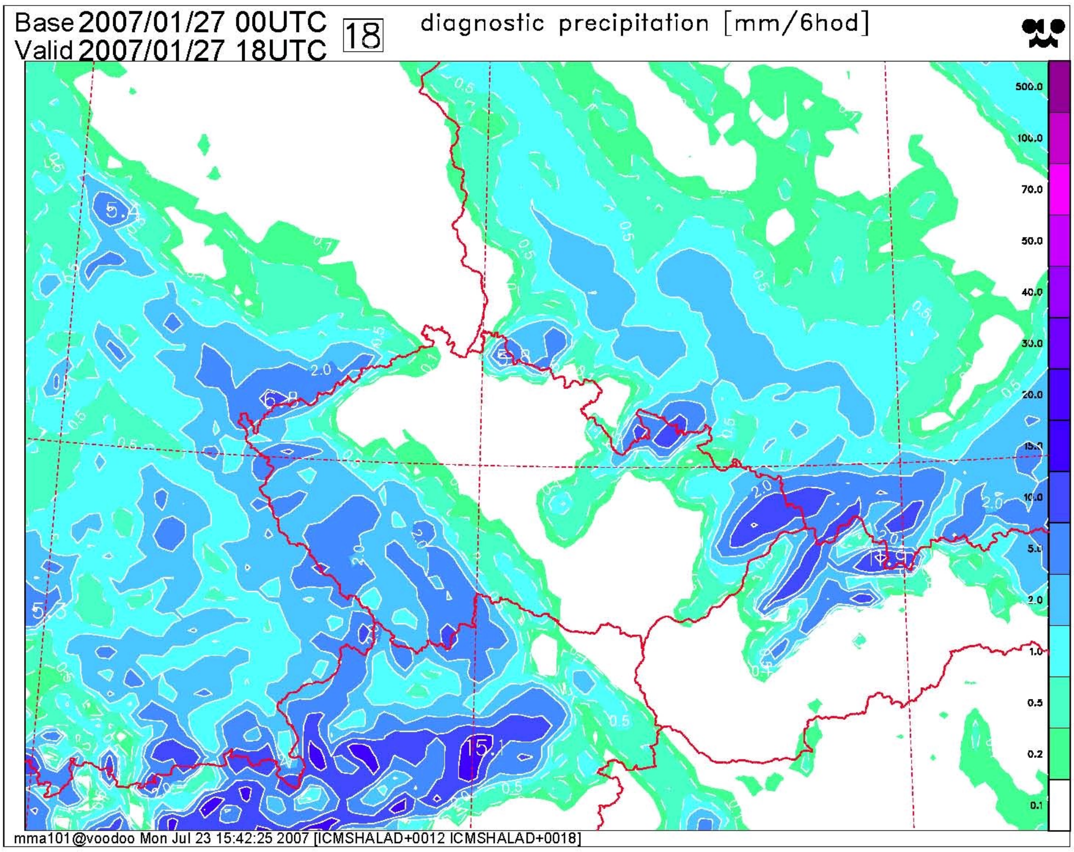


Fig 1a)

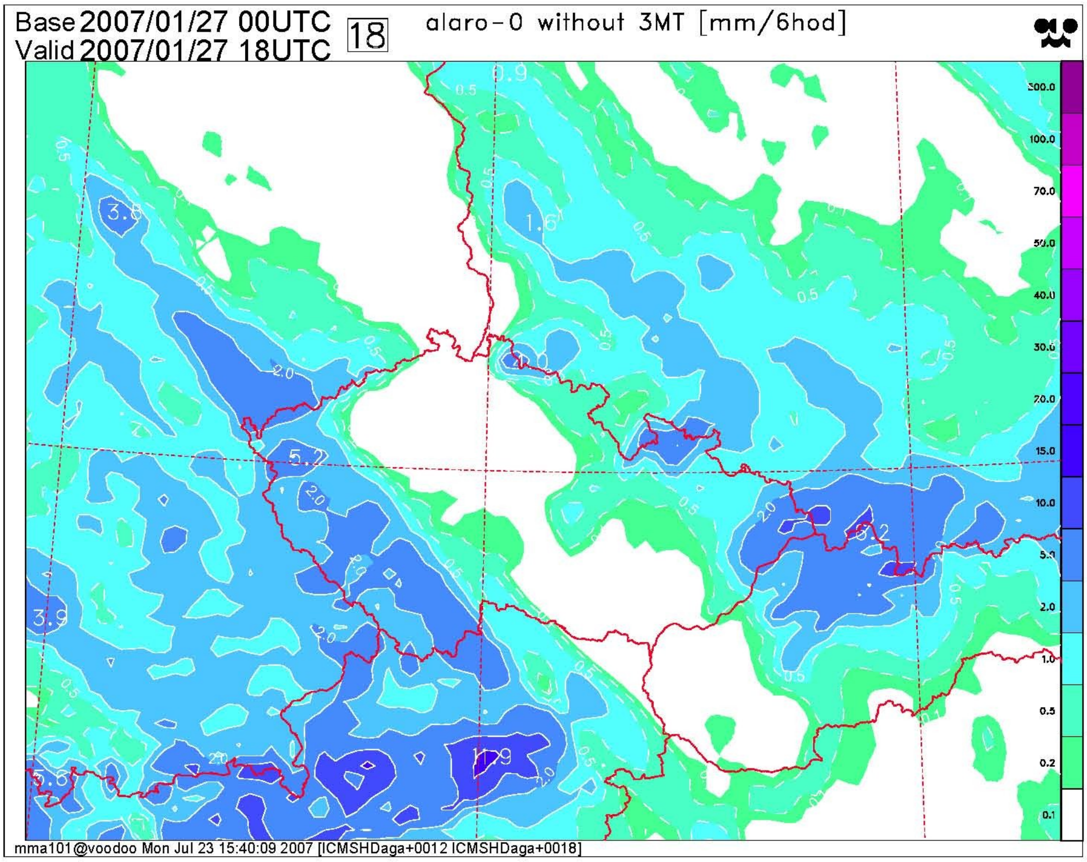


Fig.1b)

Fig.1: Example of the forecast of precipitation cumulated over 6 hours: a) using the 'old' diagnostic precipitation scheme; b) using new prognostic microphysics.

## 3.7. FRANCE

## 3.8. HUNGARY

(kullmann.l@met.hu)

The main scientific orientation of the Hungarian Meteorological Service for the ALADIN project is unchanged: data assimilation, short range ensemble prediction and high resolution meso-gamma scale modelling (AROME model).

The main scientific developments for the first half of 2007 can be summarized as follows:

### 3.8.1. DATA ASSIMILATION:

1. *Assimilation of SEVIRI data.* This work has been continued by Alena Trojáková from Czech Republic (RC LACE stay). The bias correction was recomputed for the SEVIRI data locally. The observation errors have been tuned. A preliminary report is available from Alena Trojáková.

2. *Parallel suite using MSG/GEOWIND (AMV) data.* The data were used with the settings found the best in earlier experiments (use over both sea and land with a quality indicator greater than 85%). The test has been running for a one-month period. The results are rather neutral, no significance found in the scores against observations. In spite of the small impact the data are used operationally since beginning of June.

3. *Improvement of the observation-processing.* Small technical improvements took place in the observation pre-processing at HMS (AMDAR data are now collected in netcdf format, OULAN is extended by a netcdf reader for AMDAR).

4. *Experiments with 3DVAR RUC.* 3h and 1h RUC have been implemented by a Slovenian visitor (Benedikt Strajnar, RC LACE stay). These were compared to the usual 6h cycling within a 15days period. The results of the 3h RUC have been studied in detail and it was concluded that the RUC can make some improvement compared to the 6h cycling. A preliminary report is available from Benedikt Strajnar.

5. *Use of ECMWF LBC data in the assimilation cycle.* ECMWF LBC data have been used in the 3DVAR assimilation cycling. Both a "laboratory" and an operational use have been studied concerning the availability of the LBC data. In the laboratory experiments LBC's from the ECMWF 00UTC run have also been used in the cycle (which are not available in real-time for the local 00UTC run), while in the operational experiments the LBC data from the previous day's 18UTC run have been used. A detailed article was sent to the current newsletter.

### 3.8.2. LAMEPS:

Work has continued with the ALADIN singular vectors. On the one hand the experiments concentrated on technical issues (e.g. CPU and memory usage were analyzed). In the laboratory phase of the GLAMEPS (Grand Limited Area Model Ensemble Prediction System) project everything will run at ECMWF (on the supercomputer HPCE) therefore all the necessary components running the singular vector configuration had to be installed and tested there.

On the other hand experiments were made to test the sensitivity with respect to the choice of optimization time (12 and 24 hours were tried) and also with respect to the resolution (22 and 44 km were tested) used during the singular vector computations.

The experiments are going to be further evaluated from the meteorological point of view. This work was realized during the one month stay of Richard Mladek. The report of his stay is available from Richard.

Experiments started with the downscaling of ECMWF EPS members. The script system used by the Austrian colleagues for LAEF was adapted and modified. Experiments were performed at ECMWF (on the supercomputer HPCE). For the integration of the ALADIN model the GLAMEPS domain was used with 22 km horizontal resolution. This work was realized during the stay of Joao Ferreira. A report will be available after the end of his stay.

#### 3.8.3. AROME:

We continued to study the sensitivity of AROME on coupling frequency and coupling zone size. We run AROME for a longer (10 days) period. The results were neutral regarding the coupling frequency but showed a little improvement when enlarging the coupling zone size.

We also studied the topic of initialization and coupling of prognostic hydrometeor fields. In our experiments we usually coupled AROME to our operational ALADIN forecast where the only prognostic hydrometeor is humidity, hence the initial and lateral boundary values of the other hydrometeor fields are zero. When AROME was coupled to another AROME model (running at 8km resolution as the operational ALADIN and using hydrostatic dynamic) we had non-zero hydrometeor fields at the boundaries and the forecast improved significantly. We also run case studies where we initialized the hydrometeor fields (except humidity) from an earlier AROME forecast instead of the coupling model. The preliminary results showed that forecast improves further in that case, especially at the beginning of integration.

### 3.9. MOROCCO

### 3.10. POLAND

### 3.11. PORTUGAL

## 3.12. ROMANIA

**Investigation of the PBL (Mihaela Caian, Constantin Rada)**

Aladin output has been processed in Stuwe diagram format. This is done daily for 2 chains: at 10 km and at 3 km resolution over an area centered on Bucharest (Figs. 1 and 2). The aim is to enable the study of surface exchange and boundary layer representation in the model. High resolution model output is used operationally as input for dispersion modeling over the city (Fig. 3).

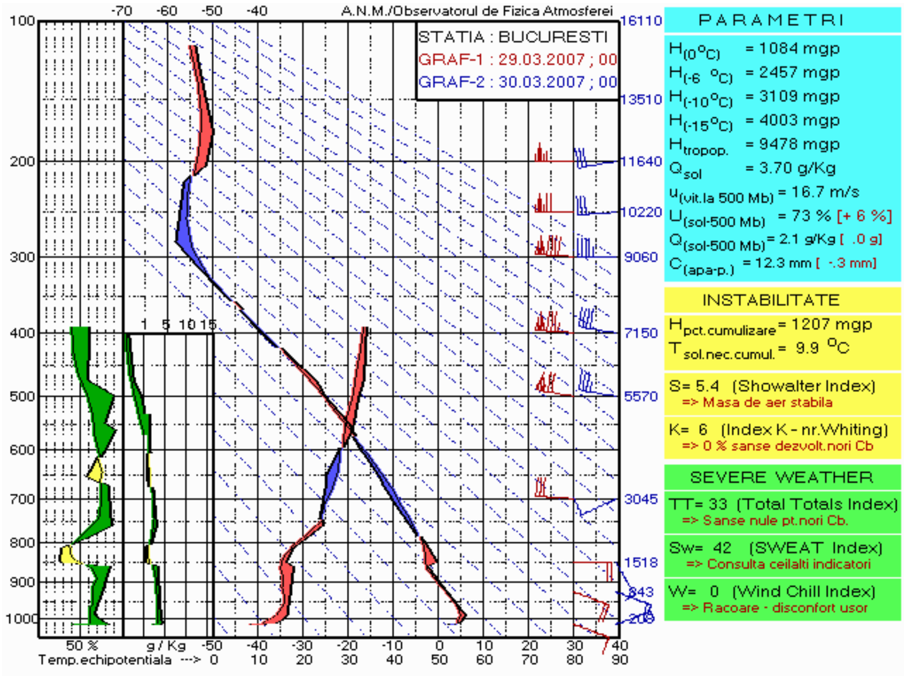


Fig 1. Stuwe diagram, Aladin 3.5 km (Read means a too cold model compared to obs Green means a too wet model compared to obs.)

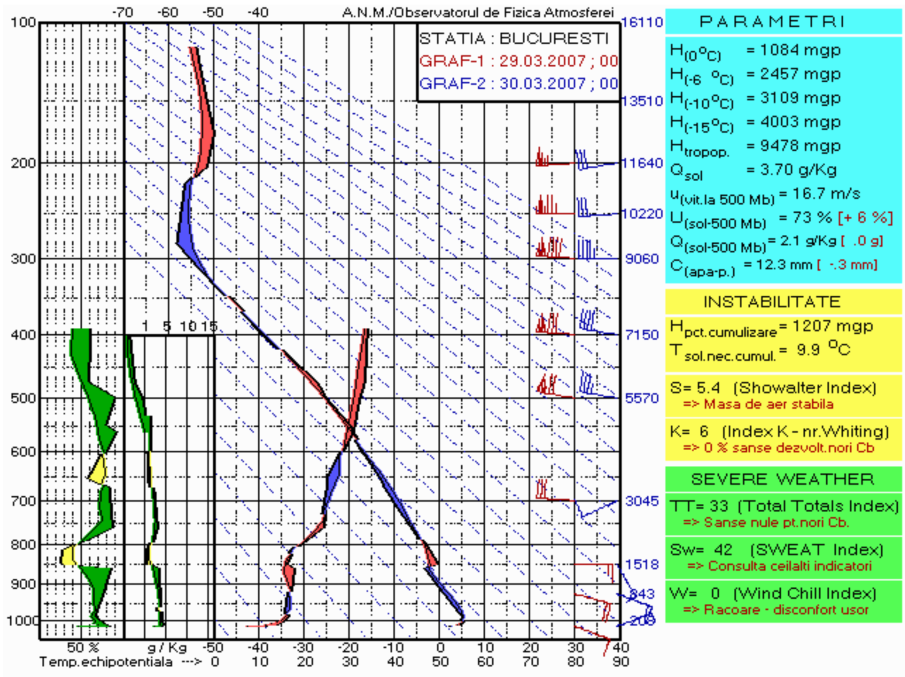


Fig.2 same as fig. 1 at 10 km

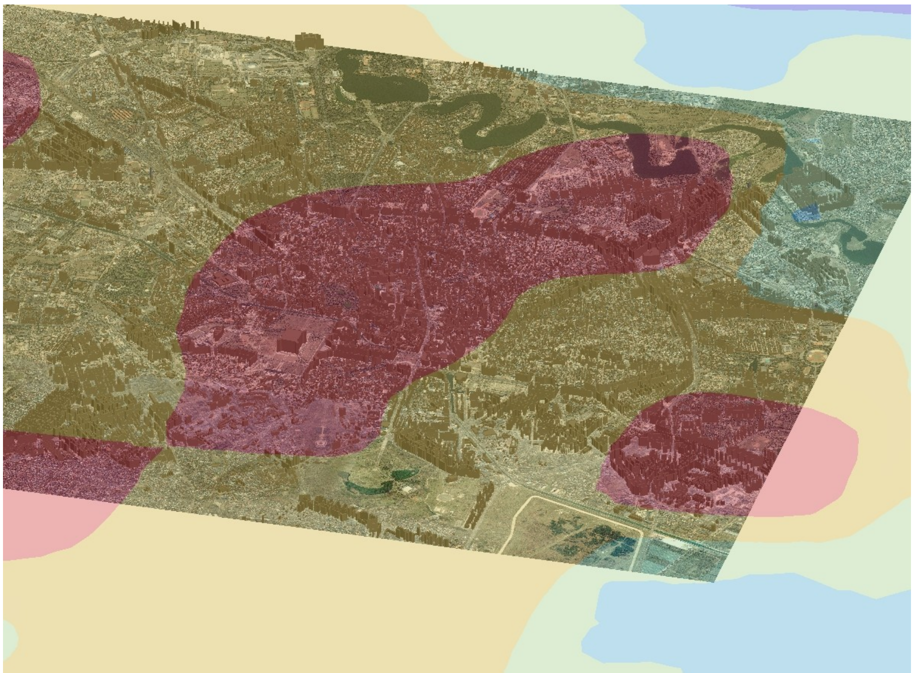

Fig. 3. Pollution dispersion over Bucharest using Aladin PBL forecast (red is high concentration value and green is "clean" air).

- **ALARO validation (Doina Banciu)**

A member of the Romanian Aladin team (Doina Banciu) attended the ALARO training course in Radostovice, Czech Republic (27-30 March, 2007) and contributed to code validation and documentation.

The ALARO validation within the cy32t1 is going on. An e-suite with ALARO is foreseen for this autumn.

### 3.13. SLOVAKIA

### 3.14. SLOVENIA

(more details neva.pristov@rzs-hm.si)

Our group was active in preparing the training course on ALARO-0 (March, Radostovice). We presented our experience with implementation of ALARO-0 and prepared documentation on autoconversion, collection, evaporation/melting processes inside microphysics.

To study how important is advection of turbulent kinetic energy (TKE) a few cases were run with AROME at 2.5 km with either TKE advection switched on or off. There were no significant difference found, except for some minor discrepancies in fields of precipitation and low level winds. The size of the domain was quite small (160x120 points), so the results depend too much on boundary conditions very likely.

In regions, where topographic forcing of the atmosphere is prevailing, such as in a complex terrain or along a complicated coastline, NWP model's resolution is important to solve the dynamic influences of the terrain. In case of precipitations, the low-level wind field and subsequent vertical motions really define the shape and the characteristics of the precipitation field. Recent experiments confirm a model's ability to correctly simulate temporal and spatial distribution of precipitation maxima in a convective situation. Moreover, accurately simulated peak intensities and peak durations (at the scale beginning at a few minutes) enable the planning of necessary emergency response for e.g. possible flash flooding. Additionally, this approach offers several possible skill scores for models with very high resolution and we are presently developing and evaluating them.

ALADIN verification project

Lovro Kalin (Croatia) spent 3 weeks in Ljubljana in June. During his stay a final content of a monthly verification report for one station with radiosoundings data was prepared. Graphs for vertical cross-sections (mean error, mean absolute error for available forecast ranges) for temperature, relative humidity, u and v wind component and geopotential height and graphs with scores for wind velocity at 250 hPa, geopotential height at 500h, relative humidity at 700 and 925 hPa, temperature at 850hPa are included into the report. Needed computation time is much shorter than for monthly reports for synop station where some optimization is still needed. Production of both types of reports will be put into operational production end of summer.

The server for ALADIN verification project has been upgraded with new disks and additional memory in June.

One of the products within verification project are also ALADIN multigrams. Products from models inside LACE countries are available in the local database soon after the model integration is finished. So we take this advantage and produce ALADIN multigrams for 7 capitals of LACE countries. The multigrams are available at www.rclace.eu each day.

### 3.15. TUNISIA

### 3.16. HIRLAM

# 4. PAPERS and ARTICLES

## 4.1. Comparison between SURFEX and ETA dust emission fluxes

Mokhtari (Algerian met office)

### 4.1.1. Introduction

The growing interest in the study of desert aerosols life cycle resulted from their many impacts on human life and on climate changes. Indeed, aerosols suspended in the atmosphere affect directly and indirectly the radiative balance. Through some studies, several numerical dust models have been developed and used for studying dust processes. [Westphal et al.,1987; Tegen and Fung, 1994; Nickovic and Dobricic,1996; Marticorena and Bergametti, 1995].

In this article, a short description of the Dust Entrainment And Deposition (DEAD) module of SURFEX model is given. This module is developed by Marticorena and Bergametti and coded by A. Grini. SURFEX, forced by the ALADIN/Algérie fields, is used in our study, to simulate the February, 20$^{th}$ and 21$^{st}$ 2007 meteorological situation which affected the major part of the Algerian Sahara. The dust emission fluxes of this simulation are analysed and compared with the ETA/Algérie model.

The main objective of this work is to check the sensibility of SURFEX to the dust fluxes injected into the atmosphere, under ALADIN forcing. Unfortunately, a thorough validation of such fluxes requires in situ measurements which are not available at the moment. The only existing products are: horizontal observed visibilities and satellite images. Since these two products reflect essentially the state of the atmosphere, their use to validate the dust emission fluxes is insufficient.

To palliate to the lack of in situ observations, the ETA dust fluxes are used as a reference after their confirmation by the two previous products, to validate the dust emission fluxes predicted by SURFEX.

### 4.1.2. SURFEX dust emission description

DEAD is a mineral dust emission module in SURFEX. It is used to compute the aerosols dust fluxes for particles less than 20 µm. The main characteristics of this module are that it is based on explicit physical theories and that it takes into account the influence of the surface states on the aerosols dust emission.

- **Physiographic fields**

For the surface processes, the driving SURFEX model uses: high resolution permanent fields of GTOPO30 for topography, ECOCLIMAP for vegetation, Covers and FAO fields for soil/texture types (sand and clay fractions [Fig.1]). Dust productive areas are distinguished from other areas by Cover004 and by Cover005, which represents respectively, bare and rock soils [Fig. 2].

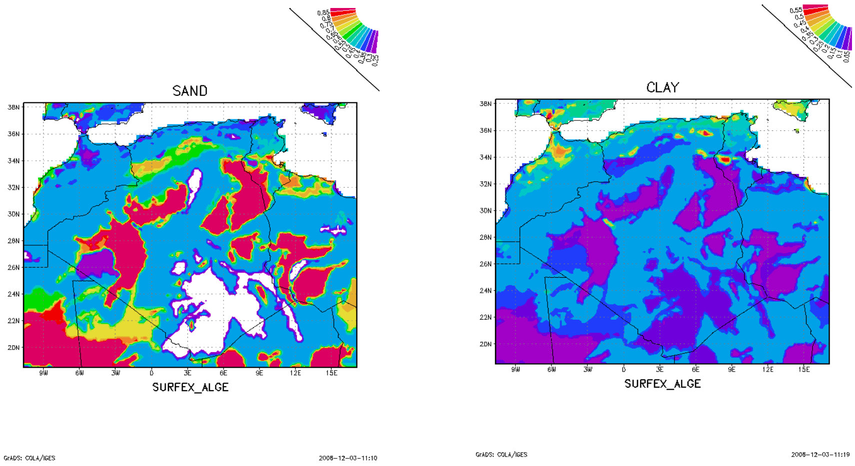


a) Sand fraction b) Clay fraction

Fig. 1: Sand and clay fraction

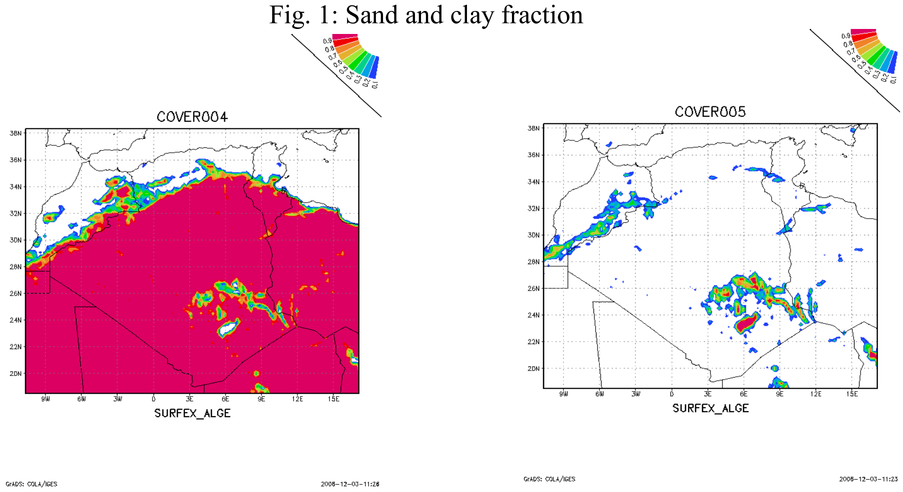


a) Bare soil fraction b) Rock soil fraction

Fig. 2: Dust production areas

### 4.1.3. Dust emission process

The movement of dust particles is mainly caused by saltation process [Alfaro, 1997], where the larger particles with diameters greater than 10 µm break soil cohesion forces and release finer particles into the atmosphere. For the wind erosion process, surface features of the atmosphere and soil, play a key role in regulating the amount of released dust. The quantity of mobilized dust depends on momentum transfer from the atmosphere to the soil. On the other hand, it is the soil state (structure, wetness, vegetation cover) which dictates how much dust will finally be injected into the atmosphere.

- **Parameterisation of the threshold friction velocity $U_*(D_p)$**

The emission of aerosols is a threshold phenomenon; it occurs only when the wind friction force exerted on the soil particles is greater than the one which maintain them on the ground. The erosion limit is named threshold friction velocity. It is parameterized in SURFEX using the formulation of Marticorena and Bergametti [1995], developed from an empirical relationship which depends only on the particle diameter. The threshold friction velocity $U_*(D_p)$ is written as follow:

$$U_{*td}(D_p)=\left[\frac{0.1666681\rho_p gD}{-1+1.928\mathrm{Re}_{*t}^{0.0922}}\left(1+\frac{6\times10^{-7}}{\rho_p gD^{2.5}}\right)\right]^{1/2}\rho^{-1/2} \qquad : 0.03\le \mathrm{Re}_{*t}\le 10 \tag{1}$$

$$U_{*td}(D_p)=\left[0.0144\,\rho_p gD\left(1-0.0858e^{-0.0617(\mathrm{Re}_{*t}-10)}\right)\left(1+\frac{6\times10^{-7}}{\rho_p gD^{2.5}}\right)\right]^{1/2}\rho^{-1/2} \qquad : \mathrm{Re}_{*t}>10 \tag{2}$$

Where: $Re_{*t} = U_{*t} .D/\upsilon\nu$ : Reynolds number ; $\upsilon\nu$: cinematic viscosity ; $D$ : particle diameter, $\rho_p$ and $\rho_a$ : respectively particle and air density

Three processes are able to modify $U_*$ and $U_{*t}$ : drag partitioning, the Owen effect and moisture inhibition. In this work, only drag partitioning and moisture inhibition will be treated.

- **Soil wetness**

Due to capillary forces on the soil grains, and to molecular adsorption, soil water increases the threshold friction velocity; therefore the amount of dust injected into the atmosphere is reduced. The soil moisture effect on the threshold velocity in SURFEX model is introduced following the method of Fecan and al. [1999]. The maximum amount of the absorbed water *w'* is an increasing function of the clay fraction in the soil. Using empirical data, Fecan and al. estimate *w'* as a second order polynomial function of clay fraction in the soil.

$$w' = 0.17\ (\%clay)\ +\ 0.14\ (\%\ clay)^2 \tag{3}$$

$$\text{for } w < w' : U_{*tw} = U_{*td} \tag{4}$$

$$\text{for } w > w' : U_{*tw} = U_{*td}[\ 1\ +\ 1.21\ (w - w')^{0.68}\ ]^{\ 0.5} \tag{5}$$

With *w:* soil wetness.

- **Aerodynamic roughness**

The effect of the internal boundary layer (IBL) relative to the presence of stones on the threshold friction velocity is parameterized in SURFEX by the formulation of Marticorena and Bergametti (1995). The distribution of energy is defined as the ratio of the IBL shear friction and the total surface boundary layer (SBL) shear friction. This ratio is given by:

$$f_{eff}(Z_0\ ,Z_{0s})\ =\ 1\ -\ [\ ln\ (Z_0\,/\,Z_{0s})\,/\ ln\ (\ 0.35\ \ (10\,/\,Z_{0s})^{0.8}\ \ )\ ] \tag{6}$$

$Z_0 = 33.3\ 10^{-6}\ m$ : Smooth roughness length

$Z_{0s} = 100.0\ 10^{-6}$ : Roughness length momentum for erodible surfaces

As a consequence, the threshold velocity is formulated as:

$$U_{*t}(D_p\,,Z_0,Z_{0s})\ =\ U_{*t}\ (D_p)\,/\,f_{eff}(Z_0,Z_{0s}) \tag{7}$$

- **Surface flux**

The horizontal flux of saltation (G) is calculated in SURFEX using the relation of White, 1979.

$$G=c.\frac{\rho}{g}U_*^3\left(1-\frac{U_{*t}}{U_*}\right)\left(1+\frac{U_{*t}^2}{U_*^2}\right) \qquad \text{with} \quad \boldsymbol{c\ =\ 2.61} \tag{8}$$

The sandblasting mass efficiency  represents the ratio between the vertical flux *F* and the horizontal flux *G*. SURFEX adopts the following relation proposed by Marticorena and Bergametti:

$$\alpha = \frac{F}{G} = 100\exp[\,(13.4\% clay - 6).\ln 10\,] \tag{9}$$

Where the mass fraction of clay particles in the parent soil is restricted to $M_{clay} < 20\%$

### 4.1.4. Numerical simulation

In order to be able to compare SURFEX and ETA/Algérie outputs, against observations, a typical situation of February, 20$^{th}$ and 21$^{st}$ , 2007, was simulated with the two previous models. The integrated domains were adapted for the two models, in order to take into account the area of interest, in both of them. The outputs of the two models are every three hours. For this simulation, the horizontal resolution is 0.2° for both models and the time-step is 300 seconds for SURFEX and 120 seconds for ETA model.

- **Overview of the meteorological situation**

The selected meteorological situation of February 20$^{th}$ and 21$^{st}$, 2007, is characterized by a low pressure centred on the south west of Algeria moving from west to east on a trajectory axed: TINDOUF-ADRAR-IN-SALAH- IN-AMENAS and reaching the Libyan and Tunisian borders, then the Mediterranean Sea on the 22$^{nd}$. The associated shallow depression at the surface (less than 1005 hPa), generated a cyclonic circulation with strong winds exceeding 100 km/h. In addition to these strong winds, these regions are very rich in erodible particles which favoured the desert aerosol emission. The reduced visibilities registered during these days showed the widespread and the intensity of the dust storms which occurred during this dust event.

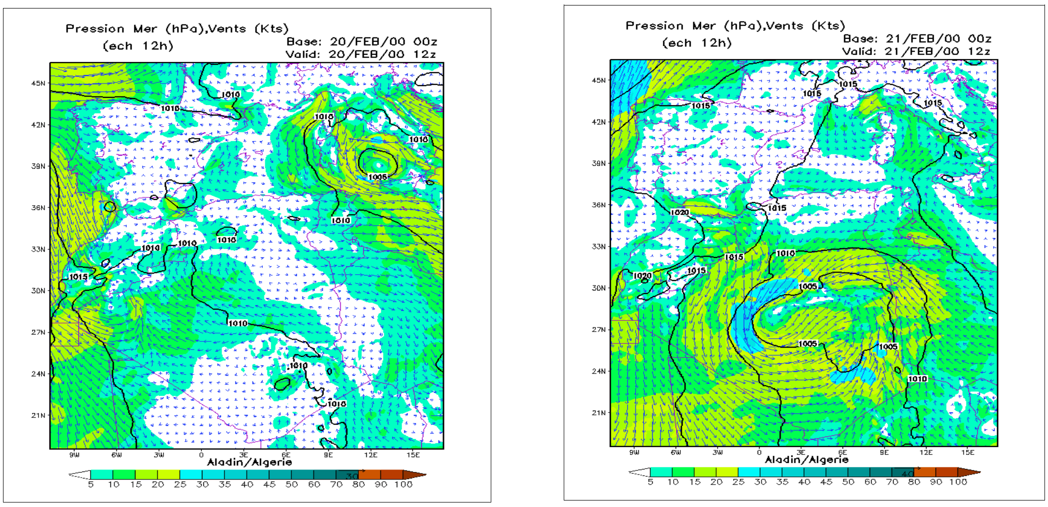


Fig. 3: Mean Sea Level Pressure and 10 m wind on 20 and 21 Feb 2007 at midday

The evolution of the dust plumes shows that the emitted dust formed big concentrated plumes on the 21$^{st}$ of February. The Moderate Resolution Imaging Spectroradiometer (MODIS) on NASA's Terra satellite took this image for that day. This image shows the concentrated dust cloud over the Algerian Sahara extending to the north.

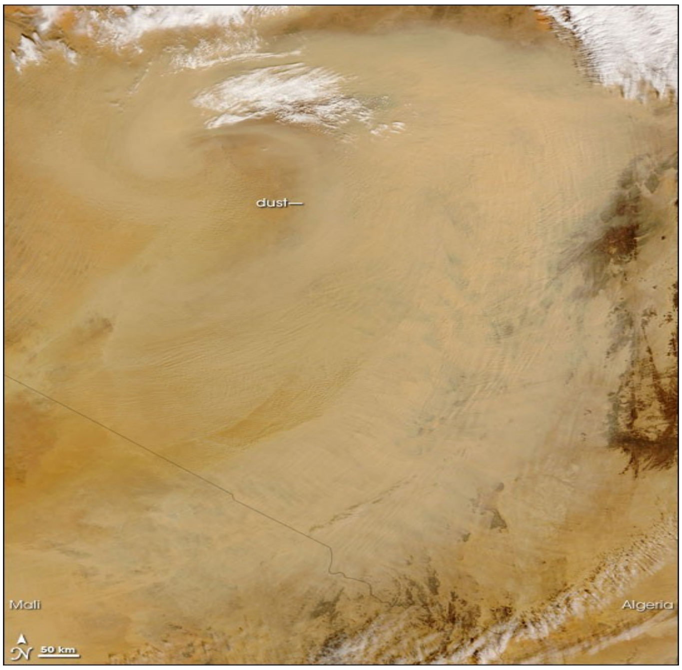


Fig. 4: Sea WIFS image showing SDS over the Algerian Sahara on 21 February 2007 at 12 z
SDS: Sand and Dust Storm

## ❑ Results and analysis

The Results which are obtained by the simulations using the two models (ETA and SURFEX), are presented in this section. First, in order to validate ETA outputs, the agreement of ETA/Algérie outputs with the observations (visibilities and satellite images), have been checked, then a comparison between ETA and SURFEX dust fluxes was done.

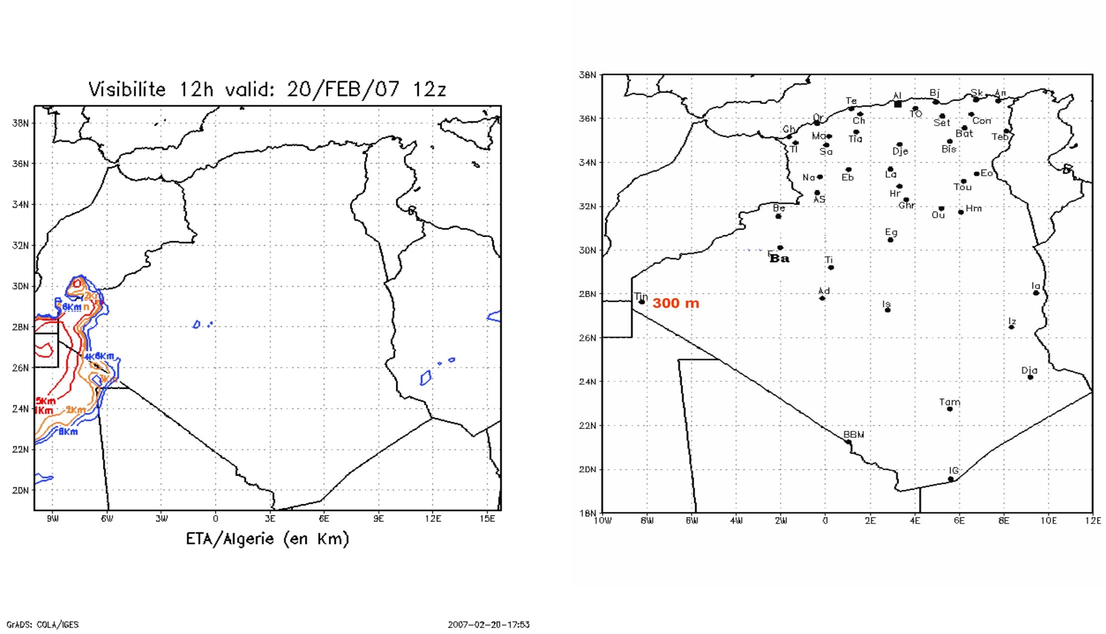


figure 5. a : Predicted and observed visibilities on 20 February 2007 at midday

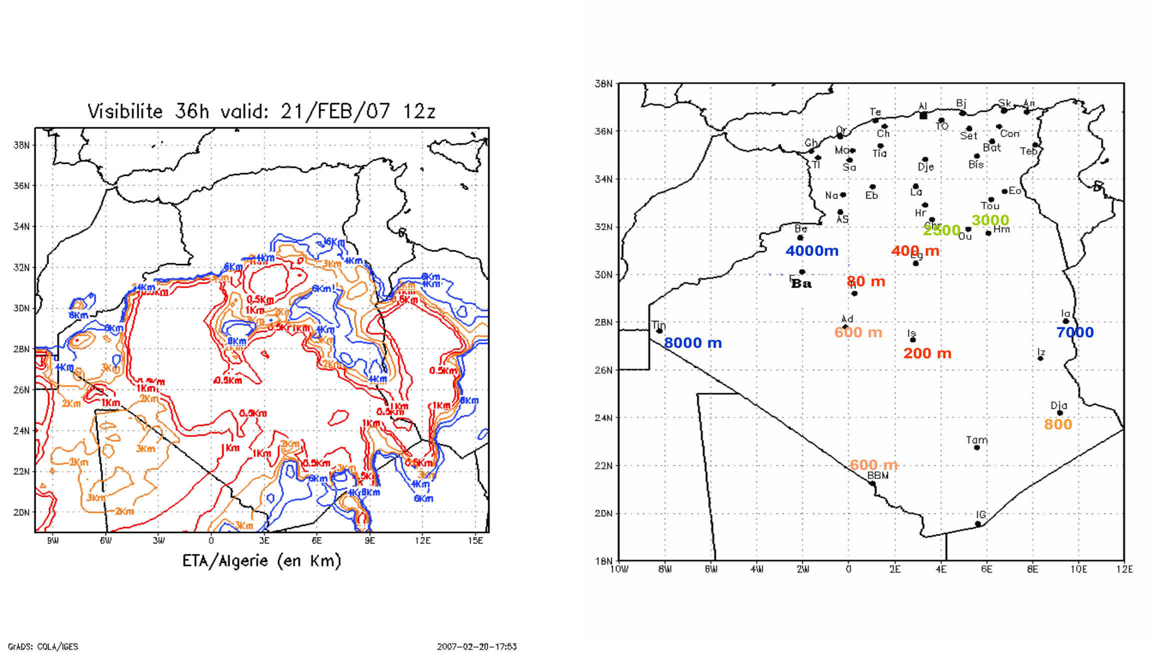


Fig. 5.b : Predicted and observed visibilities on 21 February 2007 at midday

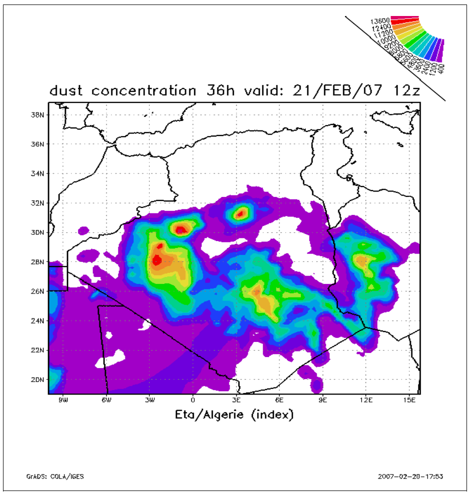


Fig. 6: Surface dust concentration forecast

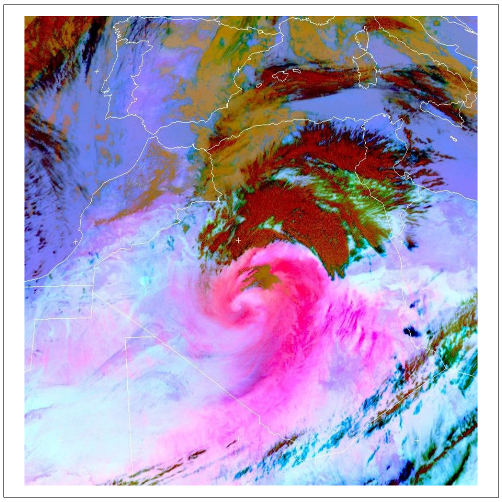

Fig. 7: Satellite image showing the dust plume extending from Algeria to Libya on 21 Feb 2007 at 12 z

Figure 5 (a and b) shows the agreement between the forecasted visibilities by ETA model and the observed ones on the 20$^{th}$ and the 21$^{st}$ of February 2007 at midday. It can be seen, despite the lack of stations, that the regions of low visibilities corresponds to that of dust storms. Figures 6 and 7 shows respectively the forecasted dust concentration by the ETA/Algérie model and the derivative dust from satellite image which indicates that the region of great dust concentration appears very coloured and in agreement with ETA model forecasts.

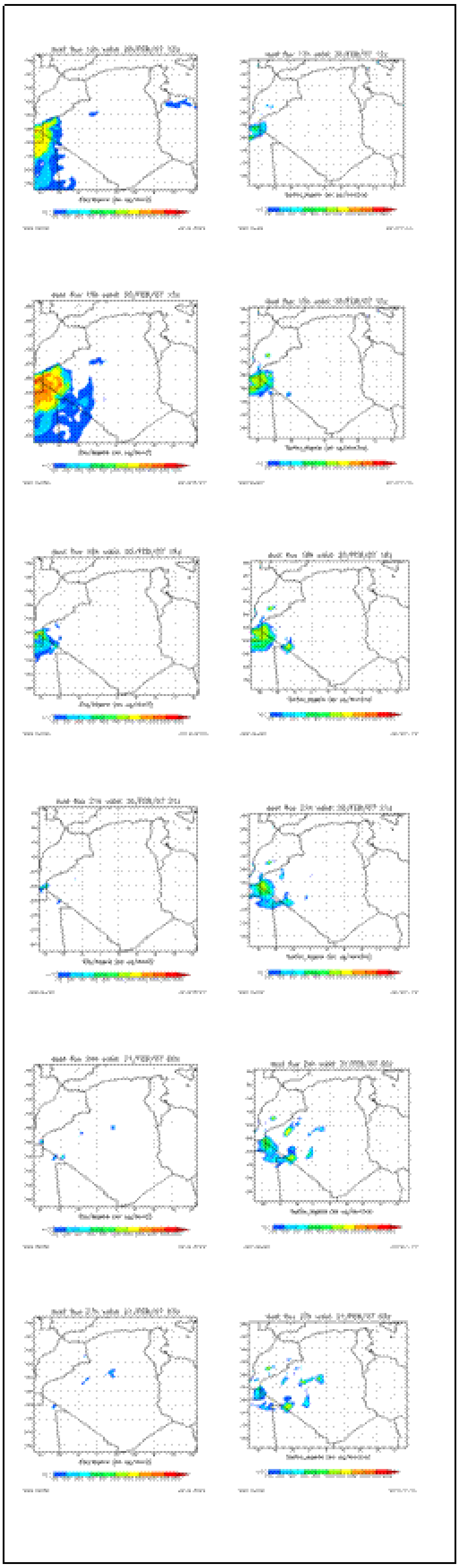

a) Dust fluxes : left ETA, right SURFEX

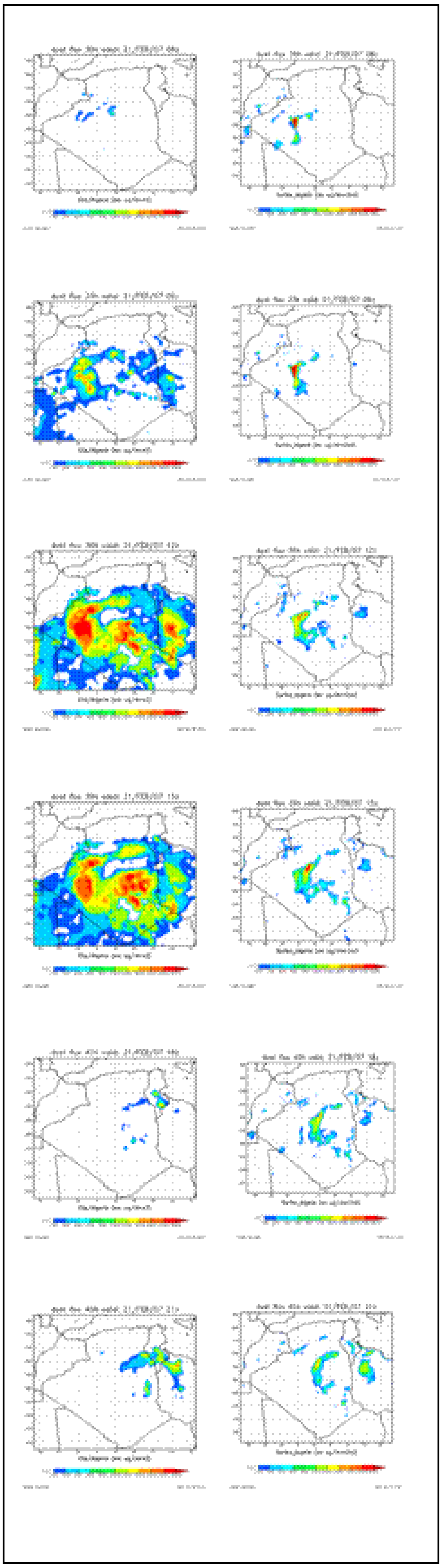

b) Dust fluxes : left ETA, right SURFEX

Fig. 8 : Dust flux predicted by ETA and SURFEX models

### 4.1.5. Discussion

As pointed out by some studies related to the subject, occurrence of sand and dust storms (SDS) and their associated dustfall is synthetically related to atmospheric movement and natural environment conditions. SDS is meteorologically defined as a wind-sand phenomenon that occurs when strong dry wind blows over a desert and adjacent areas, rising and carrying clouds of sand and dust. It is often so dense that the sun is obscured and the visibility is often reduced less than one kilometer.

In the framework of the present case study, the reduced visibilities of the 20th February 2007 at 12h and 15h was well forecasted by ETA model over the region of Tindouf (South-West of Algeria), following the strong dust fluxes, which corresponds to the injection of great amounts of dust in the atmosphere.

As ETA model, the SURFEX model well forecasted these sand risings over these areas but with less intensity and extension.

In addition, the reduced visibilities over the Center and the North East of the Algerian Sahara were well forecasted by ETA model. This can explain the strong emission forecasted by the model over these areas, but the visibilities were more over-estimated over the western and the southern parts of the Algerian Sahara. Compared to the observation (satellite image), the forecasted plumes by ETA model extended towards the east (Libya).

As ETA model, the strong risings were well forecasted by SURFEX over the central part of the Algerian Saharan but with less extension.

### 4.1.6. Conclusion

The analysis of the previous figures illustrating fields of the total sand concentration forecasted respectively by SURFEX and Eta model, leads to the following remarks:

The major problem encountered at the time of the modeling of the emissions of dust is the determination of the friction velocity threshold which is related much more to moisture and roughness of the grounds. The latter is very sensitive for the simulation of the emissions. Indeed, a friction velocity of 0.2 m/s corresponds to a wind speed of 7 m/s at 10m, or 25 km/h (case of the SURFEX model) and a friction velocity of 0.3 m/s corresponds to wind speed of 10 m/s at 10m or 36 km/h (case of the ETA model).

This difference in the friction velocity explains undoubtedly, the difference between the fluxes envisaged by the two models. The second encountered problem is in the determination of the ground moisture thresholds from which the effect of the ground moisture is taken into account. In the case of the ETA model, moisture threshold is determined by experimental data using spatial distribution of the ground texture. In the case of SURFEX, moisture threshold is determined from an empirical relation depending on the content of clay.

The results exposed in this presentation are encouraging, but it is difficult to make an unspecified assessment on SURFEX fluxes while being limited by the emission phase.

At least, it is good to make relevant that meteorological features of SDS at a particular location and across a broader geographical area are directly related to intensity and severity. Generally, strong and severe SDS greatly impact on local regions.

As such, the main objective of this work is to provide more detailed information and messages of dust warning to the general public and decision makers.

**Bibliography**

Charles S. Zender, Huisheng Bian, and David Newman, Mineral Dust Entrainement and deposition (DEAD) model: Description and 1990s dust climatology, J. Geophys. Res., VOL. 108, NO. D14, 4416, doi: 10.1029/2002JD002775, 2003.

Alf Grini, Pierre Tulet and Laurent Gomes, Dusty weather forecasts using the MesoNH mesoscale atmospheric model.

Pierre Tulet, Vincent Crassier, Fredric Cousin, Karsten Suhre, and Robert Rosset, ORILAM, a three-moment lognormal aerosol scheme for mesoscale atmospheric model: Online coupling into the Meso-NH-C model and validation on the Escompte campaign, J. Geophys. Res., VOL. 110, D18201, doi:10.1029/2004JD005716, 2005.

Slobodan Nickovic, Model for prediction of desert dust cycle in the atmosphere, U. of Athens, Depar. Of Applied Physics, Panepistimioupolis Bldg, phys-V, Athens 15784, Greece.

Benoit Laurent, Simulation des émissions d’aérosols désertiques à l’échelle continentale : Analyse climatologiques des émissions du nord-est de l’Asie et du nord de l’Afrique, Thèse de doctorat, LISA, 14.12.2005

## 4.2. Assimilation of Doppler radar radial velocities in ALADIN/AROME

C. Faccani and T. Montmerle (Météo-France, CNRM/GAME)

### 4.2.1. Summary

The FLYSAFE project aims to prevent air crashes in airports due to severe weather conditions. In the framework of this project, the assimilation of Doppler radar radial velocities is under study. The goal is to operationally assimilate these observations recorded by the French radar network ARAMIS, using the non-hydrostatic high resolution model AROME.

The main reason for assimilating Doppler radar radial velocities relies on the nature of the data themselves. Radars, which scan quite large volumes of atmosphere, provide information about the 3-dimensional precipitation pattern and wind circulation within precipitating systems. Moreover, since one complete scan is done in a quite short time, radars are able to provide data with a high temporal resolution. It allows for study of very localized small scale convective systems, which are often not forecasted or not well represented by Numerical Weather Prediction (NWP) models.

The 3DVar approach is used for the assimilation of these observations. Tests to validate the Doppler wind operator are ongoing using in parallel ALADIN and AROME, which share the same data assimilation system.

### 4.2.2. Radar data

- **The French network**

The Doppler wind source is the French radar network ARAMIS which includes 15 Doppler radars, that are mainly concentrated in the northern France (Fig.1).

Each radar performs a complete volume scan every 15 minutes at different elevation angles. Their number differs from radar to radar, from a minimum of 2 to a maximum of 11.

Raw data are available on-line, with a delay of one or two hours, in BUFR format. Each file contains values of reflectivity and radial wind (if data coming from a Doppler radar). A quality flag is also provided for each measurement in order to distinguish data of fixed echoes from those of clear sky, precipitation, or scattered by specific hydrometeors. The quality flag is used to remove unwanted echoes during the data pre-processing. The spatial resolution of radar measurements is of 1km, within a 250x250km$^2$ domain.

Nowadays, only data from 8 Doppler radars, mostly concentrated in the northern France, are recorded and archived in real time by Météo France in Toulouse, but the whole network will be operational at the beginning of 2008.

- **Doppler radar wind**

A radar is a source of electromagnetic pulses used to investigate the atmosphere. The loss of amplitude of the returning signal depends on the attenuation produced by the investigated atmosphere. Furthermore, the phase shift between emitted/received pulses is directly related to the speed of the moving target (Doppler effect). The analysis of the phase shift allows the mapping of the radial wind component for precipitating targets within the scanned area. If the elevation angle of scanning is changed, then it is possible to extract a 3-dimensional structure of the radial wind. For a more detailed description on the Doppler radar radial velocities retrieval see Tabary et al. (2005).

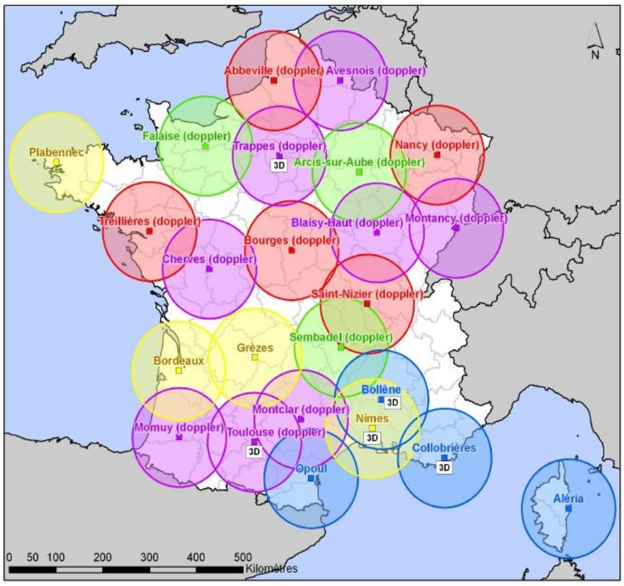


Fig.1. ARAMIS network at the end of 2007. Purple, red, and green circles are Doppler radars.

## ❑ Doppler radar wind errors

The error for Doppler wind mainly relies on three factors:

- the distance *d* of the target to the radar, because of the beam broadening with the distance,
- the signal-to-noise ratio ($S_n$), which depends on the reflectivity Z and on the distance *d*, accordingly to the formula:

$$S_n(dB) = Z + 20\cdot\log_{10}\left(\frac{100}{d}\right) \quad ,$$

- the spectral width related to each measurement, which depends on the atmospheric turbulence (an atmosphere with no turbulence has a spectral width equal to zero).

However, an additional source of error linked to the dealiasing process has to be taken into account. For a radar with a single PRT (pulse repetition time), the maximum speed recorded without ambiguity is equal to $V_N = \lambda/4\mathrm{PRT}$ , where $\lambda$ is the wavelength, a fixed parameter for each radar. All velocities larger than $V_N$ , called Nyquist velocity, are aliased of $2nV_N$ . For technical reasons, it is not possible to increase the PRT too much to get a larger $V_N$ . Therefore, the multi PRT approach is used instead.

For the French radar network, the maximum radial velocity (extended Nyquist velocity) measured without uncertainty is $\pm 60.0\,\mathrm{m}/s$ . This value is the result of a dealiasing process based on a triple-PRT scheme (Tabary et al. 2006). Three different Doppler velocities $V_1$, $V_2$, and $V_3$ correspond to three different PRT. The corresponding dealiased velocity $V_{123}$ is obtained as $V_1+2kV_{N1}$, where $V_{N1}$ is the Nyquist velocity corresponding to $PRT_1$ and k is a constant depending on $V_{N2}$ and $V_{N3}$. The error of $V_{123}$ is bigger for multiple of $2kV_{N1}$. In regions of strong turbulence, these errors are bigger than for a single PRT case. In practice, these errors may be reduced using a median filter (Tabary et al. 2006) .

## ❑ Data pre-processing

The wind data are stored as raw data, therefore, a pre-processing procedure is required to filter out the noise and the unrealistic echoes before wind measurements enter the assimilation system. The pre-processing procedure is based on the application of two different filters called respectively median and 'cleaner'. The former filters out the noise and most of the unrealistic echoes, and it also reduces the error which depends on the dealiasing process (See section 2.3). It is based on a simple replacement of data. Each grid point *i* is the centre of a 5x5 squared box. All the observations inside this box are ordered by size. The value of *i* is changed by the one in the middle of the ordered set. For a detailed description of the median filter, see Tabary et al. (2005).

Cleaner filter is based on the same principle of ordered values, and thus it removes the unrealistic echoes left after the application of the median filter. It can happen especially in areas of high turbulent flow. The complete 'cleaning' of the data is realized comparing each observation *i* with the mean values of a subset of ordered (1) data and (2) differences between *i* and the observations around it. An example of filters action is provided in figure 2. This is a case of data artificially contaminated by the action of a windmill for electric power production, working nearby the radar. Raw data from the Blaisy radar (Fig.2 left) show a circular area of noise of 20km radius, centred at the radar station (black triangle), and some additional noise on the eastern edge.

The application of the median filter (Fig.2 middle) smooths the data removing most of the noise. However, unrealistic echoes are still present in two areas, A1 and A2. The successive application of the 'cleaner' filter to this set of data completely removes the unrealistic echoes (Fig.2 right).

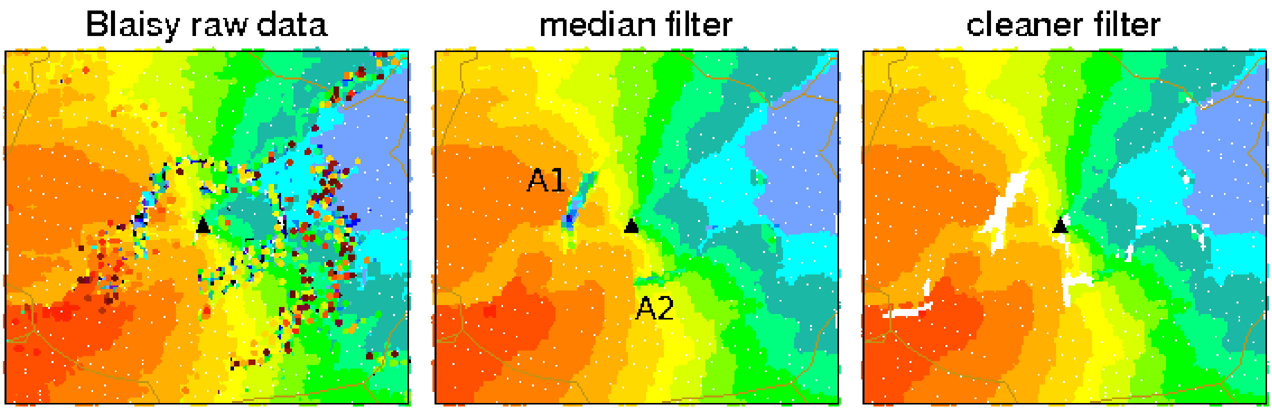


Fig.2. Action of median+'cleaner' filtering on raw Doppler wind data from the radar of Blaisy (black triangle) contaminated by windmill for electric power production.

The 'cleaner' filter is also used for elevation check before the application of the median filter, by detecting elevation at which data are potentially affected by Automatic Frequency Control problem. An example of this problem is shown in Figure 3. Measurements affected by AFC (Fig.3 left) show, at a given elevation, a distribution of mixed random echoes that can not be removed by the median filter (Fig.3, middle); the resulting wind map is still unrealistic. The application of the 'cleaner' filter to raw data (Fig.3, right) removes of more than 92% of the original measurements. The loss of such a large amount of observations is a sign of bad quality data, which have to be rejected. Since the same level of rejected data has been found for other cases affected by AFC, the cut off threshold selected in the code for rejection is of 85% for each elevation.

The last filtering of data during the pre-processing is done using the quality flag included in each file for every observation. For Doppler radial wind, only fixed echoes are filtered out. Clear air data are kept for the moment. These data, due to several non-meteorological targets such as insects or dust, are potentially very interesting for data assimilation, since they give information about the air circulation near the radar when there is no precipitation.

After this data selection, radar observations are stored as vertical profiles of radial wind, the vertical profile being produced by stacking measurements at the same location, but at a different elevation.

Finally, since the resolution of Doppler wind data is higher than the one of the model, and in order to save CPU, one vertical profile out of five is retained.

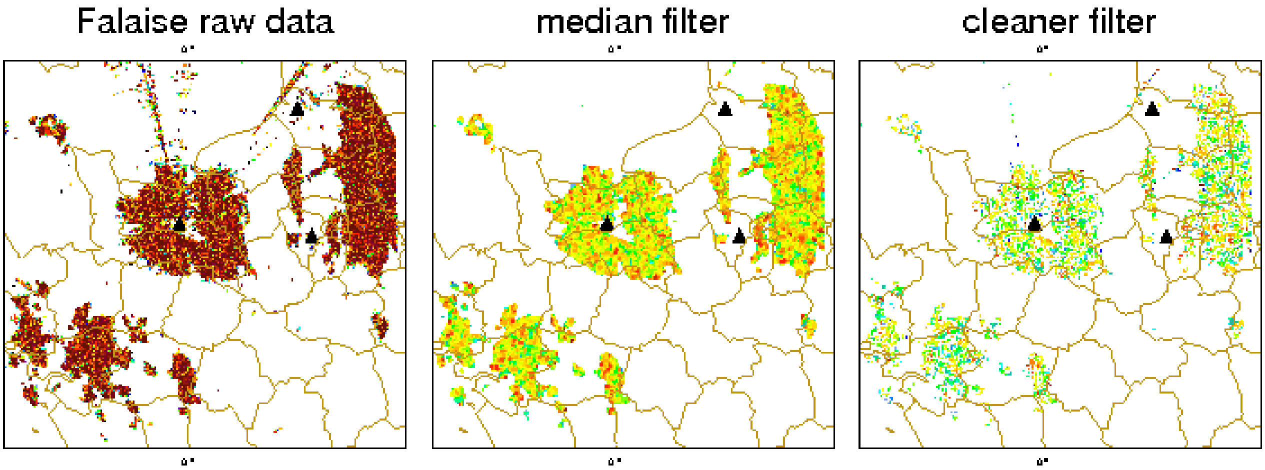


Fig.3. Example of the Automatic Frequency Control problem for radar of Falaise: raw data at 0.4° of elevation (left) after the application of either the median filter (middle) or the cleaner one (right).

### 4.2.3. Doppler radar wind operator

The assimilation of Doppler radar radial velocities is performed using the ALADIN 3DVar (Fischer et al., 2005), which is also used for data assimilation in AROME. An ad hoc observation operator (and the related Tangent Linear and Adjoint) based on Salonen et al. (2003) and Caumont et al. (2006) has been coded (Montmerle et al., 2006). This operator first computes the model's horizontal wind $V_h$ at each observation point (x,y), following the equation

$$V_h(x,y)=u\sin(\varphi)+v\sin(\varphi) \qquad (1)$$

where u and v are the model's horizontal wind components. $\varphi$ is the radar azimuth angle as shown in Fig.4. The radial component of $V_h$ (along the radar beam) is evaluated as

$$V_r=V_h\cos(\theta+\alpha) \qquad (2)$$

where $\theta$ (Fig.2) is the radar beam's elevation. This formula neglects the contribution of the vertical velocities due to falling hydrometeors. This approximation is valid only for low elevation angles, which is the case for the radars of French network (Caumont et al., 2006). The angle $\alpha$ is defined as

$$\alpha=\arctan\left(\frac{d\cos\theta}{d\sin\theta+a_e+h}\right) \qquad (3)$$

where *d* is the distance radar-target, *h* the antenna height and $a_e$ the effective radius of the earth ( $a_e=4a/3$ , where $a$ is the earth's radius), used here in order to consider the radar beam straight. It is not the case for an actual electromagnetic beam travelling through the atmosphere. The non-uniform change of the refraction index produces a bending of the beam according to the Snell's law. At radio frequencies (those used for radars), the refraction mainly depends on temperature, on water vapour partial pressure, and on total pressure. With an effective earth's radius equal to $4a/3$, the vertical gradient of the refraction index can be considered constant and equal to $-1/4a_e$ (Doviak and Zrnic, 1993). In this atmosphere, the ray path is supposed to be straight.

The broadening of the radar beam is taken into account in the operator, but only the main lobe is considered, while the secondary ones are neglected. The main lobe is represented by a Gaussian function (Probert-Jones, 1962) and the velocities are vertically averaged within the beam borders.

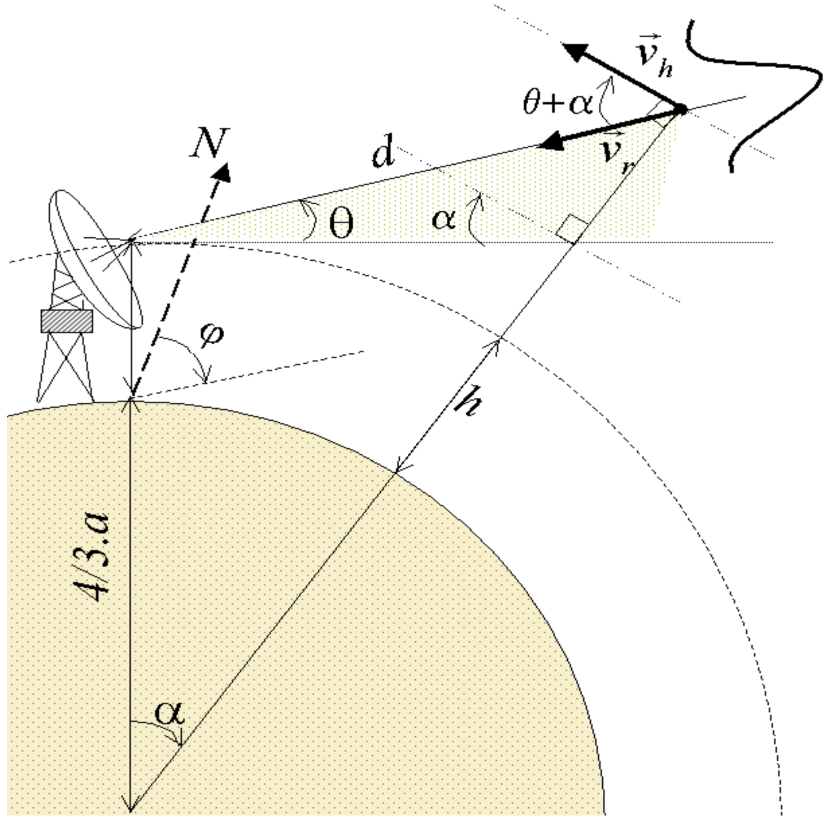


Fig.4. radar geometry. $\varphi$ Is the azimuth angle, $\theta$ the elevation of the beam, $\alpha$ the angle between the effective earth's radius $a_e$ and the target point. $h$ and $z$ are the antenna and target height respectively. $d$ is the distance between radar and target.

### 4.2.4. Screening procedure

The screening procedure for Doppler wind data is done in two steps:

1. a quality check;
2. observations thinning.

The quality check is applied to each measurement and it selects only those observations for which the departure from the background is inferior to $\pm 6\,m/s$.

The data are then thinned to avoid correlation errors among adjacent pixels. Only one profile inside boxes of $30x30km^2$ for ALADIN and of $10x10km^2$ for AROME is retained. The criterion of selection is based on the observation error of each profile and on the number of valid observations (remaining after the quality check) within each profile.

In order to take into account the beam broadening, the observation error used for radial wind depends on the horizontal distance $D$ (in km) of each wind profile from the radar,

$$\sigma(D) = \frac{1}{50} D + 1$$

Using this formula, the error is increased by 1m/s each 50km.

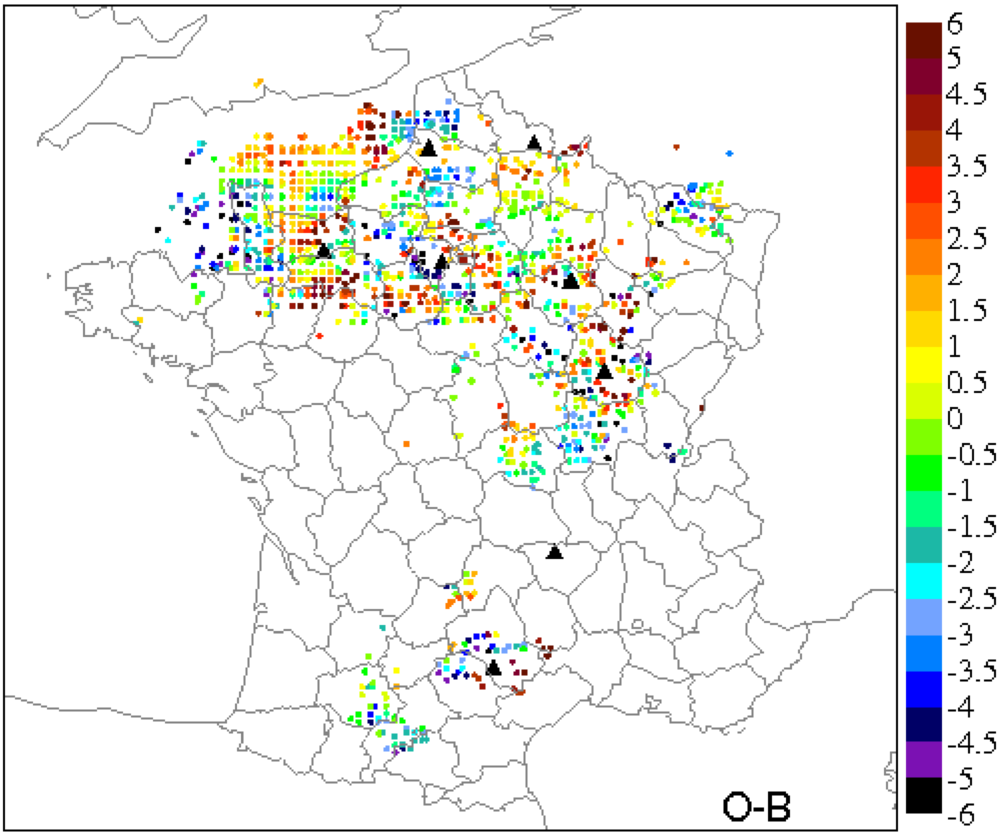


Fig.5. Example of innovations (O-B) distribution for Doppler radial velocities passing the screening procedure for a case study at 0600UTC on 13 May 2007. Only the first elevation is shown and the wind speed is in m/s. Black triangles are radar stations.

Figure 5 shows an example of active wind data resulting from the screening, for a case study at 0600UTC on 13 May 2007. The distribution of the corresponding innovations (at first elevations only) is presented. Since most of the active Doppler radar are located in northern France, the observations density is higher there. The high concentration of overlapping observations (before data screening) allows the reduction of areas where the wind field is unknown. As Figure 5 shows, this produces a sort of nearly uniform wind field distribution.

The radar at the bottom edge of the domain (Montclar, Fig.1) presents an example of clear air radial velocities, since the corresponding echoes of reflectivity (not shown) clearly indicate that no precipitation at all occurs in the south of France.

An example of Doppler wind data impact in the analysis field is provided in figure 6. Differences from a reference case, which does not include radar data, are shown for the horizontal wind field. Two different levels are considered: 850 and 500hPa. Both show increments well localized around the radar stations (triangles), larger at the radar location and at lower levels (850hPa). This result is in agreement with the observation error function (which increases with distance) and the decreasing number of observations with the increase of elevations.

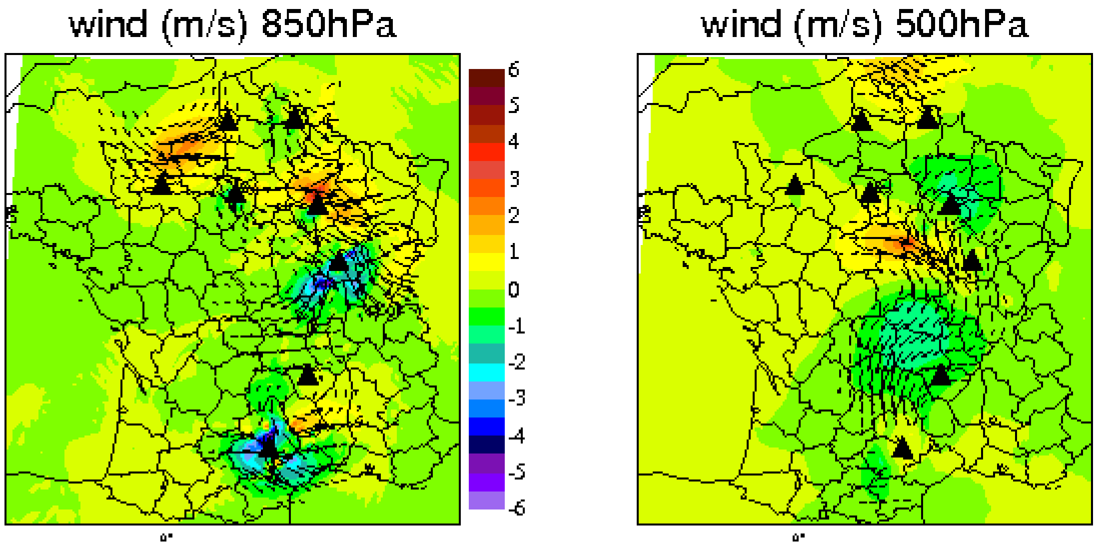


Fig. 6. Wind field differences at 850hPa (left) and 500hPa (right) for analysis produced without (reference experiment) and with assimilation of Doppler radial velocities at 1800UTC on 12 May 2007. Wind speed is in colour. Arrows unit is 5m/s.

### 4.2.5. Conclusions and Perspectives

Assimilation of Doppler radial velocities in ALADIN and AROME models, using 3Dvar, is being tested at Météo France. An ad hoc observation operator and its corresponding TL and AD have been coded. Raw data of Doppler radial velocities are currently provided by 8 Doppler radars of the French ARAMIS network. The selection of these raw measurements for data assimilation is performed using a pre-processing procedure and data screening, which filter out the noise and the fixed echoes, and reduce the data density. The tuning of observation error and the thinning procedure are still going on.

In order to assess the impact of Doppler wind data on weather forecast, experiments are performed for several case studies of heavy precipitation using both ALADIN and AROME. Experiments in a pre-operational mode will hopefully start at the end of 2007, when additional data from further operational Doppler radars will be available. The ARAMIS network will be fully operational, with 15 Doppler radars at the beginning of 2008. A proposal to increase the number of these elevations up to about 10 for each radar, when precipitation occurs, is under evaluation.

**References**

Caumont O, V. Ducrocq, G. Delrieu, M. Gosset, J.-P. Pinty, J. Parent du Châtelet, H. Andrieu, Y. Lemaître, and G. Scialom, 2006, A radar Simulator for High-Resolution Non-hydrostatic Models, *Journal of Atmospheric and Oceanic Technology,* Vol. 23, 1049–1067.

Doviak, R.J. And D.S. Zrnic, 1993: *Doppler radar and weather observation*. 2nd Ed. Academic Press. pp 562.

Fischer C., T. Montmerle, L. Berre, L. Auger, S. Ştefănescu, 2005, An overview of the variational assimilation in the ALADIN/France numerical weather-prediction system, *Quart. J. Roy. Meteor. Soc.*, Vol. 131, 3477-3492.

Montmerle T., O. Caumont, E. Wattrelot, and V. Ducrocq, 2006, Towards the operational assimilation of Doppler Wind at regional scale in Météo-France. *Proc. ERAD 2006,* Barcelona, 511.

Probert-Jones J.R., 1962: The radar equation in meteorology. *Quart. J. Roy. Meteor. Soc.*, Vol. 88, 485-495.

Salonen, K., H. Järvinen, and M. Lindskog, 2003: Model for Doppler radar radial winds. *Proc. 31st Conf. On radar Met.*, Seatlle, AMS, 142-145.

Tabary P., L. Perier, J. Gagneux, and J. Parent-Du-Chatelet, 2005, Test of a staggered PRT scheme for the French radar network. J.O.A.T., Vol. 22, 352-364

Tabary P., F. Guibert, L. Perier, and J. Parent-Du-Chatelet, 2006, An operational triple-PRT Doppler scheme for the French radar network. J.O.A.T., Vol. 23, 1645-1656

## 4.3. Using T799 IFS initial and boundary conditions in the ALADIN/HU model

Sándor Kertész, Hungarian Meteorological Service

### 4.3.1. Introduction

The work presented in this document was carried out in the framework of the ECMWF Special Project "Investigation of coupling the ALADIN and AROME models to boundary conditions from ECMWF and ERA model data". In this study the use of the T799 IFS forecasts as initial and boundary conditions to the ALADIN/HU model was investigated. This work was the direct continuation of a study that used T511 IFS forecasts to drive ALADIN/HU with dynamical adaptation (*Bölöni*, 2005). In this study not only higher model resolutions (both in IFS and ALADIN) were tested but in addition to dynamical adaptation the 3D-VAR data assimilation technique was also applied.

### 4.3.2. Description of the experiments

The experiments were carried out for the period of 8-21 August, 2006 with the ALADIN CY28T3 model version using 8 km horizontal resolution with 49 levels (up to 5 hPa). The integration domain is shown in Figure 1. In each experiment two 48 hour model integrations were performed at 00 and 12 UTC. The 3D-VAR experiments started 4 days earlier (on 4 August) but the first 4 days were regarded as a warm-up period and no forecasts were performed for them. In the 3D-VAR a 6 hour assimilation cycle was used with SYNOP (only Z), AIREP, AMV, TEMP and Wind profiler observations and satellite radiances (NOAA AMSU-A and AMSU-B sensors). All the IFS initial and boundary conditions were prepared on the HPCE system of ECMWF using the scripts developed for the Special Project (*Kertész*, 2006).

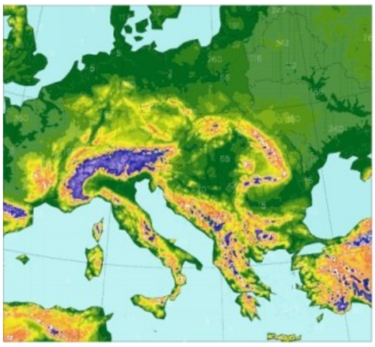

Figure 1: The integration domain and orography of the ALADIN/HU model

### 4.3.3. Handling of the surface fields

One of the problems of the BC generation process stems from the fact that IFS and ARPEGE/ ALADIN use different surface schemes. It means that not all the required surface fields for ARPEGE/ALADIN are directly available in the IFS analyses/forecasts. Although this problem is handled by configuration 901 (it converts IFS GRIBs into ARPEGE FA files) by deriving all the required fields, it is well known that the present solution in 901 is not satisfactory. Instead it was suggested that for the IFS-driven ALADIN runs all the surface fields in the initial condition file should be replaced with the surface fields of the corresponding ARPEGE analysis. This replacement has to be done only for the initial conditions since surface fields are not coupled from the boundary conditions files during the ALADIN integration. The effect of this change can be clearly seen in Figure 2 showing that the surface field replacement provides better results for surface parameters.

As a consequence, this solution was applied in all the experiments presented in this paper.

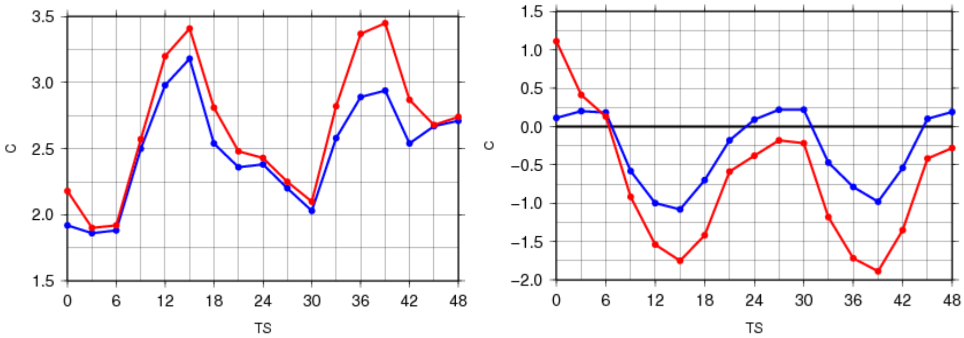


Figure 2: RMSE (on the left) and bias (on the right) scores for T2m for one 48 h ALADIN/HU integration using T799 IFS BCs. The red curve represents the default surface handing solution while the blue curve the modified one. The verification was performed against SYNOP observations.

### 4.3.4. Using the 00 and 12 UTC IFS runs as BC

In the first set of experiments dynamical adaptation driven by ARPEGE and IFS was tested. Two experiments were carried out:

- **ARPE_dyna**: initial and boundary conditions provided by ARPEGE
- **ECMF_dyna**: initial and boundary conditions provided by IFS T799 (stream oper)

Regarding the surface fields the two experiments gave similar results for both the 00 and 12 UTC runs (Figure 3). It is not surprising at all because all the surface fields in the initial condition files were taken from ARPEGE.

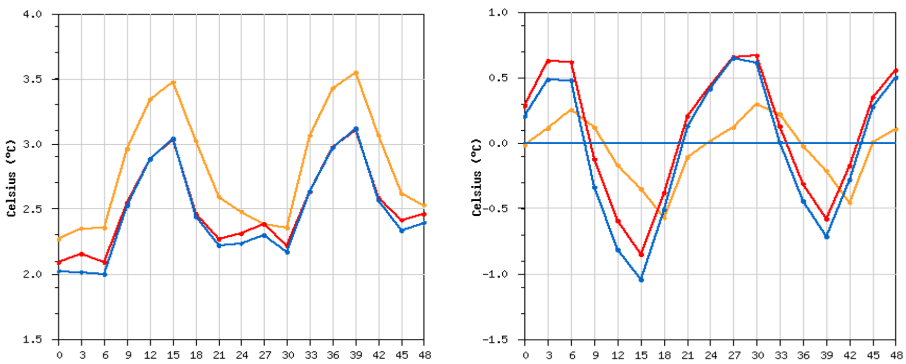


Figure 3: RMSE (on the left) and bias (on the right) scores for T2m for the 00 UTC runs. The red curve denotes ARPE_dyna, the blue curve denotes ECMF_dyna and the orange one represents the operational IFS forecast available at HMS. The verification was performed against SYNOP observations.

The verification of the upper air fields exhibited large differences between the experiments: ECMF_dyna proved to be significantly better both in terms of RMSE (Figure 4) and bias scores. The difference is larger at 00 UTC and smaller at the 12 UTC where it occurs only in the upper troposphere. ARPE_dyna is proved to be better than ECMF_dyna only for relative humidity in the upper troposphere. However, it is well known that relative humidity measurements from the European TEMP soundings at this height are not fully reliable so this feature should be neglected.

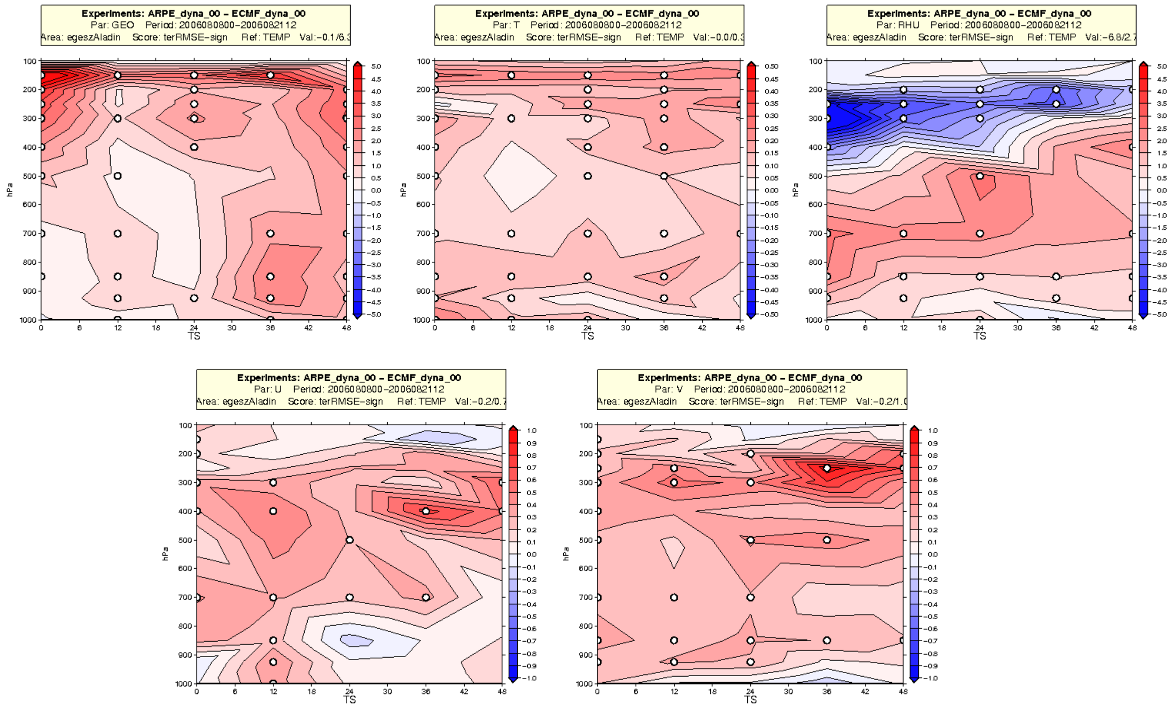

Figure 4: Difference of RMSE scores of the 00 UTC forecasts of ARPE_dyna and ECMF_dyna. Red shades indicate that ECMF_dyna is better, while blue shades indicate the opposite. White circles show that the difference is significant on a 90% confidence level. The verification was performed against TEMP observations in every 12 hours. The figure order is the following (from left to right): Z, T, RHU, U and V.

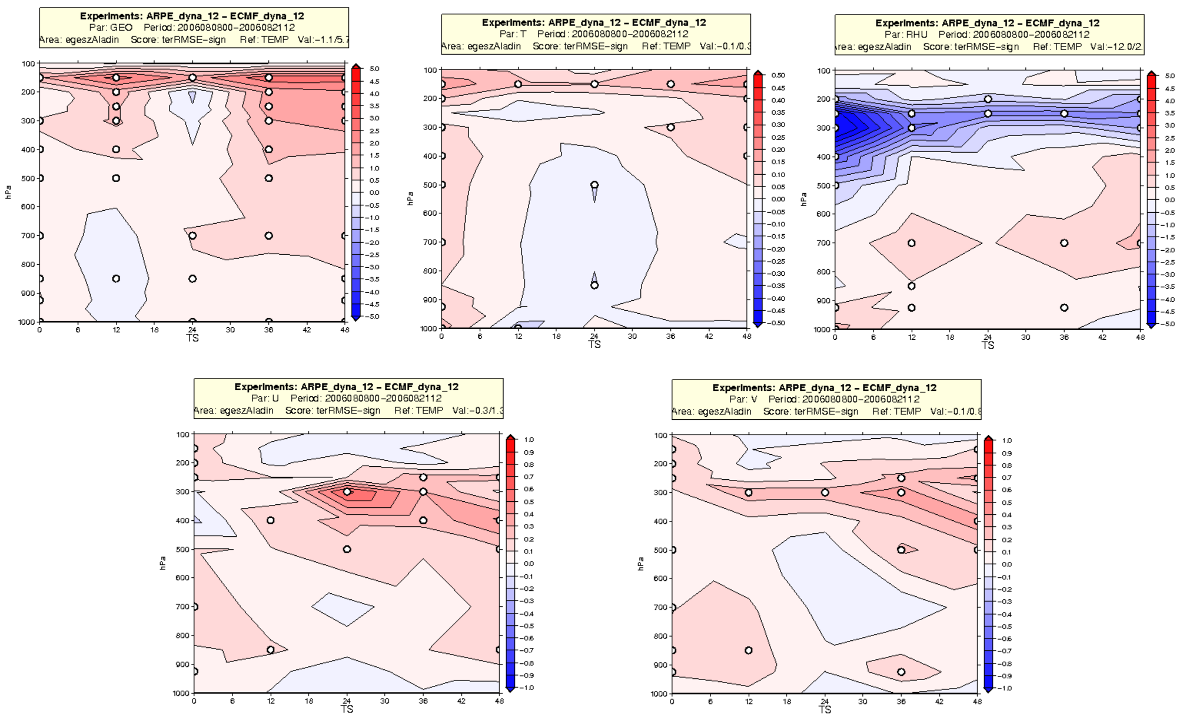

Figure 5: The same plots as in Figure 4 but this time for the 12 UTC runs.

#### 4.3.5. Using the 06 and 18 UTC IFS runs as BC

Unlike ARPEGE, the operational IFS runs are not available at the desired time for the operational ALADIN applications. For instance, the 00 UTC ALADIN/HU run ends at 3:30 UTC but the 00 UTC IFS integration starts only after 5:00 UTC. Thus for operational purposes only the previous IFS runs could be used as initial and boundary conditions to ALADIN. These runs are as follows:

- the 18 UTC IFS run (stream SCDA) providing BCs for the 00 UTC ALADIN run
- the 06 UTC IFS run (stream SCDA) providing BCs for the 12 UTC ALADIN run

This 6h-shifted BC usage was tested both with dynamical adaptation and 3D-VAR data assimilation. The following experiments were carried out:

- **ARPE_dyna**: dynamical adaptation using ARPEGE as initial and boundary conditions (in fact it is the same experiment as in the previous chapter)
- **ARPE_3d**: 3D-VAR with ARPEGE (both in the analysis cycling and in the forecast production ARPEGE was used as BC)
- **ECM6_dyn**: dynamical adaptation using IFS SCDA runs as initial and boundary conditions
- **ECM6_3d**: 3D-VAR with IFS SCDA runs (both in the analysis cycling and in the forecast production IFS SCDA was used as BC)

In the 3D-VAR experiments the same method as in the dynamical adaptation was applied to the surface: the surface fields in the first guess were replaced with the surface fields of the corresponding ARPEGE analysis.

- **Surface verification**

Regarding the surface parameters the largest difference between the experiments was found for T 2m (Figure 6). It can be seen that the two 3D-VAR runs performed similarly for both RMSE and BIAS.

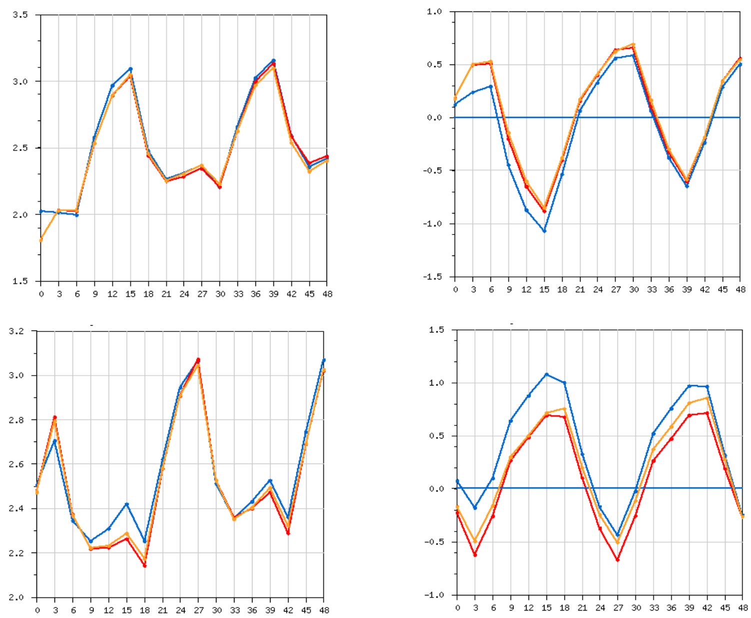

Figure 6: RMSE (on the left) and BIAS (on the right) scores for T2m for the 00 (top row) and 12 (bottom row) UTC runs. The red curve denotes ARPE_3d, the orange curve denotes ECM6_3d and the blue one denotes ECM6_dyna. The verification was performed against SYNOP observations.

Concerning the ECM6 experiments the use of 3D-VAR could slightly improve the RMSE scores but the bias scores indicate a systematic difference between dynamical adaptation and 3D-VAR. For RHU 2m and wind 10 m the differences were even smaller.

The verification of the precipitation forecast was also performed against SYNOP observations. ARPE_3d and ECM6_3d were compared using contingency tables for 12 and 24 h precipitation sums. The main conclusion is that for precipitation existence and for smaller precipitation rates (< 2 mm) ECM6_3d performed slightly better, but for large values (> 10mm) ARPE_3d is slightly better. Nevertheless, the differences are rather small. The results for the 24h precipitation for the 00 UTC runs are summarized in Figure 7 and 8.

| előrejelzés \ megfigyelés | =0 | <=2 | <=10 | >10 | Osszesen |
|---|---|---|---|---|---|
| =0 | 918 | 213 | 170 | 79 | 1380 |
| <=2 | 1908 | 1262 | 421 | 99 | 3690 |
| <=10 | 500 | 1089 | 907 | 339 | 2835 |
| >10 | 68 | 199 | 396 | 401 | 1064 |
| Osszesen | 3394 | 2763 | 1894 | 918 | 8969 |

| | =0 | <=2 | <=10 | >10 |
|---|---|---|---|---|
| B= | 0.407 | 1.336 | 1.497 | 1.159 |
| PC= | 0.672 | 0.562 | 0.675 | 0.868 |
| POD= | 0.270 | 0.457 | 0.479 | 0.437 |
| FAR= | 0.335 | 0.658 | 0.680 | 0.623 |
| F= | 0.083 | 0.391 | 0.309 | 0.082 |
| KSS= | 0.188 | 0.066 | 0.170 | 0.354 |
| TSS= | 0.238 | 0.243 | 0.237 | 0.254 |
| ETS= | 0.119 | 0.031 | 0.096 | 0.198 |
| HSS= | 0.212 | 0.060 | 0.145 | 0.331 |
| OR= | 6.090 | 1.308 | 2.052 | 8.643 |
| ORSS= | 0.718 | 0.134 | 0.345 | 0.793 |

Figure 7: Contingency tables and the corresponding parameters for the 24h precipitation forecasts (from 3 to 30h) of the 00 UTC ARPE_3d runs.

| előrejelzés \ megfigyelés | =0 | <=2 | <=10 | >10 | Osszesen |
|---|---|---|---|---|---|
| =0 | 945 | 226 | 148 | 87 | 1406 |
| <=2 | 1888 | 1270 | 451 | 104 | 3713 |
| <=10 | 483 | 1078 | 911 | 347 | 2819 |
| >10 | 78 | 189 | 384 | 380 | 1031 |
| Osszesen | 3394 | 2763 | 1894 | 918 | 8969 |

| | =0 | <=2 | <=10 | >10 |
|---|---|---|---|---|
| B= | 0.414 | 1.344 | 1.488 | 1.123 |
| PC= | 0.676 | 0.561 | 0.678 | 0.867 |
| POD= | 0.278 | 0.460 | 0.481 | 0.414 |
| FAR= | 0.328 | 0.658 | 0.677 | 0.631 |
| F= | 0.083 | 0.394 | 0.305 | 0.081 |
| KSS= | 0.196 | 0.066 | 0.176 | 0.333 |
| TSS= | 0.245 | 0.244 | 0.240 | 0.242 |
| ETS= | 0.124 | 0.031 | 0.098 | 0.188 |
| HSS= | 0.221 | 0.060 | 0.150 | 0.316 |
| OR= | 6.330 | 1.310 | 2.112 | 8.029 |
| ORSS= | 0.727 | 0.134 | 0.357 | 0.778 |

Figure 8: Contingency tables and the corresponding parameters for the 24h precipitation forecasts (from 3 to 30h) of the 00 UTC ECM6_3d runs.

#### 4.3.6. Upper air verification

For the upper air parameters (Figure 9-12) ECM6_dyna obviously turned to be worse than ECMF_dyna but it is still nearly of the same quality as ARPE_dyna (see the first column in Figure 9-12). The introduction of 3D-VAR improved the forecast quality in the first 12 hours for both ECM6 (see the middle column in Figure 9-12) and ARPE (not shown). Thus both for ECM6 and ARPE 3D-VAR turned to be better than dynamical adaptation. Comparing the 3D-VAR configurations we can conclude that the effect of 3D-VAR is more significant for ECM6 and ECM6_3d is even slightly better in the first 12 hours then ARPE_3d. Similar results were found for the other parameters.

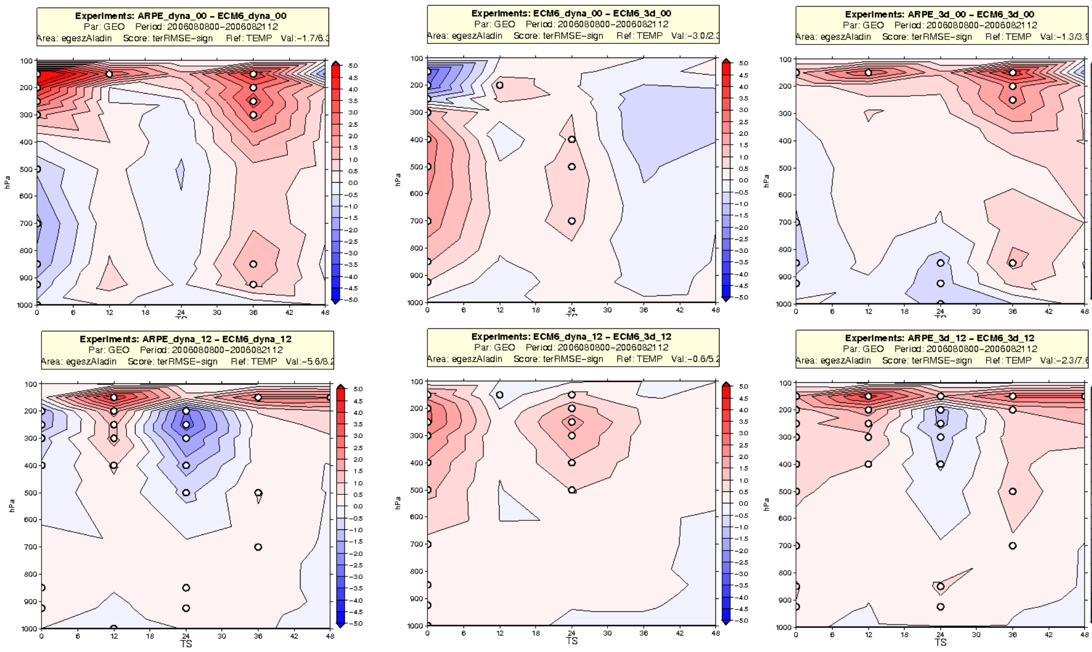


Figure 9: Difference of RMSE scores of the 00 (top row) and 12 UTC (bottom row) forecasts for Z. Left column: ARPE_dyna minus ECM6_dyna. Middle column: ECM6_dyna minus ECM6_3d. Right column: ARPE_3d minus ECM6_3d. Red shades indicate that the model to be subtracted is better (e.g. ECM6_dyna in the left column), while blue shades indicate the opposite. White circles show that the difference is significant on a 90% confidence level. The verification was performed against TEMP observations in every 12 hours.

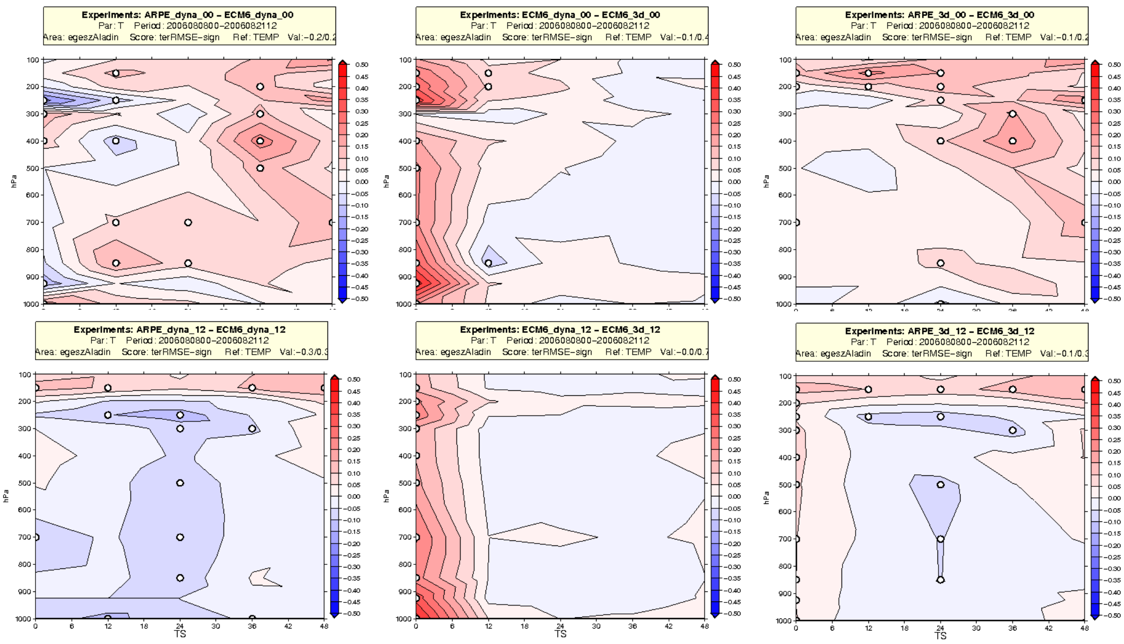


Figure 10: The same plots as in Figure 9 but this time for the temperature.

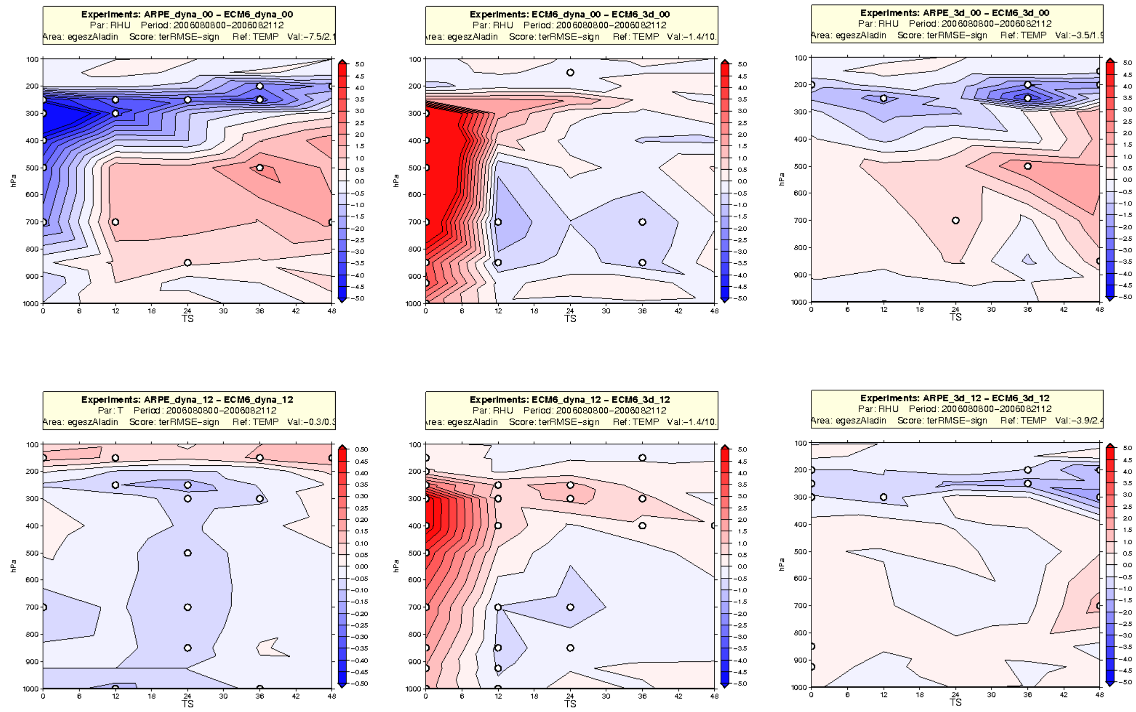

Figure 11: The same plots as in Figure 9 but this time for the relative humidity.

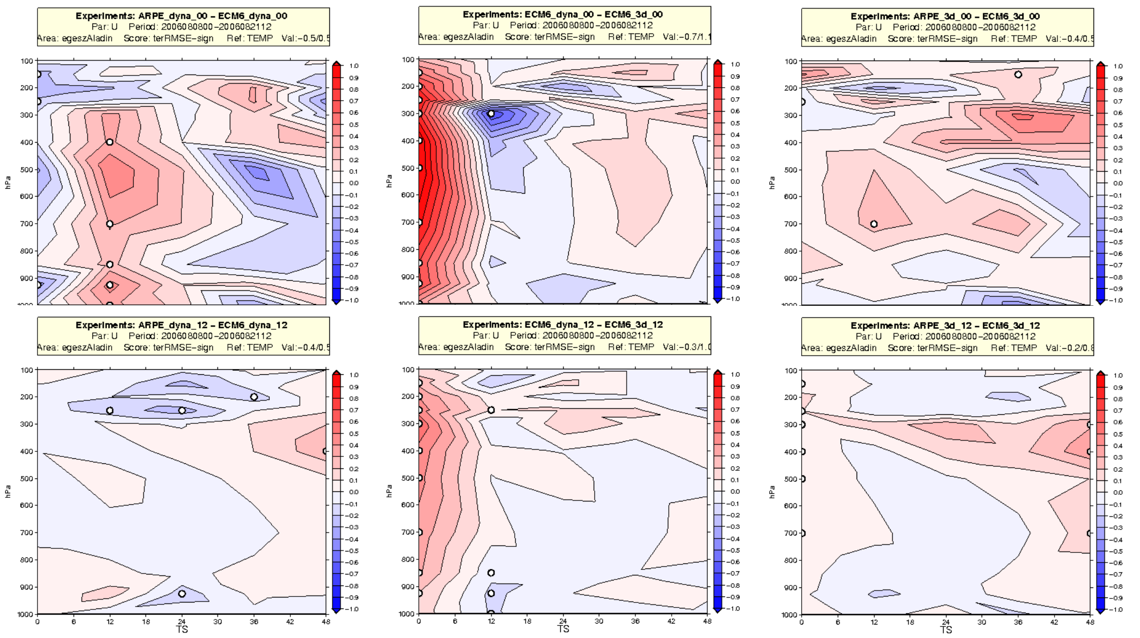

Figure 12: The same plots as in Figure 9 but this time for the U wind component.

### 4.3.7. Conclusions

It was shown that ALADIN based on dynamical adaptation performs better for the upper air parameters with IFS BCs than with ARPEGE ones. However, unlike ARPEGE, in a real-time environment only the 6h earlier IFS run is available as BC to ALADIN. The usage of the 6h earlier IFS run was tested both with dynamical adaptation and 3D-VAR data assimilation. It turned out that this kind of IFS BC usage is optimal when 3D-VAR is used in ALADIN. In this case the upper air scores are even slightly better than in 3D-VAR with ARPEGE. The detailed evaluation of the results (weather events, case studies) is still to be done.

Another important issue is the question of the optimal use of IFS surface fields. The recent solution should be further developed and a more advanced method should be applied.

**References**

Bölöni G., 2006: ALADIN coupled with ECMWF/IFS, Presented at the 16th ALADIN workshop, May 16-19, 2006, Sofia. Available online at:

http://www.cnrm.meteo.fr/aladin/meetings/Wk2006/presentations/tuesday/G_boloni_ECM_LBC.pdf

Kertész S., 2006: Preparing ALADIN BCs on ECMWF HPCF. Available online at:

http://www.rclace.eu in the Documents -> Local Documents menu

## 4.4. Downscaling of ARPEGE global ensembles (PEARP) by ALADIN model - heavy rain case study

Richard Mládek, Czech Hydrometeorological Institute

### 4.4.1. Summary

In the recent studies (Hágel and Szépszó, 2005; Hágel, 2006) there was found generally no real improvement when using direct downscaling of the global ensemble system (PEARP) by the local area model with high resolution ALADIN. Mainly 500 hPa geopotential, 850 hPa temperature, mean sea level pressure and 10 meter wind speed were examined in detail in those studies. In our work we are trying to evaluate the influence of the same downscaling on the specific situations where our local model had the biggest problems with precipitation forecast for Czech republic during last three years. The probabilistic verification of 6 and 24 hour cumulated precipitation for 17 chosen cases is presented. The aim of the study is to find out if the downscaling of the global ensemble forecasts by the local model can improve precipitation forecast for those difficult situations and to compare resulting probabilistic forecasts of ALADIN model to the global ones provided by ARPEGE model. It is shown that the direct downscaling in our test cases made worse most of the computed probabilistic scores. It can be said further that there is prevailingly no real improvement neither quantitative nor qualitative when exploring each case individually. The best results are obtained with the combination of both model ensembles global and local.

### 4.4.2. Model settings

To have consistent results we recomputed the global ensemble forecasts with PEARP methodology and spectral resolution TL358 but with different target domain (Europe and some of the Atlantic (70N/330W/30S/35S) and different optimization time (24 hour). These modified settings were chosen according the results of above mentioned studies. PEARP ensemble system is singular vector based and limited to 11 members (10 perturbed + 1 control) but run with high spectral truncation of TL358 with a stretching coefficient of 2.4. It gives horizontal resolution around 23 km over the central Europe. For more information about PEARP see Nicolau, 2006. The ALADIN model with 9 km horizontal resolution and 43 vertical levels was used for downscaling. Further, exactly the same model physics setting both for global and local models was used based on the developmental version 29t2mxl (so called "Prague" physics operational until January 2007 in Prague yet without prognostic cloud water). The integrations started at +18 UTC (as in operational PEARP) day before the rain event and the forecast length was 36 hour.

### 4.4.3. Experiment setting

Only the days with RMSE bigger than 10 mm/24 hour (average of 33 Czech synoptic stations verified against the closest model point from integration starting at 0 UTC) during the period 2003-2006 were chosen for the study. This period was selected because regular verification in Czech Hydrometeorological Institute has been done since summer 2002 and also because for the same period there were available ARPEGE global analyses with spectral resolution T358 for PEARP integrations. The verification was done against rain gauges data spatially averaged to the approximately 10x10 km latlon grid. The model forecasts were interpolated to the same grid. A similar verification method was used in more precipitation verification studies (e.g. Mullen and Buizza, 2000) and reflects well the character of model outputs. In Czech we have available around 150-240 resp 800 observed observational data for 6 resp. 24 hour cumulated precipitation. After spatial averaging it gives around 150-210 resp. 550 defined gridboxes (see Pict. 1).

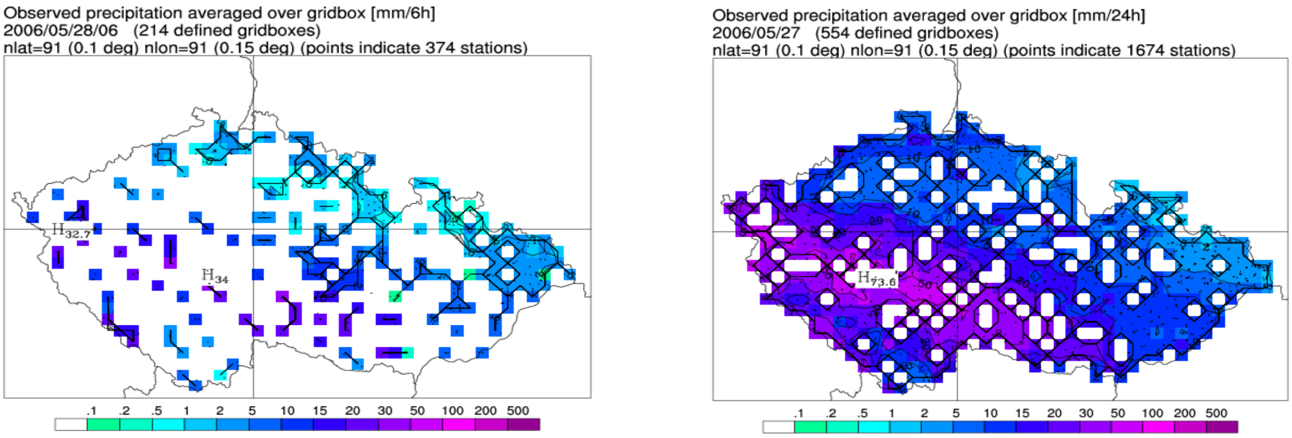


**fig. 1** Regular latlon mesh used for the the verification. 6 (left chart) resp. 24 hour (right chart) cumulated precipitation are averaged over each gridbox. The model forecasts are interpolated to the same points.

### 4.4.4. Verification

The common probabilistic scores (ensemble mean, spread, RMSE and BIAS; Talagrand, reliability and ROC diagram; Brier score) were computed using verification package developed in the frame of ALADIN-LACE group. The statistical signification of the results is limited due to a low number of cases (17 days) and the number of verified gridpoints on the area of Czech republic with defined both model and observed precipitation data. We remind that for 6 hour cumulation periods there is even approximately three times less defined gridboxes than for 24 hour one. In all pictures ALADIN resp. ARPEGE ensemble results are denoted as experiment HER1 resp. HER2. The used precipitation thresholds are 0.2, 1, 2, 5, 10, 20, 50 and 100 mm.

The high amounts of observed rain as follows from the selection procedure are typical for all cases. The observed maxima in individual cases are at least around 20-30 mm/24 hour and often around 40-50 mm/24 hour (70 mm absolute maximum). From the contingency tables computed for control runs (table 1) can be seen that the most represented category is between 10-20 mm/24 hour, but there are only 28 resp. 1 event(s) over 50 mm forecast by ALADIN resp. ARPEGE model (51 events in reality). Both models tend to underestimate precipitation below 0.2 and above 20 mm/24 hour. ETS scores are better for ARPEGE control runs except for the class 1-2mm /24 hour.

| ***mm/24h*** | ***0-0.2*** | ***0.2 - 1*** | ***1 - 2*** | ***2 - 5*** | ***5 - 10*** | ***10 - 20*** | ***20 - 50*** | ***50 - 100*** | ***> 100*** | ***sum*** |
|---|---|---|---|---|---|---|---|---|---|---|
| **obs** | 650(7.2) | 411(4.5) | 491(5.4) | 1467(16.2) | 2170(24.0) | 2346(25.9) | 1457(16.1) | 51(0.6) | 1(0.0) | 9044(100.0) |
| **arp ctrl** | 266(2.9) | 573(6.3) | 478(5.3) | 1369(15.1) | 2226(24.6) | 3152(34.9) | 979(10.8) | 1(0.0) | 0(0.0) | 9044(100.0) |
| **ald ctrl** | 246(2.7) | 532(5.9) | 566(6.3) | 1511(16.7) | 2470(27.3) | 2658(29.4) | 1033(11.4) | 28(0.3) | 0(0.0) | 9044(100.0) |

Table 1. Extract (cumulated values for every category) from the contingency tables computed for ARPEGE and ALADIN control runs over all cases. In parentheses there are percentages.

| ***mm/24h*** | ***0,2*** | ***1*** | ***2*** | ***5*** | ***10*** | ***20*** | ***50*** | ***100*** |
|---|---|---|---|---|---|---|---|---|
| **ETS arp ctrl** | 0,062 | 0,153 | 0,203 | 0,253 | 0,220 | 0,142 | 0,000 | 0,000 |
| **ETS ald ctrl** | 0,164 | 0,178 | 0,189 | 0,199 | 0,177 | 0,120 | -0,002 | 0,000 |

Table 2. ETS scores (computed multicategoricaly) for ARPEGE and ALADIN control runs.

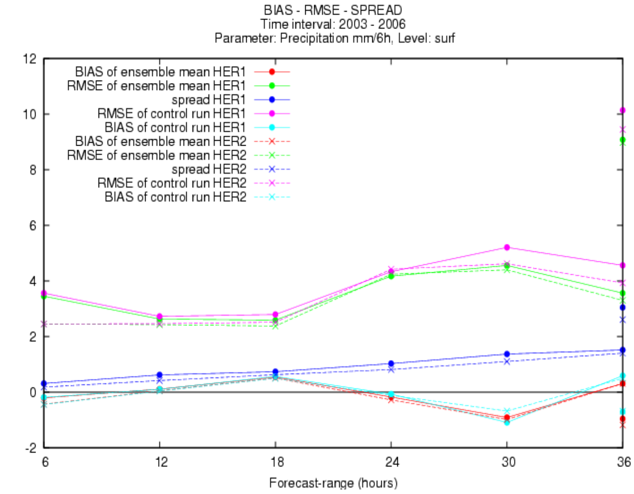


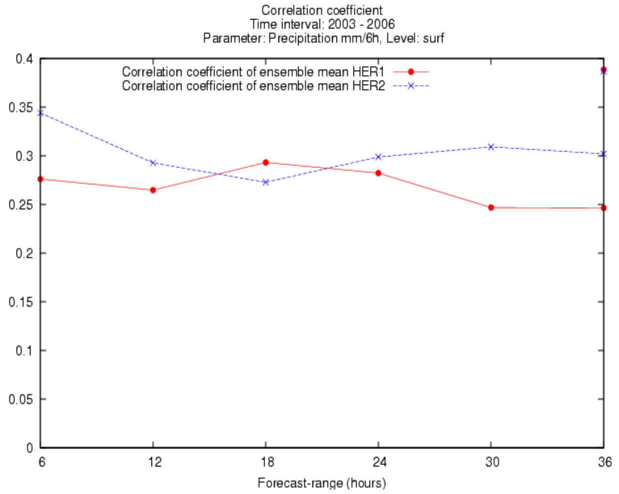


Fig.2: Averaged values over the whole period of BIAS, RMSE computed for control run and ensemble mean; ensemble spread. Markers on the right Y axis are valid for 24 hour sums.

Fig.3: Averaged values over the whole period of correlation coefficient of ensemble mean. Markers on the right Y axis are valid for 24 hour sums.

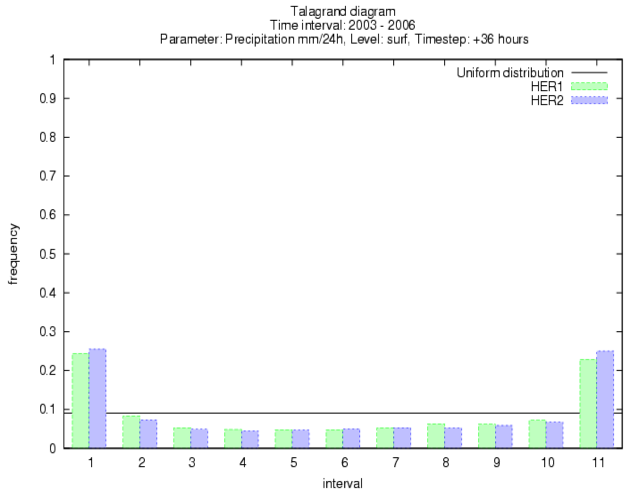


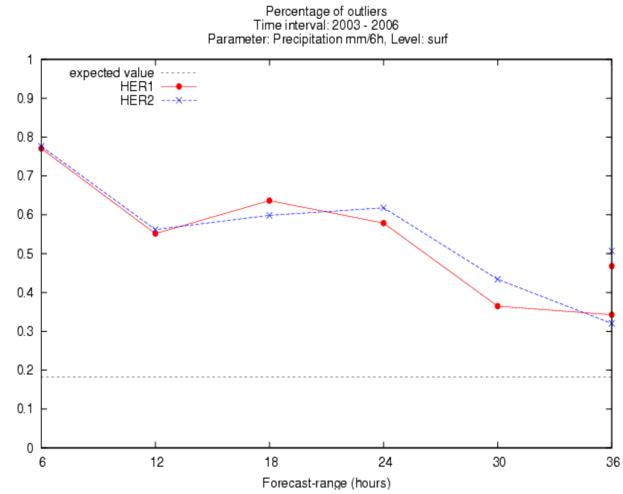


Fig.4: Talagrand diagram for ARPEGE and ALADIN ensembles. Only 24 hour sums averaged over the whole period are considered. Horizontal line denotes ideal uniform distribution.

Fig.5: Percentage of outliers for ARPEGE and ALADIN ensembles. Markers on the right Y axis are valid for 24 hour sums. Horizontal line denotes ideal uniform distribution.

The better averaged continuous statistics for ARPEGE based ensemble system and the control runs are shown in fig. 2. For all time ranges are averaged values of RMSE of ARPEGE control runs even better then the ALADIN ensemble mean values. The ensemble mean is not always the best product of probabilistic forecast of precipitation (extremes are smoothed sometimes) but as we can see, its values are always better then the values of control runs for all time ranges (6 hour cumulated rain) and also if 24 hour sums are considered (see the values marked on right Y axis in fig. 2). The improvement between the values computed for control runs and ensemble means is bigger for ALADIN based ensembles but it is still insufficient to beat at least the results of ARPEGE control runs. Another important feature which can be seen in fig. 2 is generally very low spread and its very slow increase within the forecast time. Its value reaches at the most one third of the averaged RMSE value considering 24 hour sums.

Even if one examines the same curves as in fig. 2 but computed for each case separately the values of ensemble spread are never higher than 2 mm for 6 hour cumulated precipitation. The lack of spread is clear also from U-shaped Talagrand diagram (fig. 4). The slightly better number of outliers for ALADIN ensemble is shown for 24 hour and most of 6 hour sums in fig. 5. In fig. 3 is shown that 6 hour sums computed for PEARP are better correlated with the observations than the ALADIN values (except for time range +18 hour). In fig. 6 is shown an example of ROC scores for ALADIN ensemble and every threshold. ROC area values are displayed in parentheses in legend. The ROC diagram for PEARP looks very similar.  In fig. 7 is shown an example of reliability diagram again for ALADIN ensemble. The forecasts of both models (for PEARP not shown) are overconfident (distributions for every threshold are flatter than 45 deg.). It means that the low risks are underestimated and the high risks overestimated.

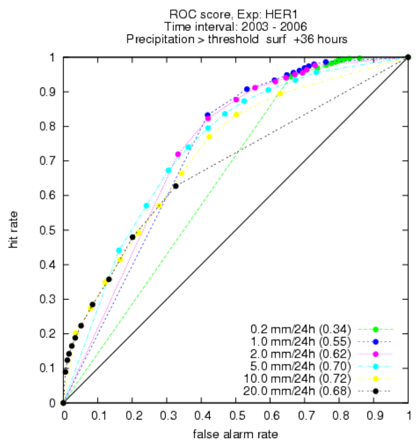


Fig. 6: ROC diagram for ALADIN ensemble, 24 hour sums and all thresholds. In parentheses in legend there are ROC area values.

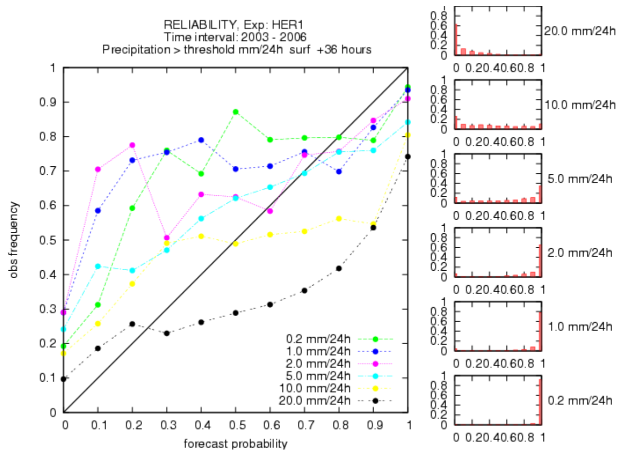


Fig. 7: Reliability diagram for ALADIN ensemble, 24 hour sums and all thresholds. In the plots on the right the frequency of forecast probabilities for every thresholds are plotted.

The slightly better results than those given by pure ARPEGE ensemble can be obtained by merging of both ensembles global and local (see Fig. 8). After study of individual cases (see below) it seems that the global model might compensate e.g. too high precipitation on the windward side in ALADIN paradoxically due to its lower horizontal resolution and thus smoothed orography. On the other hand a higher horizontal resolution of ALADIN ensemble lead to slightly bigger spread and might compensate other kinds of errors present in global forecasts. In fig. 9 is shown a parameter which derives the biggest benefit from merged ensemble – the number of outliers.

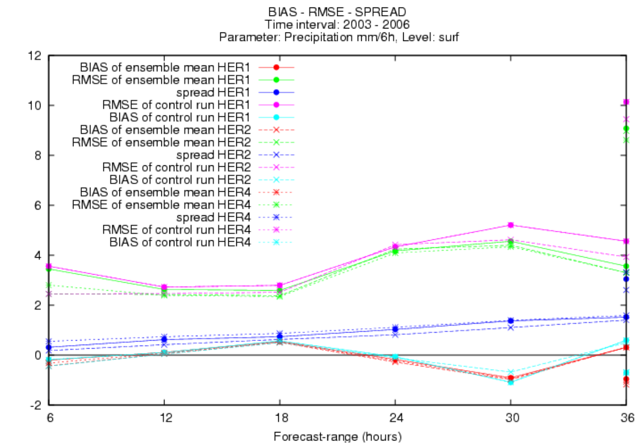


Fig. 8: Averaged values over the whole period of BIAS, RMSE computed for control run and ensemble mean; ensemble spread. As exp. HER4 is denoted merged eps. Markers on the right Y axis are valid for 24 hour sums.

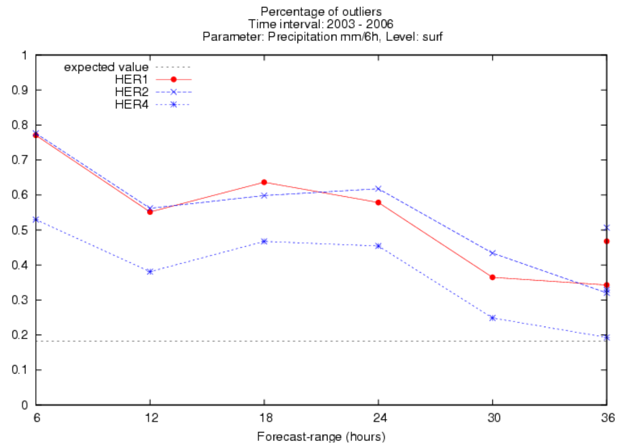


Fig. 9: Percentage of outliers for ARPEGE and ALADIN ensembles. As exp. HER4 is denoted merged eps. Markers on the right Y axis are valid for 24 hour sums. Horizontal line denotes ideal uniform distribution.

### 4.4.5. Cases examination

It is the aim to obtain more additional informations coming from ALADIN ensemble prediction than from the results of ALADIN/ARPEGE control integration or probabilistic forecast of PEARP. Unfortunately it seems that it's not the case almost never at least when looking in detail to the results of each of our 17 events. For each case the plots as in fig. 2 –5 were produced, then the maps of cumulated forecast and observed rain for every 6 and 24 hour interval (also large-scale and convective part separately). Both ensemble mean charts and stamp plots with individual ensemble members were examined too.

The weather in virtually all cases is connected with the passage of cold frontal line over Czech republic from west, north-west or south-west directions. There are two typical groups of seven resp. nine situations in our sample. The first are the winter or transient season cases with predominant large-scale rain in the model forecasts. The highest amounts of cumulated rain are often more than 40 or 50 mm/24 hour. In both models the maxima are also not seldom too strictly joint with the windward side of Czech mountains what is a well know problem. Nevertheless the forecasts of such events are generally pretty good and we can see very strong signals in the probabilistic charts even for the precipitation over 40 mm/24 hour although the pattern of raining areas is not the best (see event9 from October 23, 2004 in fig. 10-13 as an example). The fact that these very satisfactory forecast events are included in our sample is because of our selection method and very high observed rain sums. The inaccuracy in predicted maxima or the locations of the rain gives then bigger RMSE values. The second group of cases is characterized by much more convective activity during warm seasons. The rain patterns in the model forecasts are given here by the convective part of the total rain but the large-scale component always contributes significantly to the precipitation maxima. There is no case of a pure subgrid convection in our sample. As can be expected such situations are much more difficult to forecast and here we would like to see a positive impact of ensemble methodology itself or the impact of the higher ALADIN resolution. Unfortunately exploring our nine cases subgroup doesn't give any any clear results in favour of ALADIN ensemble forecast. The ensemble mean gives mostly only too smoothed maxima and the signal in the probabilistic charts of precipitation over 40 mm is only the lowest one (5-35%) if any (it is valid for both models). The differences between ALADIN and ARPEGE ensembles are indeed bigger but the usage of downscaled ALADIN ensemble doesn't help in a lowering of the uncertainty of prediction of such events. The spread values are not bigger than in the first group of well predictable situations and only a very few ensemble members can be found sometimes qualitatively better than the control forecasts. There is one interesting case in the second group from August 24, 2005 (not shown). All ensemble members looks virtually the same and the almost zero spread values are constant within a forecast range. This event looks to be the most unpredictable from the view of used models and singular vector based method of perturbation generation. This case was studied in past also with the non-hydrostatic AROME with very high resolution and a slightly better results were obtained (Janousek, 2006).

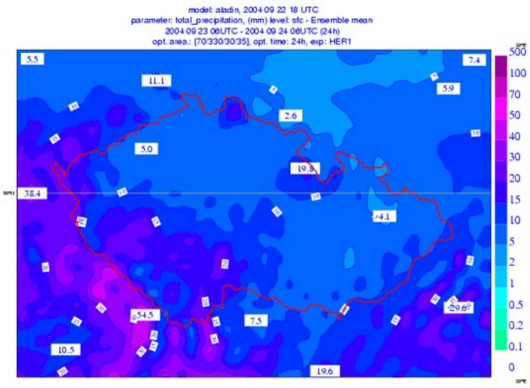

Fig. 10: Total cumulated precipitation of the ALADIN ensemble mean, October 23, 2004. The picture is almost the same for the control run. The results of PEARP are very similar.

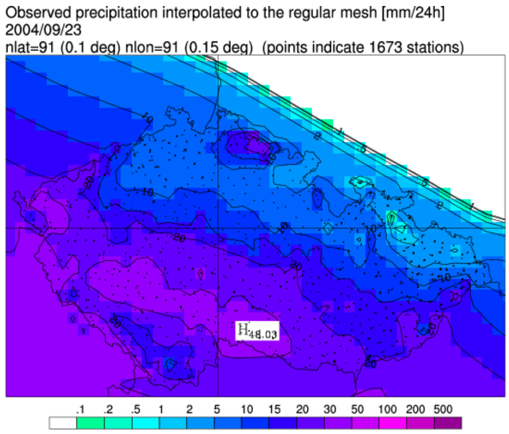


Fig. 11: Observed precipitation for the same day as in Fig. 7.

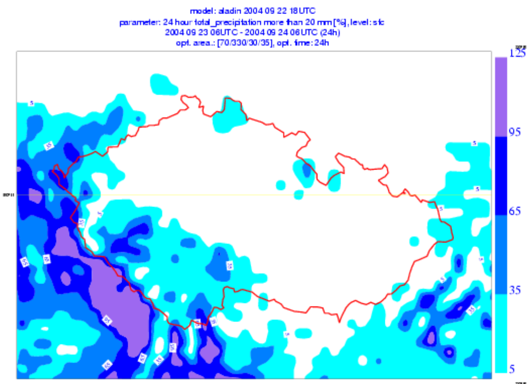

fig. 12 Probability chart of the precipitation over 20 mm and the same day as in Pict. 7 for ALADIN ensemble. The results of PEARP are very similar.

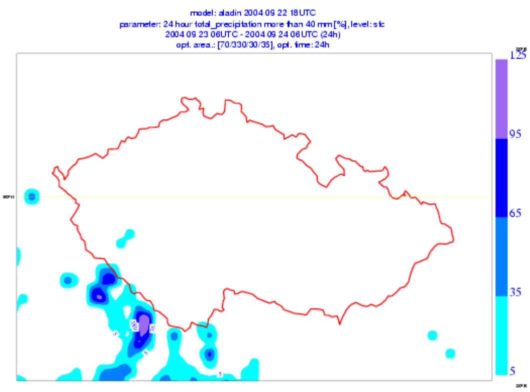

fig. 13 Probability chart of the precipitation over 40 mm and the same day as in Pict. 7 for ALADIN ensemble. The results of PEARP are very similar.

### 4.4.6. Conclusions

The downscaling of ARPEGE ensemble by ALADIN model in our test cases made worse most of the computed probabilistic scores when comparing ALADIN versus ARPEGE ensemble performance. There is prevailingly no real improvement neither quantitative nor qualitative when exploring each case individually. On the top of it the interpolation of observations to the mesh used for verification with resolution of 10 km is favourable for ALADIN model which had horizontal resolution closer to it. The ensemble spread for precipitation is very low and it would be interesting to try moist singular vector computations. The regular long-time probabilistic precipitation verification against the dense observations as in our study is necessary to fully explore the usefulness of similar ensembles for heavy rains prediction. The probabilistic charts with the high values of probability of heavy rains can give the forecasters more confidence in their daily routines as was shown on the results of the first subgroup of the sample with well predictable situations.

The best results (a bit better then PEARP ones) were obtained by merging of both ensembles global and local. The slightly better spread and thus more scenarios of possible weather with reasonable accuracy of both model ensembles is behind it.

Further on the basis of our results it could be interesting to consider a computation of more members in PEARP ensemble instead of downscaling them. The verification of the closest model point to the observation stations should be also done in future as a variation to the observation averaging to fully evaluate a possible usefulness of the increase in the model horizontal resolution when using ALADIN instead of ARPEGE ensembles.

**References**


E. Hágel, Latest results of the LAMEPS experiments, ALADIN newsletter 27.

M. Janousek, 2006, personal communication after the stay in Météo-France

Mullen and Buizza, 2000, Quantitative Precipitation Forecasts over the United States by the ECMWF Ensemble Prediction System, MWR, vol. 129, p. 638-663

J. Nicolau, Short range ensemble forecasting, http://www.wmo.ch/web/www/DPS/TC-DPFS-2002/Papers-Posters/Topic1-Nicolau.pdf

## 4.5. The (pre-) operational status of ALADIN Limited Area Ensemble Forecasting (LAEF)

A. Kann, Ch. Wittmann, Y. Wang (ZAMG, Vienna, Austria)

### 4.5.1. Introduction

In 2006, the experimental ALADIN regional EPS system LAEF (Limited Area Ensemble Forecasting, Wang and Kann, 2006) has been implemented at ZAMG. Work has been focused on the initial condition perturbation (comparing Breeding, *E*nsemble *T*ransform, *E*nsemble *T*ransform *K*alman *F*ilter) and on the impact of different physical parameterizations using dynamical downscaling technique (Kann and Wang, 2006). Further investigations have been carried out on the problem of adequate boundary conditions (Kann and Wang, 2007).

Since March 2007, the Limited Area Ensemble System ***ALADIN – LAEF*** runs in (pre-) operational mode. In the following, a description of the complete system will be given.

### 4.5.2. The configuration of the Ensemble System

The main methodological ingredients of the ensemble generation are:

Initial perturbation: Downscaling of ECMWF Singular Vector Perturbation.

Lateral boundary perturbation: Coupling with the ECMWF EPS system.

The model – related part of the system is implemented as a quasi time-critical application on hpce at ECMWF and consists of the following steps (Kertesz, 2006; Tascu, 2006; Stjepan Ivatek-Šahdan, 2007):

- Getting the relevant ECMWF EPS data from MARS archive
- Conversion from ECMWF to ARPEGE File format (configuration e901)
- Interpolation from ARPEGE to LAEF domain (configuration e927)
- Dynamical downscaling (configuration e001)

Dynamical downscaling is performed for the first 16 EPS members, for the control run (T399) and for the high-resolution deterministic model (T799) (altogether 18 members).

- Transfer of the output FA Files to ZAMG using ectrans
- FA to GRIB-I conversion
- Generation of products (EPSgrams, probability plots, poststamp charts, etc…)

The model version of Aladin used for downscaling is cycle31T1. It runs in hydrostatic mode with a horizontal resolution of 18 km and 37 vertical levels using Lopez-microphysics. The forecast covers the time range up to +54 hours and the operational procedure is performed twice a day (00 and 12 UTC model runs).

### 4.5.3. The ALADIN – LAEF integration domain

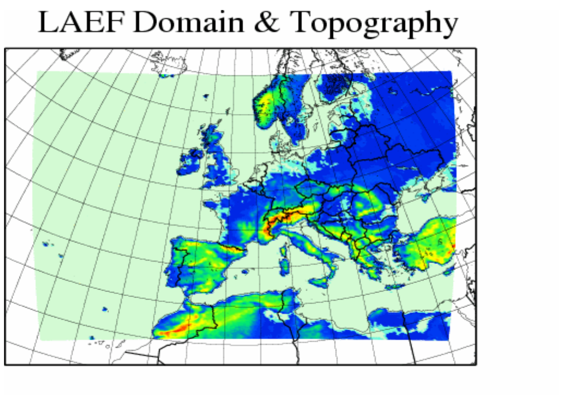


Fig. 1: ALADIN – LAEF integration domain and orography. The domain covers large parts of Europe, northern areas of Africa and the north Atlantic.

### 4.5.4. The ALADIN – LAEF products

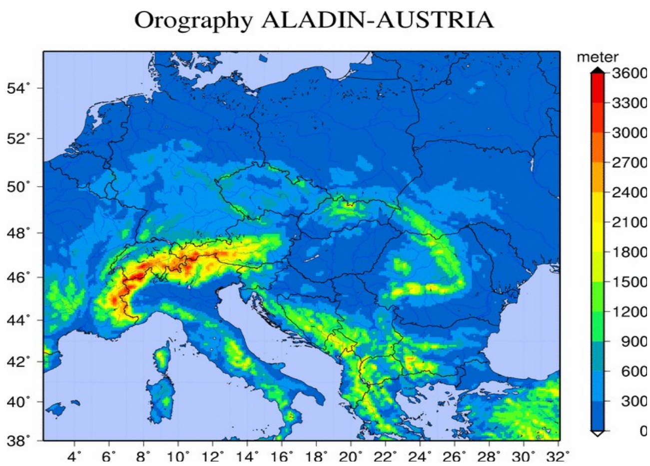


Fig. 2: ALADIN – LAEF post-processing domain for products is identical to the LACE telecom domain.

The post-processing domain covers the area 38.53N to 54.98N in latitude and 2.55E to 31.8E in longitude with 0.15 degrees grid spacing in both directions (regular lat-lon grid). The temporal resolution of post-processing is 3 hours from +6 to +54 hours.

The following types of plots are generated in operational mode:

EPSgrams, Probability plots, Poststamp charts, Ensemble Mean & Spread charts, Spaghetti plots

The elaborated parameters are:

500hPa Geopotential Height, 850hPa Temperature, 2m-Temperature, 2m-Maximum Temperature, 2m-Minimum Temperature, Precipitation, 10m Wind – Speed, 10m Wind – Gusts, CAPE, Mean Sea Level Pressure, 2m – Relative Humidity

## ❑ EPSGRAMS

2 EPSgrams are produced for a variety of stations within Europe, reflecting the frequency distribution of the main weather parameters. Total Cloudiness, Total Precipitation, Wind speed and 2m – Temperature are shown in EPSgram-1, Convective Cloudiness, CAPE, Gust Speed and 2m – Relative Humidity in EPSgram-2 (Figure 3).

As generally applied in this type of plots, the box-and-whisker diagrams represent the minimum, 25%-percentile, median, 75%-percentile and the maximum of the ensemble distribution.

The temporal evolution of the downscaled control forecast (blue solid line), the downscaled high-resolution deterministic forecast (red solid line) and the operational ALADIN – AUSTRIA forecast (black solid line) are added to the distribution of the ensemble system.

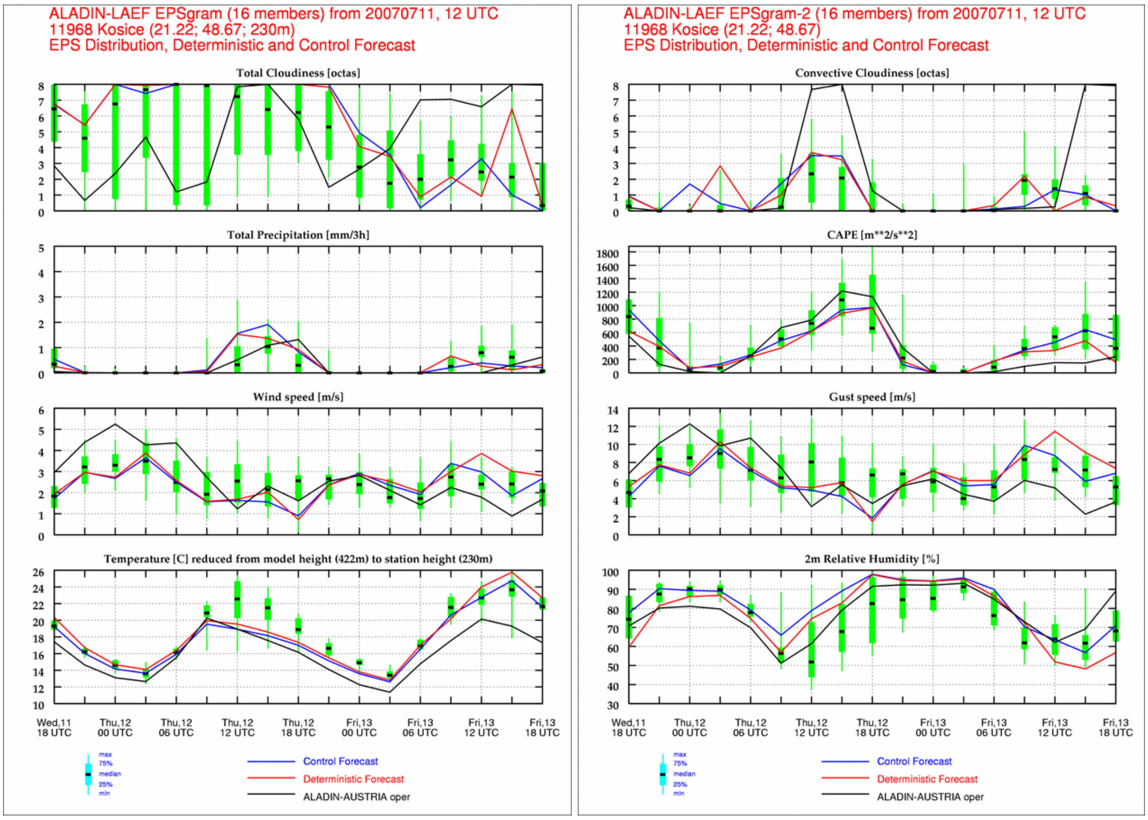


Fig. 3: Example of EPSgram-1 and EPSgram-2 for Kosice (SK).

## ❑ Ensemble Mean & Spread

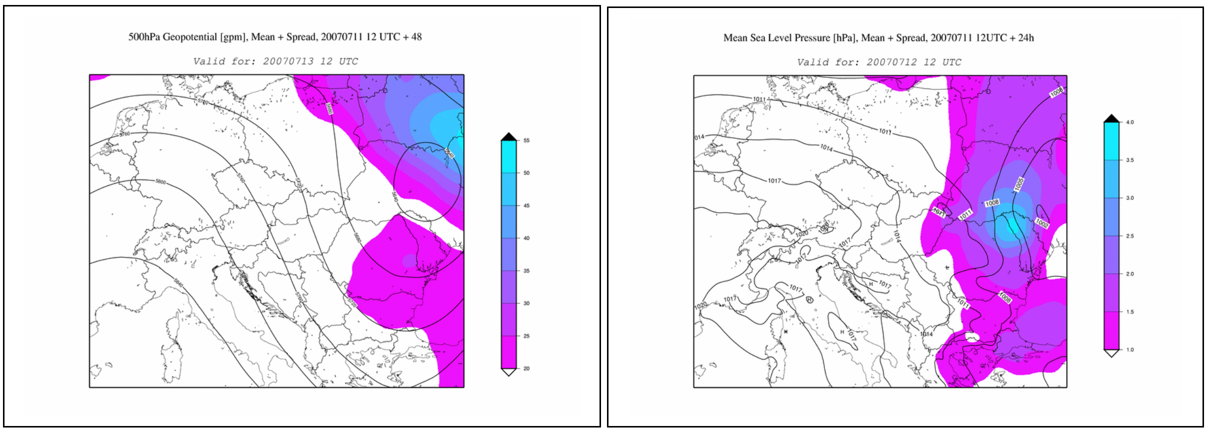


Fig. 4: Example of Ensemble Mean & Spread: Left: 500hPa Geopotential Height, right: Mean Sea Level Pressure. The solid contour lines denote the ensemble mean, the coloured areas indicate the spread.

## ❑ Spaghetti plots

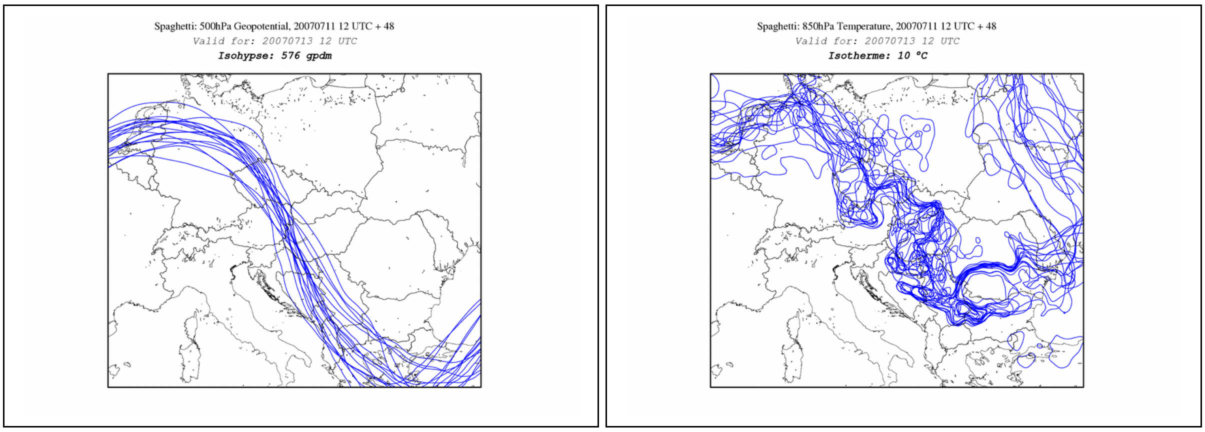


Figure 5: Examples of Spaghetti plots: Left: 500hPa Geopotential showing the Isohypses 576 gpdm of all ensemble members. Right: 850hPa Temperature showing the 10 degC isotherme of all ensemble members.

## ❑ Poststamp charts

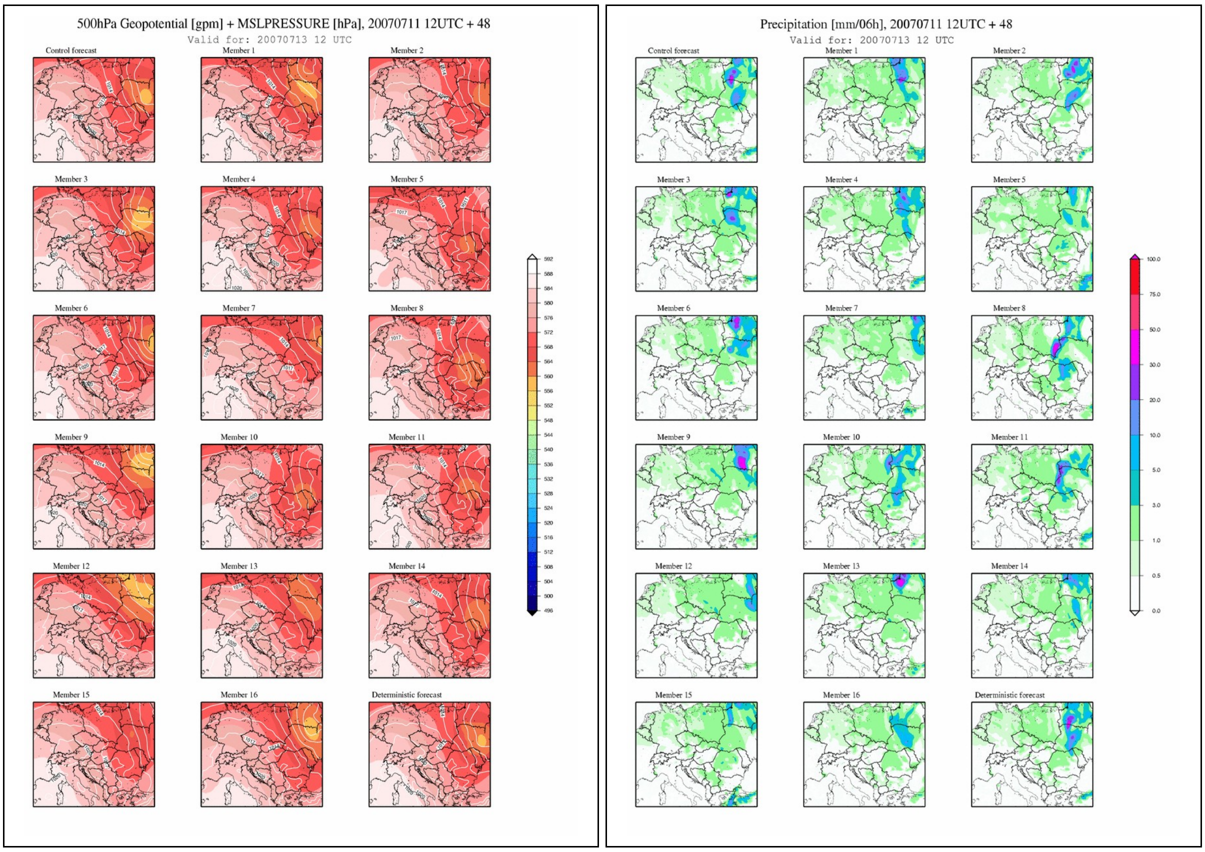


Figure 6: Examples of pststamp charts: Left: Forecast for 500hPa Geopotential Height (coloured areas) and Mean Sea Level Pressure (contour lines) for all ensemble members + control forecast + (downscaled) high resolution deterministic forecast. Right: 6 hours accumulated precipitation forecast for all ensemble members + control forecast + (downscaled) high resolution deterministic forecast.

## ❑ Probability plots

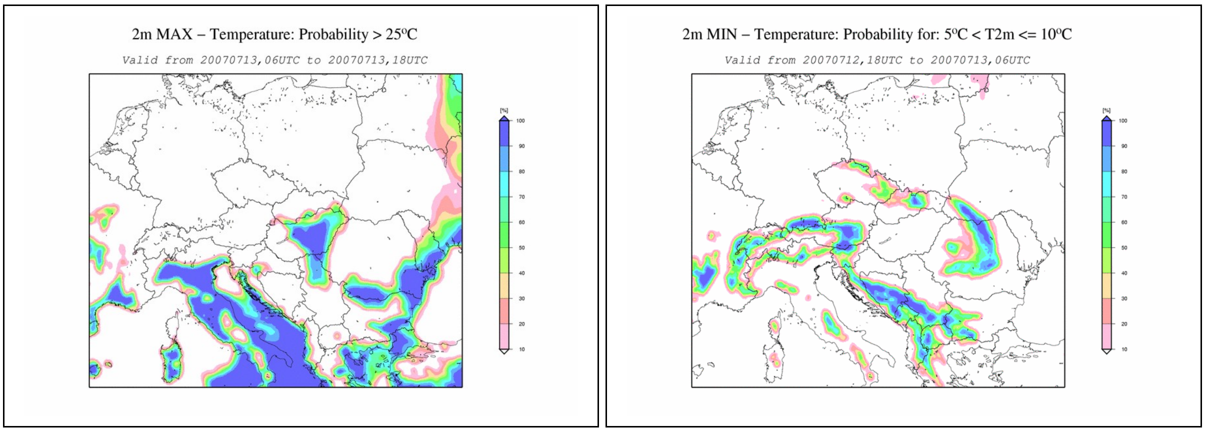


Fig. 7: Examples of Probability plots: 2m Maximum Temperature exceeding 25°C (left) and 2m Minimum Temperature between 5°C and 10°C (right) within a certain time range.

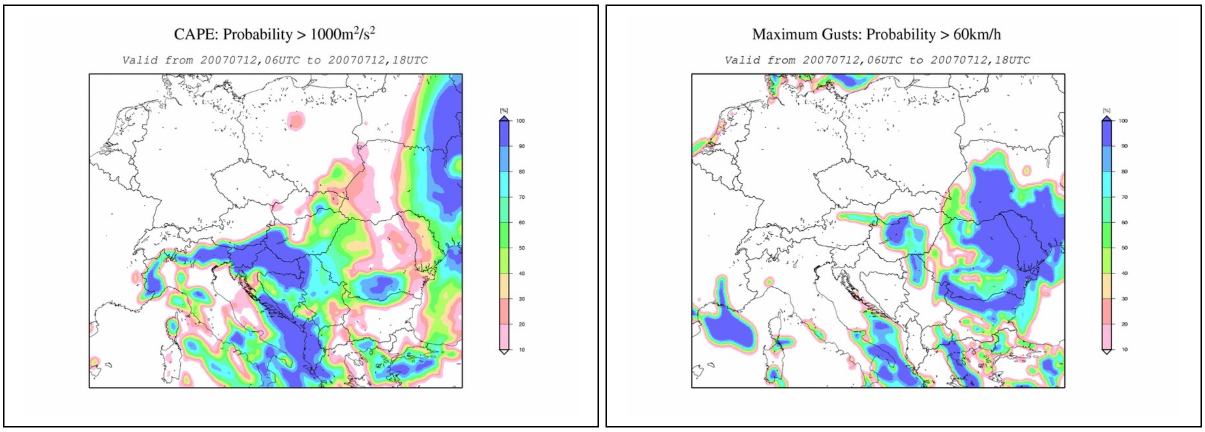


Fig. 8: Examples of Probability plots: CAPE exceeding 1000m²/s² (left) and Gusts exceeding 60 km/h (right) within a certain time range.

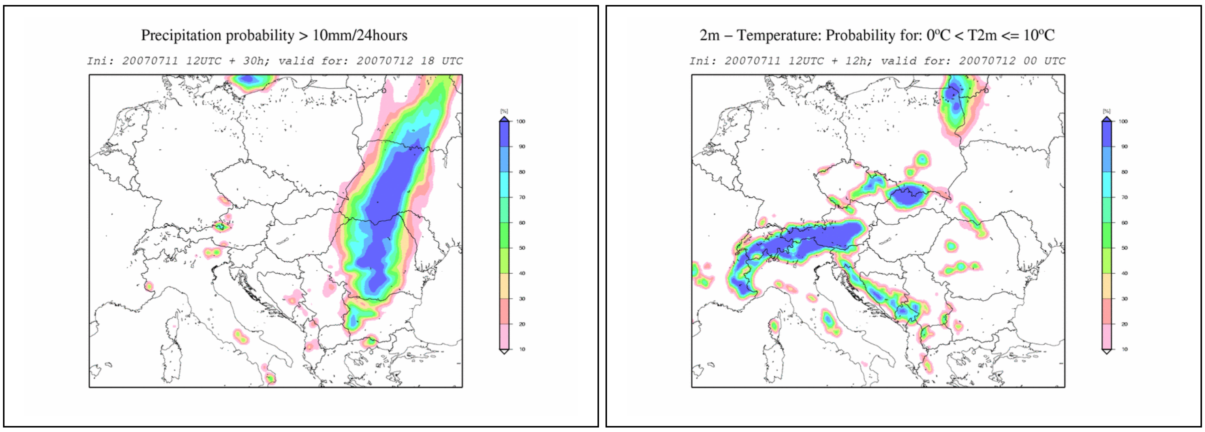


Fig. 9: Examples of Probability plots: 24 hours accumulated precipitation forecast exceeding 10mm within a certain time range (left) and 2m Temperature between 0°C and +10°C at a certain verification time (right).

The products shown above are available on RC LACE Homepage in real time.

### 4.5.5. Outlook

Up to now, the ensemble system simply consists of dynamical downscaling of the first 16 ECMWF EPS members using the Aladin model. As the members are statistically independent, the way of choosing the members should be negligible. Nevertheless, information from unused ensemble members is lost and maybe leads to worse performance. In the (near) future, a clustering algorithm will be applied in order to select representative members from the whole ensemble system. This method should provide a better probability distribution to the system and improve the quality. Furthermore, applying the blending technique (Bellus, 2006), that combines large scale initial perturbation and small scale initial perturbation gained by breeding method, is planned to be introduced. Additional investigations within the framework of LAEF will focus on the implementation of Breeding, ETKF and ET. Regarding post-processing, a bias correction will be implemented in the near future in order to eliminate systematic deficiencies.

Apart from the work on the ensemble system itself, the final preparation of the LAEF verification package (Hagel, 2006; Mladek, 2006) is planned to be finished within the next months.


### Acknowledgements

As ALADIN – LAEF has been fully established by LACE contributions, we would like to thank all colleagues, who have worked on its birth. Our special thank go to Martin Bellus, Edith Hagel, Richard Mladek, Georg Pistotnik, Stjepan Ivatek-Sahdan and Simona Tascu for their work during their LACE stays.


#### References


Belluš M.: Combination of large scale initial conditions uncertainty with small scale initial perturbations obtained by breeding method using blending procedure. Report on stay at ZAMG, 2006.

Hagel, E.: Report on work in Vienna on the common verification package. Report on stay at ZAMG, 2006.

Ivatek-Šahdan, S.: Downscaling ECMWF EPS for ALADIN. Report on stay at ZAMG, 2007.

Kann A., Wang Y.: ALADIN Limited Area Ensemble Forecasting (LAEF) experiments: Multiphysics downscaling of PEARP. Aladin Newsletter **30**, 2006.

Kann A., Wang Y.: Limited Area Ensemble Forecasting (LAEF) experiments: Dealing with Uncertainties in the LBC. Aladin Newsletter **31**, 2007.

Kertesz, S.: Investigations of coupling the ALADIN and AROME models to boundary conditions from ECMWF and ERA model data, 2006.

Mladek, R.: Work on the Common Verification Package for the evaluation of ensemble forecasts. Report on stay at ZAMG, 2007.

Pistotnik, G.: Coupling ALADIN LAEF with ECMWF EPS. Report on stay at OMSZ, Budapest, 2006.

Tascu, S.: Coupling ALADIN LAEF with ECMWF EPS. Report on stay at ZAMG, 2006.

Wang Y., Kann A.: ALADIN Limited Area Ensemble Forecasting. Aladin Newsletter **29**, 2006.

## 4.6. Validation of FOG and VISIBILITY forecasts for Lindenberg, Germany with ALADIN/ AUT cy25 and cy29 within COST722 project

Harald Seidl, ZAMG

### 4.6.1. Introduction

COST (=European COoperation in the field of Scientific and Technical Research) action 722 was raised to develop advanced methods for short range forecasts of fog, visibility and low clouds. It was split into 3 working groups (WG1 initial data, WG2 numerical models and WG3 statistical methods).

ZAMG has been involved mainly in WG2 focussing on intercomparison period from September until December 2005 on a subdomain centred in Berlin, Germany.

Operational limited area model ALADIN cy25 with sub-inversion cloudiness scheme (SK-scheme) and some extended post processing was used to gain reasonable visibility thresholds for the whole period.

ALADIN cy29 experimental suite with prognostic cloud liquid water, Lopez microphysics and SK-scheme for cloudiness parameterization were used to perform simulations on certain fog/Stratus events out of the whole period.

DMI-HIRLAM, FOG-NMM-BERLIN and LM-PAFOG participated in the Lindenberg intercomparison as well.

In Lindenberg (sited southeast of Berlin in rather flat terrain) many meteorological parameters relevant for boundary layer processes are continuously observed at 10 and 100m masts. Also flux and soil measurements are available every 10 minutes. This comprehensive data set was used to validate model forecasts for the whole intercomparison period and for selected fog cases as well.

### 4.6.2. Some results and comments

All participating models are able to simulate fog and low stratus, parameterization of visibility seems useful (though tunable) as well, these are the positive aspects from COST722 model intercomparison. On the other hand comparing real and modelled distributions of fog or liquid water contents, respectively, still reveals a few weaknesses on the NWP side.

The analyses of the radiative fluxes at the surface have pointed out the difficulties of the models to forecast the cloud parcel at the exact position. The cloud cover influences strongly the forecast quality (fog formation delayed). Moreover, the parameterizations of the low atmosphere evolution show a limited accuracy. The vertical profiles underline the difficulty of the models to reach the saturation at the surface. The latent and sensible fluxes have large bias during the day and the model forecasts for these variables have a large dispersion.

But, the lack of accuracy is partially corrected by the visibility parameterization.

Figures below are depicted from radiation fog event end of September 2005.

From time evolution of visibility at Lindenberg (figure 1) we capture the fact that ALADIN (green line) is able to forecast fog though with a delay of approximately 4 hours and some damping.

Horizontal visibility distribution for the small domain around Lindenberg on 27 September 2005, at 03 UTC indicates the ability of ALADIN to forecast the radiation fog event as a whole at the same time missing in accuracy. - Fog is not forecast exactly at Lindenberg observatory but somewhat North of it. (figure 2 – observations, figure 3 – ALADIN postprocessed forecast)

ALADIN 2m-visibility is computed according to Gultepe et al. 2006, however using the 2 lowest model levels (figure 4) instead of (interpolated) 2m values of liquid water content.

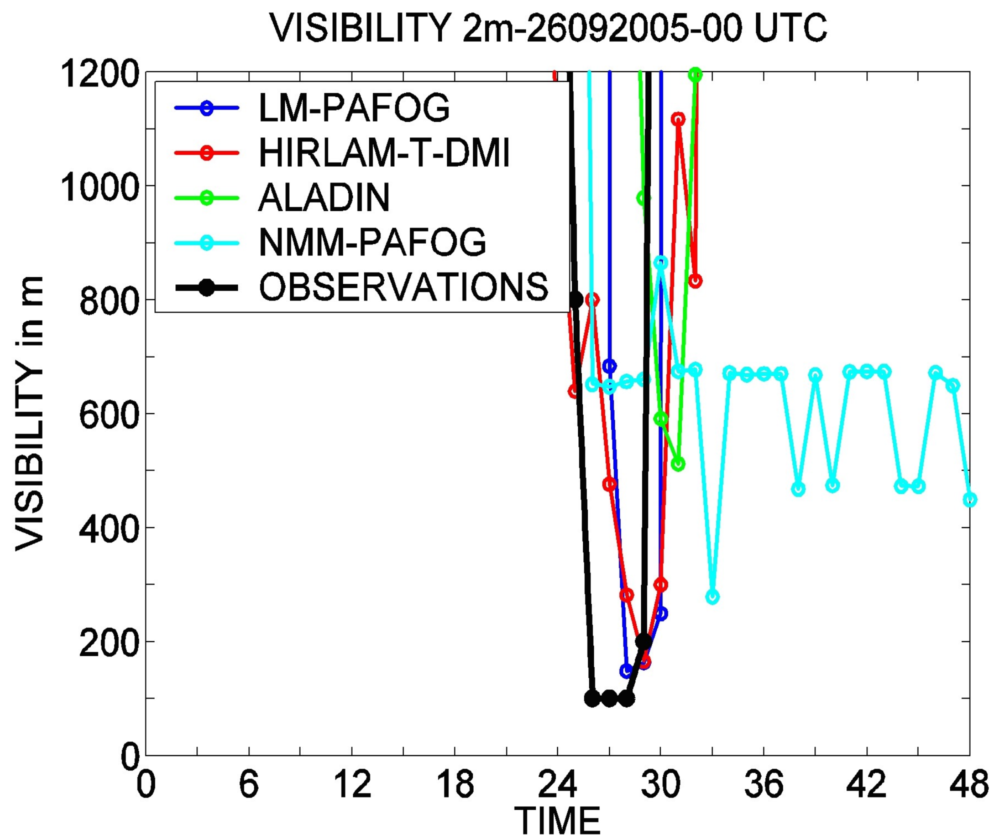


Fig.1: Model forecasts of 2m visibility (green curve is for ALADIN) at Lindenberg compared to observation curve (black curve)

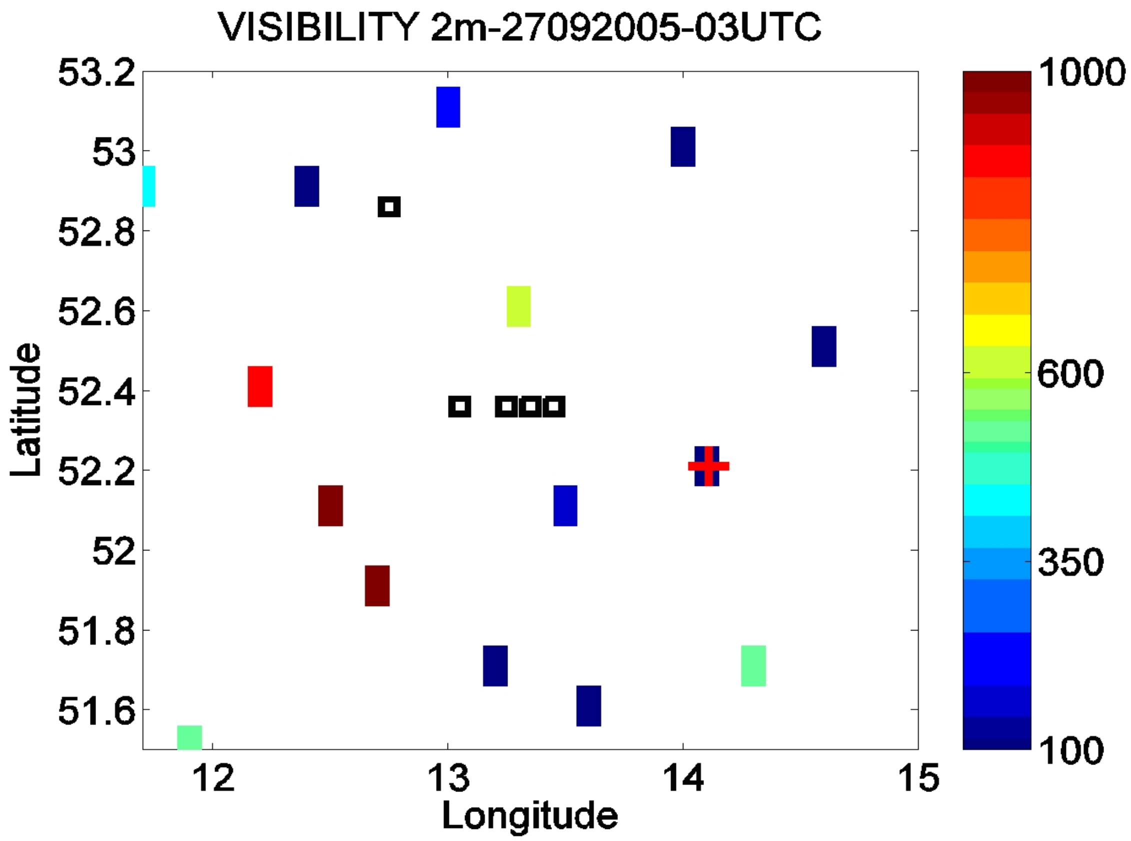


Fig. 2: network of 2m visibility measurements

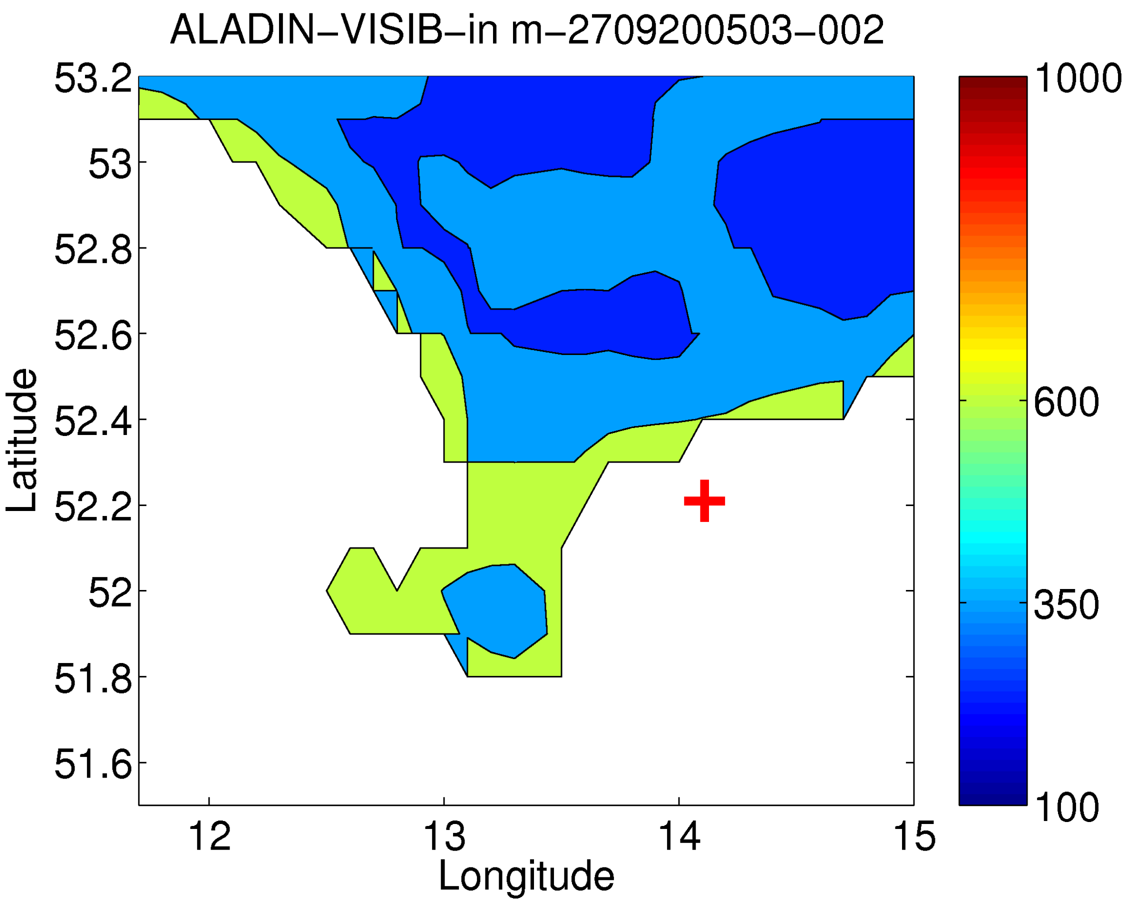


Fig.3: Visibility computed from ALADIN forecasts of liquid water content from combination of level 45 and level 44 (lowest model levels) values

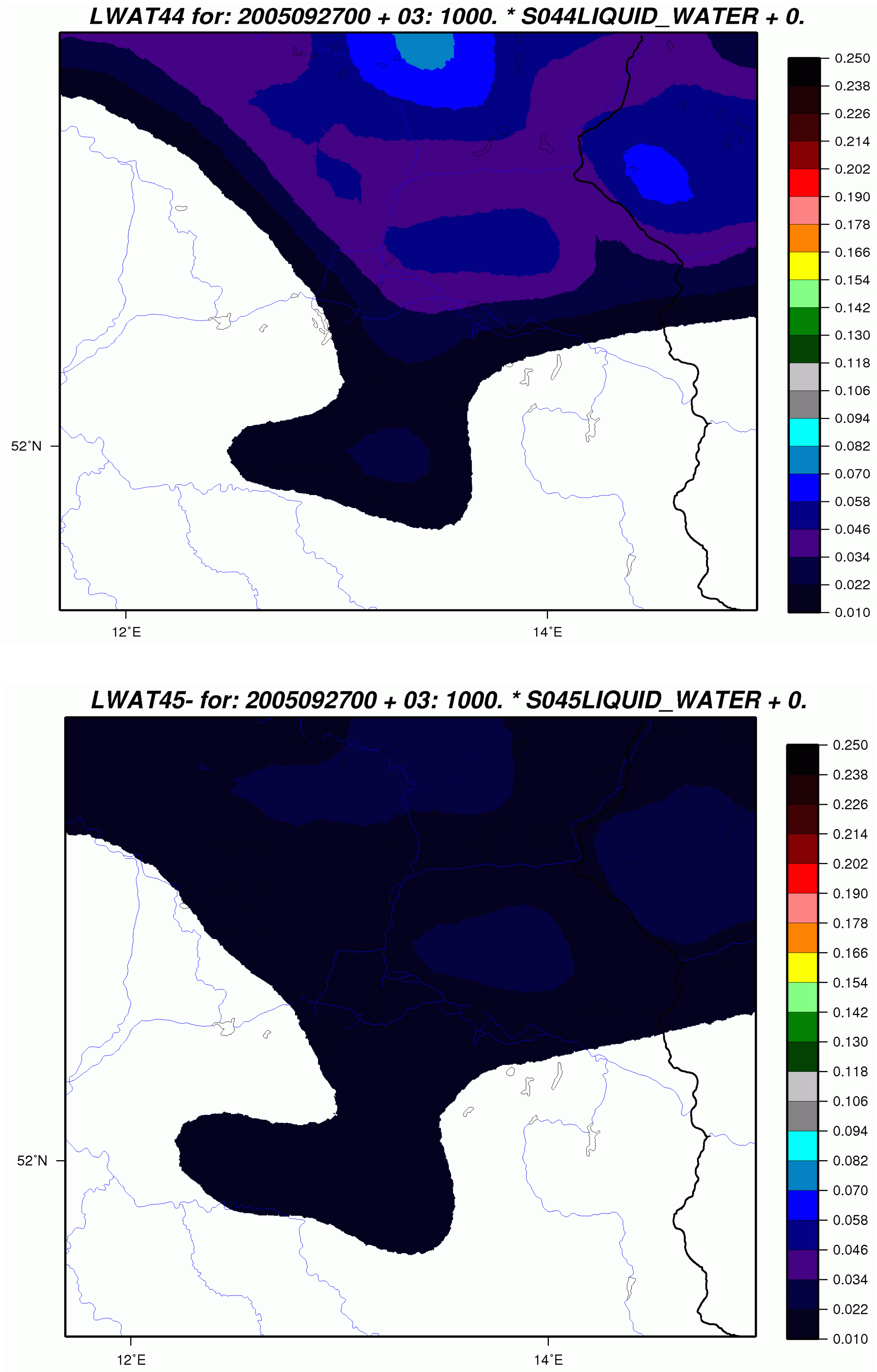


Fig. 4: ALADIN cloud liquid water [g/kg] at level 44 (top) and level 45 (bottom)

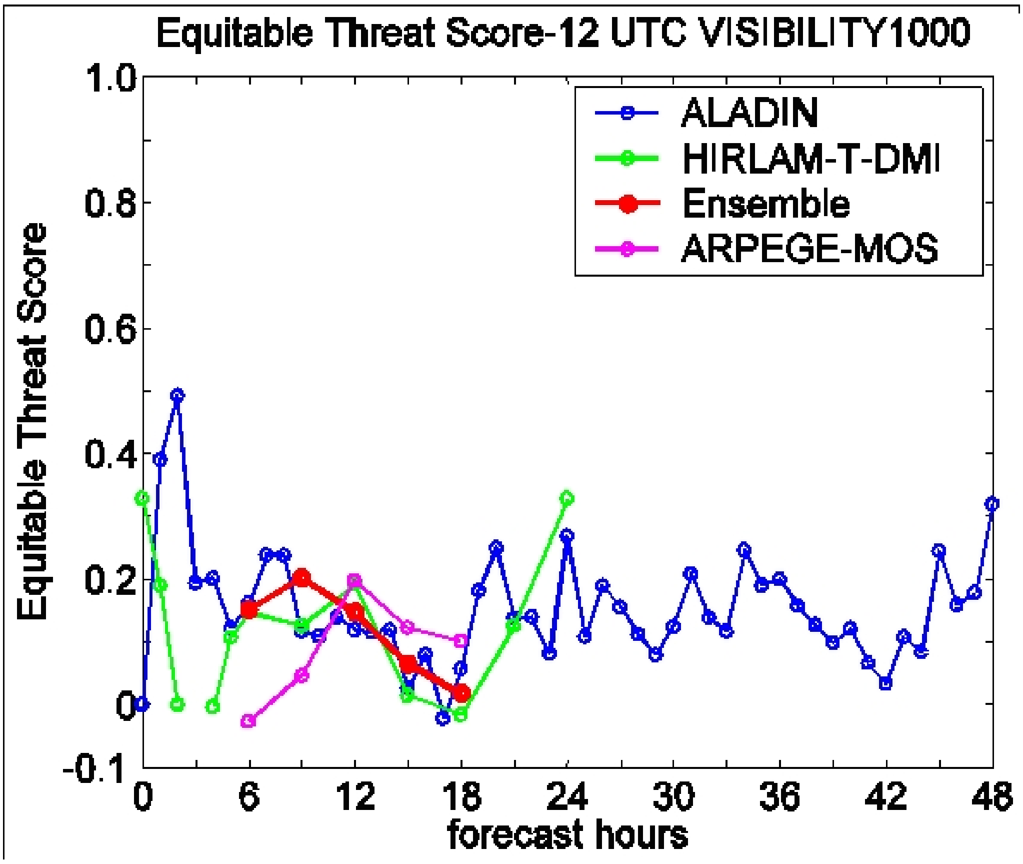


Fig. 5: Time evolution of equitable threat score (ETS) per forecast hour and per fog forecast model for a visibility threshold 1000m based on the forecasts initialized at 12 UTC

Equitable threat score for three months of validation at Lindenberg, Germany (figure 5) indicates the potential of ALADIN to reach relatively high performance in the shortest forecast range up to 2 hours while keeping some skill also for larger forecast periods. In contrary to the case studies these forecasts were computed from operational ALADIN/AUT version cycle 25 after some simple post-processing.


**Acknowledgements**

Many thanks to all colleagues participating in COST722, Lindenberg intercomparison, especially to Andreas Bott for coordinating and to Matthieu Masbou for compiling all together.


**References**


More results and also the individual contribution from ZAMG, entitled "Low stratus and fog forecast for Central Europe introducing an empirical enhancement scheme fo sub-inversion cloudiness" by Harald Seidl, Alexander Kann and Thomas Haiden can be found in COST722, 2007, final report: available online at:

http://www.staff.uni-marburg.de/~cermak/cost/final_report_cost722.doc

http://www.staff.uni-marburg.de/~cermak/cost/final_report_cost722.pdf

Gultepe et al., 2006: "Visibility parameterization from microphysical observations for warm fog conditions and its application to the Canadian MC2 model", Proceedings of the AMS meeting in Atlanta (January 2006)

### 4.7. LACE contribution to MAP D-PHASE

Sabine Leroch, Alexander Kann, Yong Wang (ZAMG)

#### 4.7.1. Introduction

D-PHASE (Demonstration of Probabilistic Hydrological and Atmospheric Simulation of flood Events in the Alpine region) is the forecast demonstration project (FDP) of the world Weather Research Programme (WWRP) using the achievements of MAP (Mesoscale Alpine Programme) to predict heavy precipitation and related flooding events in the alpine region. Where MAP addresses the entire forecast chain ranging from limited-area ensemble forecast, high-resolution atmospheric modelling, hydrological modelling and nowcasting. ALADIN AUSTRIA (deterministic run) as well as ALADIN limited area ensemble forecasting (LAEF) deliver contributions to the project within the D-PHASE operation period from 1 June to 30 November 2007. Grib files,warning files and several plots are generated for both models twice (00:00 and 12:00 UTC) a day and transfered to an archive in Hamburg (archive.dkrz.de) where the data is available to all project participants. In the following we present some of the generated results.

#### 4.7.2. Created Grib-files

- **Deterministic Model**

The ALADIN AUSTRIA has a horizontal resolution of 9.6km on 45 levels in the vertical. The D-Phase domain spans a region of 142x102 grid points with lon/lat coordinates at the left bottom corner of 2.53/42.94. The coupling frequency to ARPEGE amounts to 3 hours, simulation timestep is 415s.

Within the deterministic or so called driving model four different grib files are created by each model run using an output timestep of one hour and lead times of 48 hours. The FIX file containing constant single level fields related to the geological and geographical surface data of the domain like geometrical height of the earth surface, geopotential, land-sea mask and vegetation. The SURF file giving the simulated single level fields on the ALADIN topography including the surface pressure, 2m temperature, 2m specific humidity, wind-speed and gust, as well as all types of precipitation , low, middle and high cloudiness, boundary layer top height and the convective available potential energy. The TPT2 file giving the 2m temperature and the total precipitation needed to produce the alert files. The PLEV file containing all upper air fields on 8 pressure levels (1000, 925, 850, 700, 500, 300, 200 and 100 hPa) i.e. temperature, geopotential, wind velocity, relative and specific humidity.

- **ALADIN limited area ensemble forecasting (LAEF)**

The limited area ensemble prediction system has a horizontal resolution of 18km on 37 levels in the vertical. Its domain consists of a quadratic grid of 105x49 points with the left bottom corner at lon/lat 2.55/42.95. The coupling frequency to Arpege amounts to 6 hours, simulation timestep is 720s. LAEF consists in total of 16 ensemble members from which the ensemble mean is deduced. The output timestep is 3 hours with lead times of 48 hours. For each of the 16 members the four grib files (see above) are generated. The grib files for the ensemble mean are used to generate the plot files.

#### 4.7.3. Plots and Alerts

For a selected number of sites on the domain accumulated precipitation rates for 3, 6, 12, 24 and 48 hours are calculated, and if required (after comparison with a site typical allowed maximal precipitation rate) alert files are generated. Regions for which alerts are issued are marked by certain collors on the D-Phase domain monitored on www.d-phase.info. Below a selection of generated plots for Aladin-Austria and LAEF are given. All plots refer to the heavy rain event on July 10 2007 caused by a cold front crossing the domain from northwest to southeast from July 9 to July 10.

## ❑ ALADIN Austria

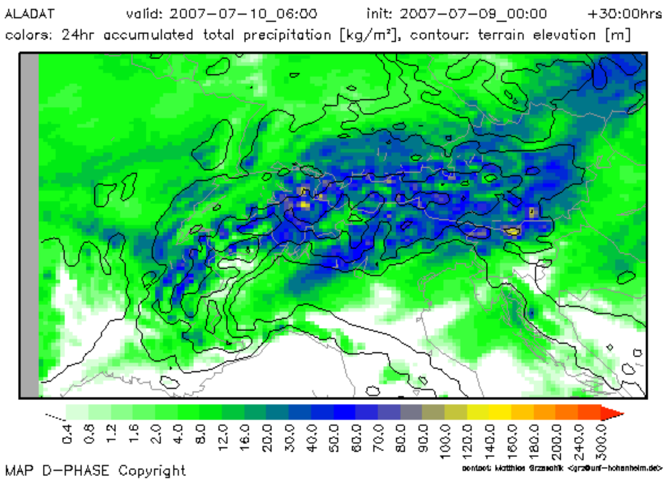


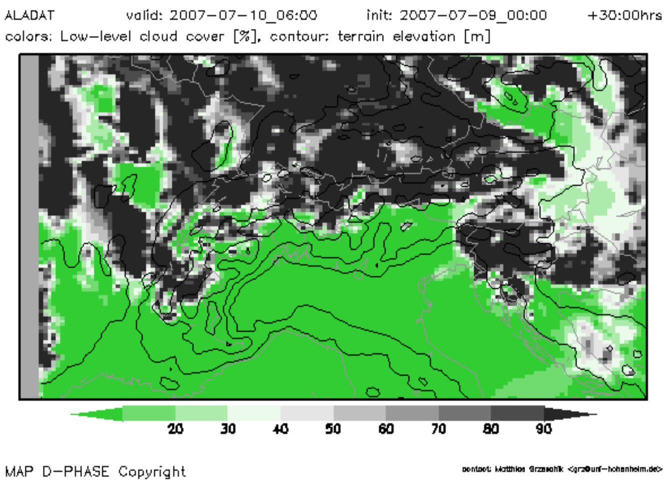

ALADAT valid: 2007-07-10_06:00 init: 2007-07-09_00:00 +30:00hrs
colors: 700hPa relative humidity [%], contour: 700hPa omega [Pa/s], vector: 700hPa horiz

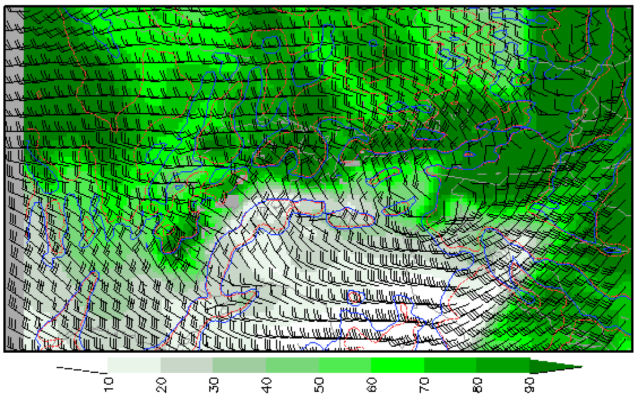


MAP D-PHASE Copyright

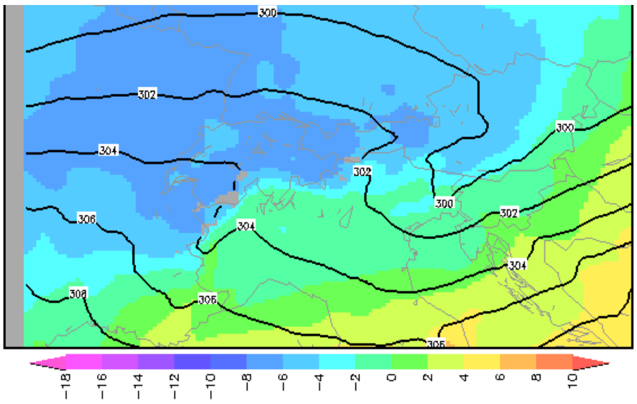


MAP D-PHASE Copyright

ALADAT valid: 2007-07-10_06:00 init: 2007-07-09_00:00 +30:00hrs
colors: 2m temperature [deg C], contour: Terrain elevation [m]

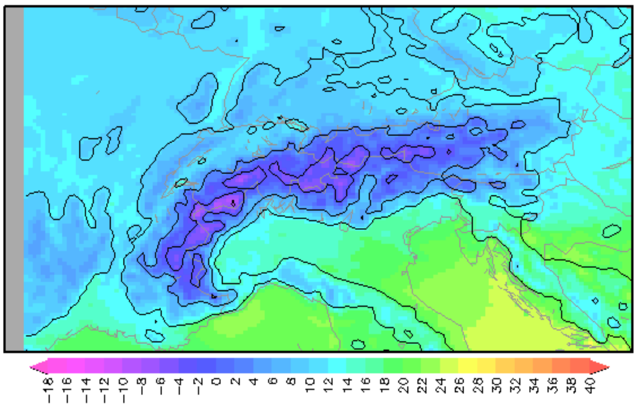


MAP D-PHASE Copyright

## ❑ ALADIN LAEF

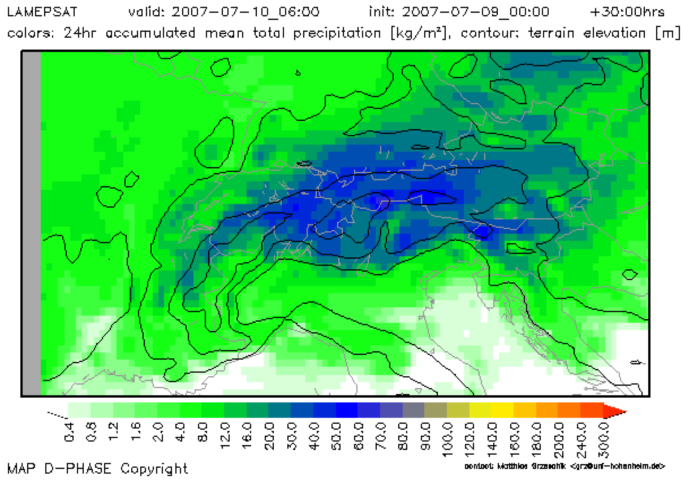


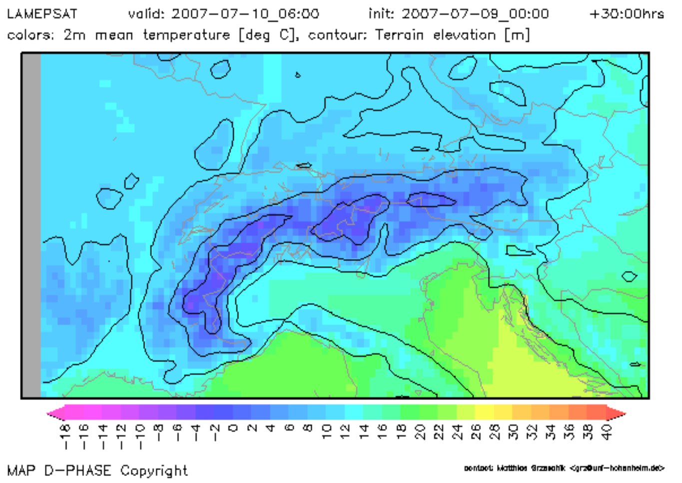


### 4.7.4. Summary/Outlook

MAP D-PHASE aims to establish a distributed real-time end-to-end forecasting system for heavy precipitation and subsequent flood events in the alpine region. In a first step probabilistic forecast provides first guesses for heavy rain events and its spatial distribution with lead times between 2 and 5 days. On this way so-called (pre)alerts can be issued. In a second step two days before the event happens, high resolution deterministic forecasts are performed for the alert region. The data from the deterministic forecast is then used to drive hydrological models. In the nowcasting range (0-6 hours before the event) finally the precipitation data is adapted to current measurements of radar and gauge stations giving new input for the hydrological models.

MAP D-PHASE should provide the end-user with both long pre-warning times through the use of EPS forecasts delivering probabilities for intense rain several days before it sets in and rather accurate data for short lead times produced by highly resolved nowcasting tools.

## 4.8. Evaluation of METEO-FRANCE Numerical Weather Prediction Models during AMMA 2006-SOP.

M. Nuret*, J-P. Lafore*, N. Asencio*, H. Bénichou***, O. Bock**, F. Favot*, T. Montmerle*, Y. Seity*

(summarized by F. Bouttier, please contact nuret@meteo.fr for the full version of this paper)

*Météo-France/GAME, Centre National de la Recherche Scientifique, **Centre National de la Recherche Scientifique, *** Météo-France

**Abstract**: *This preliminary study aims at evaluating the forecast skill of Météo-France NWP models operationally run during the AMMA SOP in 2006. The global models (~50 km) performed better than ALADIN LAM model at higher resolution (10 km) specifically deployed during the 4 months of the SOP. A specific problem is the increase of total precipitation with the resolution. CRM AROME model (2.5 km) improves the distribution and timing of precipitation, except for intense rain events (>20mm/day) that are too frequent.*

### 4.8.1. INTRODUCTION:

In order to fulfil the needs of the AOC (AMMA Operational Center) NWP centres (ECMWF, METEO-FRANCE, UKMO, NCEP/African Desk) and AMMA partners provided a wide range of analysis, forecasts products and specific diagnostics, made available to forecasters and AMMA scientists on the AOC-Web[1] site or through the Synergie RETIM-Afrique forecast system. The main objectives of this note are presenting and evaluating the forecasts operationally provided by METEO-FRANCE during the 4 months of the AMMA-SOP (June – September 2006). Only punctually we will present some results relative to ECMWF products.

METEO-FRANCE has operationally run 3 models:

- The global models ARPEGE with a stretched grid with its pole over France, resulting in a ~50km resolution over West Africa. The 4D-var assimilation is performed with a short cut-off (1hr) allowing forecasters to use output (available at +3hr in Africa) for the 2 daily briefings of 07UTC and 17UTC.
- The global model ARPEGE-Tropiques mainly differs from ARPEGE by its regular grid of ~50km and a longer cut-off (3hr) enabling the assimilation of more data than ARPEGE.
- The limited area model ALADIN-AMMA at a resolution of ~10km with a 3hr cut-off is initialized by a 3D-var analysis specifically tuned for this tropical domain. The Jb matrix error has been computed by Montmerle et al. (2005) from a set of twin lagged simulations over the AMMA domain over a 2 months period of the 2003 monsoon season. Specific developments have been made to assimilate the MSG-1 SEVRIRI radiances. As for ALADIN-France operational model, Quikscatt surface winds (over ocean) are assimilated with a significant positive impact. The ALADIN-AMMA domain covers the whole West Africa (Fig. 1) between 2°N and 24°N. It includes the major West African mountainous areas such as the Fouta-Djalloun to the SW (maximum elevation 1752m), Mont Cameroon massif to the SE (4095m) and to the North the Aïr/Hoggar (2918m).

A fourth model has been run on request (15 cases available) in almost real time for testing purposes. It corresponds to the next AROME operational high resolution system currently under development at Météo-France. Its 2.5km resolution allows explicit resolution of the deep convection. Initial conditions and lateral boundaries were provided by the ALADIN-AMMA analysis and forecasts respectively. The AROME domain covers a smaller area [6-16°N; 0°-10°E]

1 AOC web site address: http://aoc.amma-international.org/

including Bénin, South Niger and West Nigeria (Fig. 1). Simulations started at 00UTC and lasted 30hr.

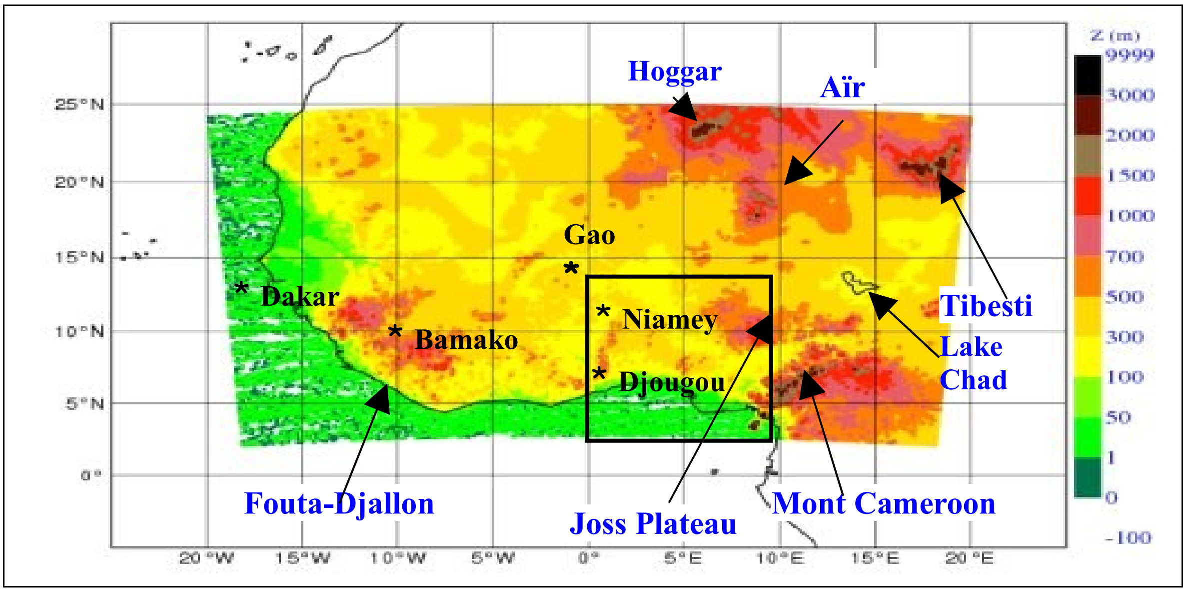


***Figure 1**: Topography map within the ALADIN-AMMA model domain. The AROME domain is also outlined, and major mountainous areas are indicated.*

After a description in section 2 of data that have been received in real time and assimilated at Météo-France, we will evaluate the forecasts over the West Africa domain. Conventional operational scores (NWP monitoring division DP/PREVI/COMPAS) comparing models with observations (TEMP, SYNOP) are presented in section 3. Section 4 compares forecasted precipitation to a precipitation satellite estimate. In section 5 the Integrated Water Vapor (IWV) retrieved from 3 GPS surface stations on meridional transect (Djougou, Niamey and Gao) provided by Bock et al. will be used as an independent set of data for comparison with forecasts. Finally in section 6 an evaluation in term of Quantitative Prediction Forecast (QPF) is proposed, with emphasis on the AROME model. Main conclusions are drawn and some recommendations are proposed in section 7.

### 4.8.2. DATA RECEPTION

The number of information entering the assimilation system in real time have been significantly increased during the 4 months of the SOP in 2006. Most notable events include:

**SYNOP-SHIP** (a): 10m wind (over sea), mean sea level pressure (MSLP), T2m and Hu2m are used. The number of messages received dropped mid of August 2006 due to a failure of the Niamey telecommunication center. It increased later on. Up to 200 messages are received at 12UTC.

**SATOB**(c): satellite wind vector are used. The failure of MSG-1 end of September 2006 is a major event.

**DRIBU**(d): MSLP, 10m wind and T2m from buoys are used. There is a strong increase of the number of received messages beginning of July 2006 (from 10 in June 2006 up to ~40 messages in July 2006 and after) as a consequence of the EGEE campaign in the Gulf of Guinea.

**TEMP**(e): corresponding to the soundings network strongly reinforced since 2006 beginning due to the AMMA major effort. T, Hu and wind from all sounding levels are used. Roughly 10 soundings at 00UTC were already received in June 2006 at the SOP beginning; either a doubling as compared with previous years. The 2 periods of reinforcement of the sounding frequency (up to 8/day) can be identified by an increase of soundings received in June (20-30) and August ($1^{st}$ –$15^{th}$) with a maximum of 20 received messages for the 12UTC slot. Later (September 2006) the number of received messages is similar to June 2006.

**PILOT**(f): corresponding to low levels wind profiles. In June 2006, 5 messages per slot were received; there was a constant increase up to 15 messages beginning of August 2006, which stabilized later on at 10 messages/slot in September 2006. Wind at all levels from the sounding are used.

**RADIANCES**(g): the number of radiances was fairly constant during the 4 months period (polar orbiting satellite + MSG-1). The failure of MSG-1 end of September 2006 is noticeable.

### 4.8.3. COMPARISON TO RADIOSONDES AND SYNOP

The operational scores performed at Météo-France by the NWP monitoring division COMPAS have been computed for the 4 months period for ARPEGE and ALADIN-AMMA analysis and forecasts. Results of these scores are presented for 2 different initial times (00 and 12UTC). The relative performance of the 2 models is discussed in this section as compared with the radiosondes and synop observations. The models biases and root mean squares (rms) relative to observations correspond to straight lines and to lines with * respectively.

- ❑ **Comparison to radiosondes:**

About 1000 TEMP messages over the 4-months SOP period have been used to compute the statistics documenting the behavior of the models (ALADIN-AMMA, ARPEGE) against soundings as a function of forecast range. We should nevertheless keep in mind that it is believed that humidity measurements from some soundings are themselves biased (Vaïsala RS80 sondes – see AMMA-EU[1] deliverable D4.1.1.d: Report on sondes statistics by Agusti-Paraneda 2006).

- ☑ **Temperature (Fig.2):**

00UTC run: <0 bias (analysis too cold), increasing with forecast range –maximum in lower and upper troposphere, minimum in mid-troposphere. At initial time the bias is stronger in ALADIN-AMMA than in ARPEGE; this difference decreases with increasing forecasting range. ALADIN improves the rms at the analysis, but they are similar in both models for the forecast.

12UTC: >0 bias (analysis too warm) at 1000hpa, and then small weaker <0 bias than the one observed for 00UTC runs.

1 https://www.amma-eu.org/ workspaces/work_package_s_workspace/tools-methods/wp4_1/deliverables/

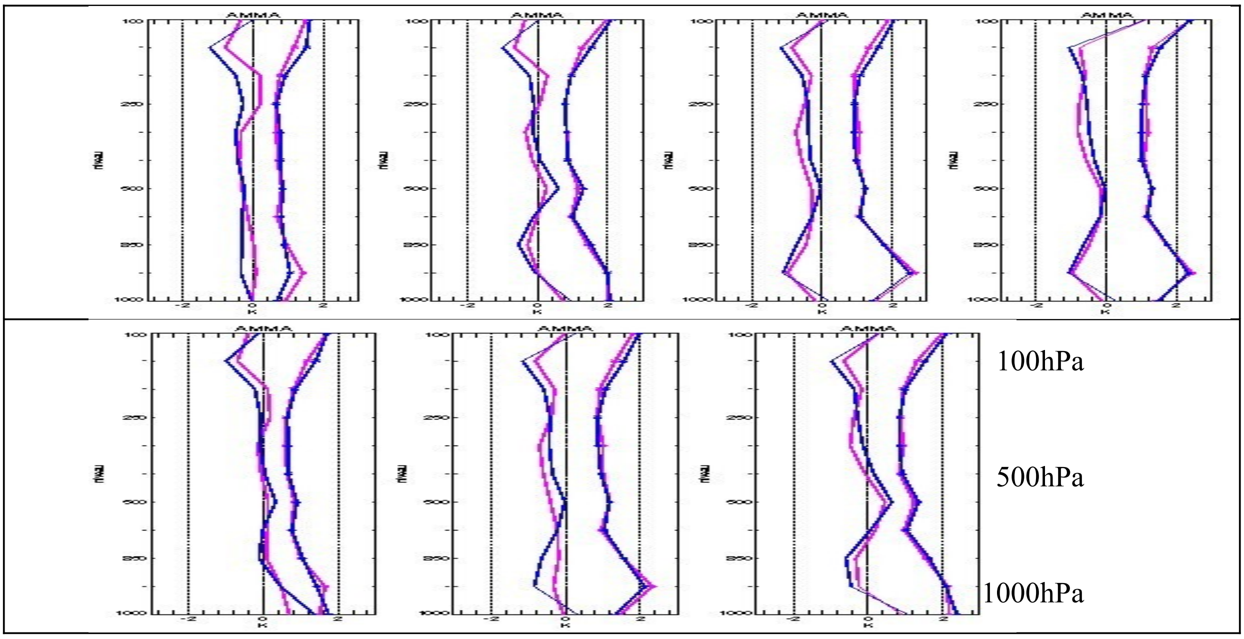


**Figure 2**: Vertical profiles of the temperature bias and rms for ARPEGE (pink) and ALADIN-AMMA (blue) models against TEMP (radiosondes). Runs starting at 00UTC (ranges 00, +12, +24, +48 hours - upper row) and 12UTC (ranges 00, +12, +24 hours - lower row). Vertical lines correspond to –2°C, 0°C and +2°C.

☑ **Relative humidity:**

Negative bias (analysis too moist) above 400hpa at initial time (00 and 12UTC runs). Both models are too moist in the lower and upper troposphere; bias reaching +10% in the lower troposphere at 24 hours range.

☑ **Wind speed:**

A weak negative bias (maximum ~ -1m/s) is found at analysis time (00 and 12UTC). During the forecast the bias becomes more or less neutral; one can notice a low level (~950hPa) positive bias at 00UTC (+24 hour range forecast of the 00UTC run and +12 hour range forecast of the 12UTC run).

The rms increases quickly with the range (4 m/s at 24hr range).

ALADIN improves a little the rms for the analysis, but the forecasts are not improved.

☑ **Wind vector difference module :**

A mean difference of 1.5m/s at analysis time increasing to 2m/s (+12 hour range) and then 4m/s in lower and upper troposphere (+36 hour range) is found. Score is better for ALADIN-AMMA analysis, worse for ALADIN model. Same conclusions for the 12UTC comparison.

In the models 2 maxima appear: one in the lowest level (925 – 850hPa) and one in the upper levels (200hPa, corresponding to the TEJ). At the AEJ level (~600hPa) there is a relative minimum discrepancy.

❑ **Comparison to SYNOP**

About 5000 SYNOP messages have been used to perform the statistics.

A positive bias is noticed ( ~ +0.5hPa increasing to +1hPa with increasing forecast range); it is slightly weaker in ALADIN-AMMA than in ARPEGE. A diurnal cycle of the error is observed with a maximum at 06UTC.

The rms increases with time (1 to 2 hPa) with a slight improvement for ALADIN.

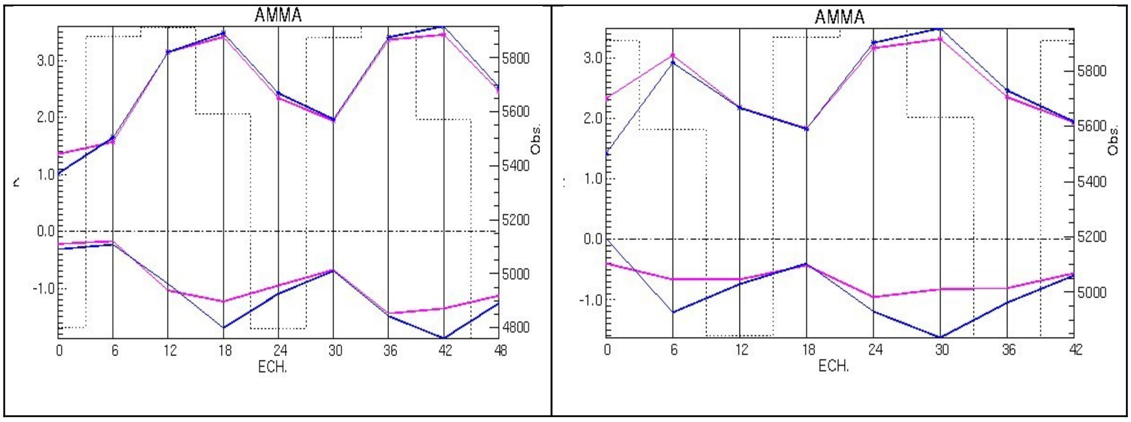


**Figures 3 and 4**: Evolution as function of the forecast range of 2m temperature bias and rms for ARPEGE (pink) and ALADIN-AMMA (blue) models against the SYNOPs. Left and right panels correspond to runs starting at 00UTC and 12UTC respectively. Bars and right axis correspond to the number of observations involved in the comparisons.

### ☑ 2m Temperature (Fig.3 and 4)

A <0 bias is observed in the analysis (too cold). It strongly increases with forecast range (-0.5°C to -2°C). The maximum bias occurs at 18UTC (00UTC and 12UTC runs) and is slightly weaker in ARPEGE than in ALADIN-AMMA.

The diurnal cycle of the rms is strong, also maximum at 18UTC corresponding to the maximum of convective activity. ALADIN doesn't improve the rms except for the analysis.

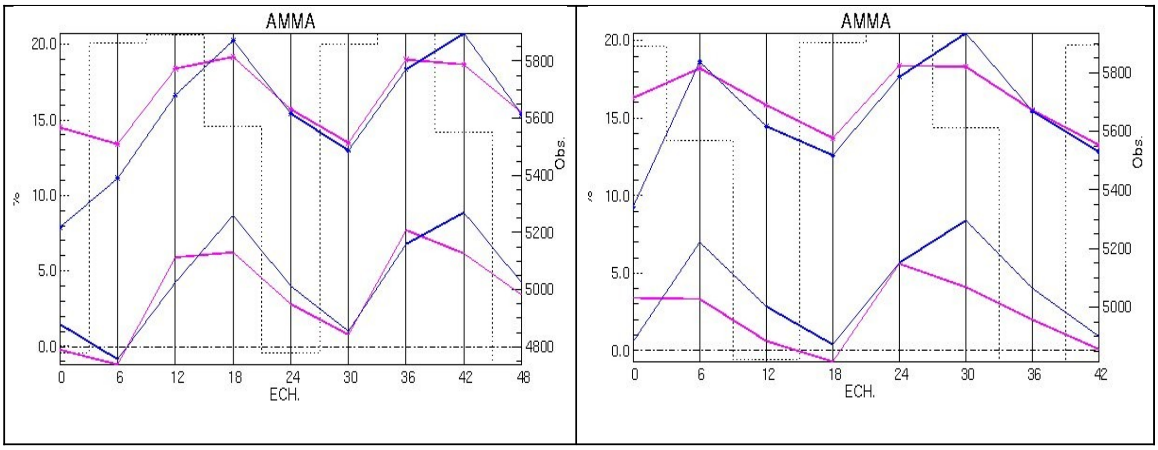


**Figure 5:** same as Fig.3 but for **2m humidity.**

### ☑ 2m Humidity (Fig.5):

The ALADIN analysis is clearly improved, but it is lost by the forecast after 12 hr range. The bias is positive, it increases with time and even more for ALADIN.

As for temperature the diurnal cycle of bias and rms is intense for humidity, and maximum at 18UTC, probably in relation with the diurnal cycle of the convection. It should be noticed that the rms and bias maxima occur later for ALADIN.

☑ **Wind direction :**

Similar weak biases (±5°) for both models but large rms (50° to 60°) although slightly greater for ALADIN. It may be related to a weak wind regime prevailing at the surface.

☑ **Wind speed :**

Positive bias (~ +1m/s) with a strong diurnal cycle maximum at 06UTC. Better results for ALADIN (bias and rms).

❑ **Comparison of ALADIN-AMMA to ARPEGE:**

The figures below display the evolution of the profiles of the differences between ARPEGE and ALADIN for different variables (those statistics are not available for ARPEGE-Tropiques). Improvements (degradation) of ALADIN relative to ARPEGE correspond to areas with blue (red) isolines on these figures.

☑ **Temperature :**

Some improvements can be noticed for the temperature field (mainly in the mid-troposphere for all forecast ranges), but degradation is found in lower and upper troposphere.

☑ **Humidity:**

The bias is weakly reduced by ALADIN only for the upper troposphere (250-500hPa) at all ranges greater than 12hr from 00UTC runs. For all others cases a negative impact is found; i.e. too much moisture in ALADIN forecasts.

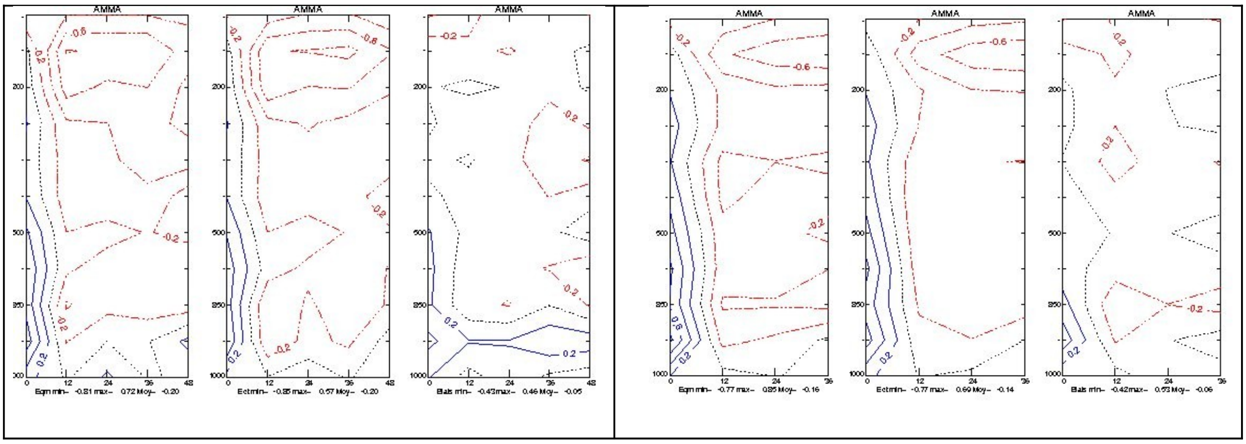

**Figure 6:** same as Fig. 12 but for **vector wind difference**.

☑ **Wind field (Fig. 6):**

Clear improvements can be seen at any analysis time (00 and 12UTC), but as forecast range increases ALADIN performs slightly worse than ARPEGE.

In summary, those comparisons show that the mesoscale analysis (ALADIN-AMMA analysis) has a better fit to the observations than the ARPEGE analysis, but the scores also show that the ARPEGE model performs better than the ALADIN model. In other words the highest resolution (10 km) doesn't allow improving the forecast skill of ALADIN LAM model over the West Africa as compared with global model ARPEGE.

❑ **Analysis increments:**

Monthly mean analysis increments for the humidity field have been computed (guess-analysis) for ARPEGE model

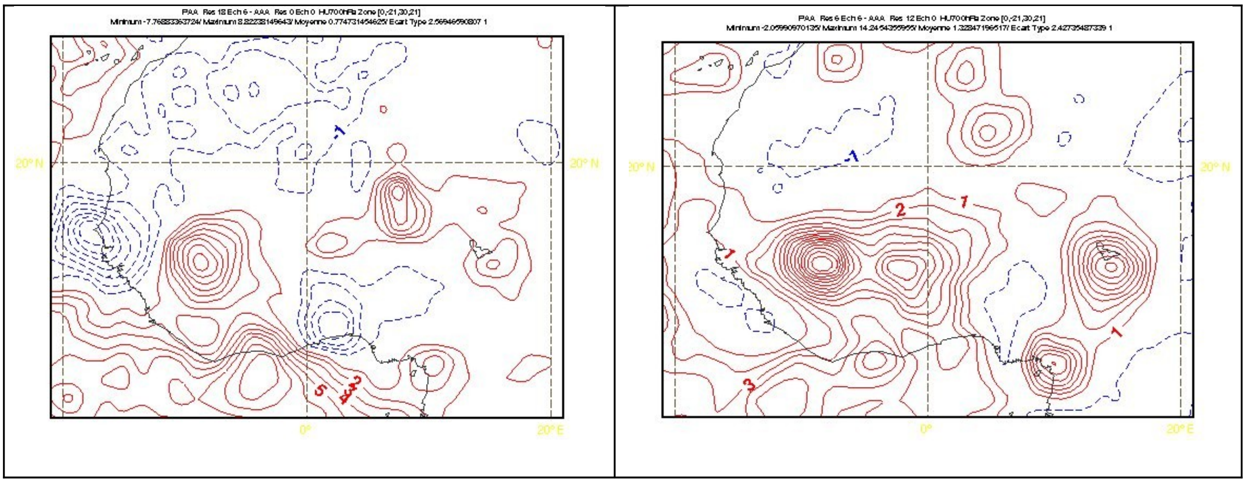


**Figure 7:** Monthly mean ARPEGE analysis humidity increment (guess-analysis) at 700hPa (1% isoline interval). Left column for 00UTC, right column for 12UTC ; in September.

Positive increments on Fig.7 (red isolines) indicate a guess moister than the analysis (i.e. analysis drier than the guess) due to the assimilation of observation. Blue isolines indicate the reverse. Even at a month scale the analysis increment field stays strong with spotty structures centered at some radiosondes locations. It could be related to bad model skills depending on the weather situation changing during the season. For example in June at 00UTC, there are no intense structures of increments contrary to other months during the active monsoon period. Nevertheless systematic positive humidity increments (red targets on Fig. 16) are detected at some location such as: Bamako (Mali), Tamale (Ghana) and in a lesser extent at the sounding Cameroon stations (Douala, Ngaoundere). At these locations these large discrepancies between the guess and the analysis could be a trace of a well-known problem of dry bias in the sounding measurements currently examined at ECMWF. Douala may be concerned by an orographic representativity problem (proximity of Mt Cameroon). Also it should be noticed that the analysis increment exhibits a strong diurnal cycle with larger increments at 12UTC (up to 15% at Bamako) than at 00UTC. Some blue targets appear from time to time mainly centered on Dakar at night.

In short the analysis of humidity increment confirms that some sondes exhibit an intense dry bias that can dramatically reduce the moist energy at some location in the analysis. As it may strongly affect the forecast skill of convection, it is a priority to correct such bias for the further AMMA studies as undertaken at ECMWF. Results displayed in the present note should be carefully examined at the light of this bias and it will prevent us drawing general conclusions.

### 4.8.4. EVALUATION OF PRECIPITATION

Precipitation estimates provided by NOAA/CPC (RFE2) (Laws et al., 2004) are used to evaluate the precipitation forecasts of METEO-FRANCE and ECMWF. These data correspond to daily estimate (from 6UTC to 6UTC following day) and are available at a resolution of 10km.

Precipitation forecasts corresponding to the 00UTC run (i.e. difference between the +30hr and +6hr forecast ranges) are evaluated here. All data have been interpolated onto a regular 1°x1° degree grid.

From the CPC data plotted on Fig. 8a, one can see two maxima associated with orography (Fouta Djalloun and Mount Cameroon on the western and eastern part respectively) separated by a region of weaker precipitation in the southern central part of the domain (10°W, 5°E). The northern part of the domain (Sahel) is characterized by a strong north-south gradient of precipitation localized along ~10°N.

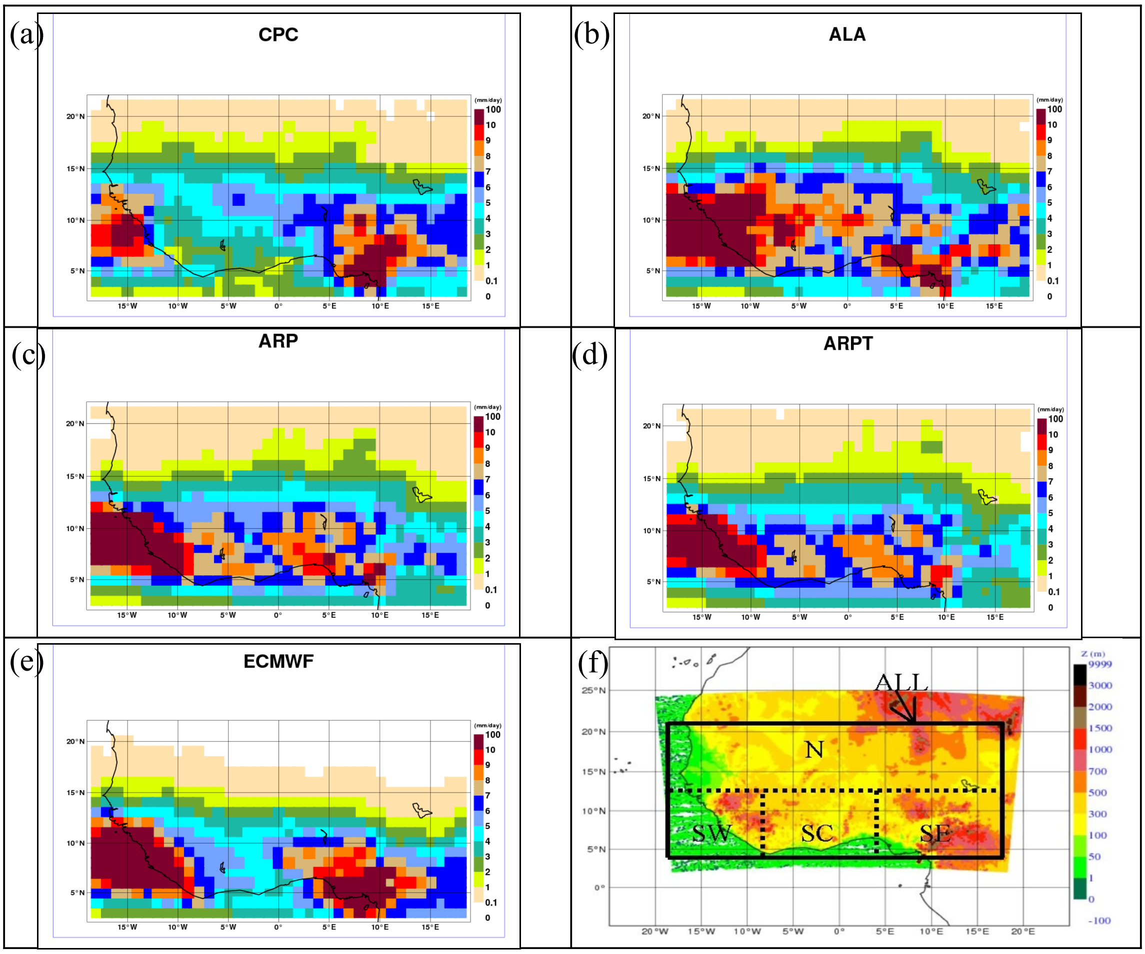


**Figure 8**: *1°x1° box averaged daily rain rate (mm/day) for the 4 months period (June-September 2006) as (a) estimated by CPC and forecasted by (b) ALADIN, (c) ARPEGE, (d) ARPEGE-TROPIQUE and (e) ECMWF. Orography of West Africa on the ALADIN domain with the geographical partitioning used in Table 1 (ALL, N, SW, SC, SE) is shown on (f).*

The 4 models reproduce the main features of the averaged precipitation field, particularly the position of the north-south gradient zone along 10°N, but some systematic errors can be noticed (Fig. 9):

b) Too much precipitation on the Fouta-Djalloun mountains (western part of the domain), but too less on the Mount Cameroon mountains (eastern part) except for ECMWF.
c) Too much precipitation in the south central part (west of 5°E) except for ECMWF, and not enough precipitation east of 5°E.
d) Southward shift of the gradient zone in ECMWF

This excess of precipitation noticed over the Fouta-Djalloun for all global models is magnified in the ALADIN-AMMA LAM model as confirmed by Fig.18. Over the rest of the domain, the behavior of the 3 models is quite similar, except the northward penetration of precipitation over Sahel is better represented with ALADIN than global models.

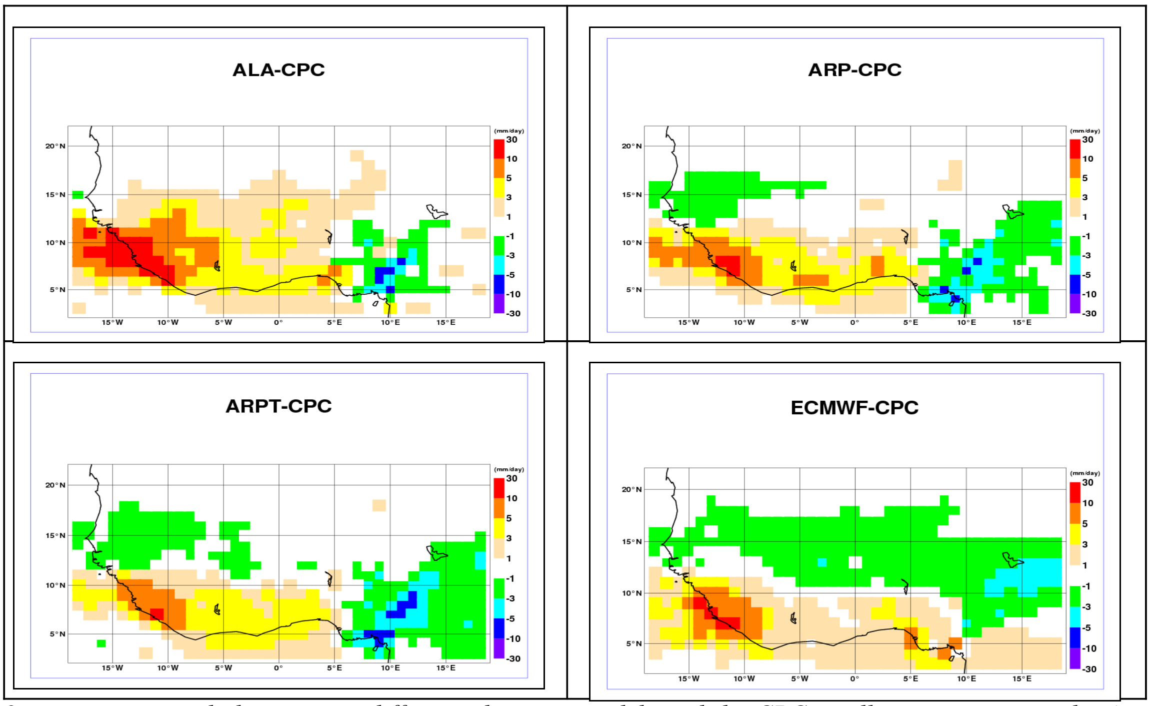


**Figure 9:** *average mean daily rain rate difference between models and the CPC satellite estimate over the 4 months period (June-September 2006).*

The correlation and biais have been computed between observed and forecasted precipitation for the 4 months period. Those have been computed for the whole domain (ALL line) and for the geographical zones shown on Fig. 17.f (N, SW, SC, SE). Concerning METEO-FRANCE models, the best correlation over the whole domain (ALL) 0.29 is obtained by ARPEGE-Tropiques (0.27 for ARPEGE, 0.28 for ALADIN). In term of bias there is a clearer signal with global models giving the best results (+1% for ARPEGE-Tropiques, +11% for ARPEGE) while ALADIN-AMMA is clearly strongly biased (+42%).

Similar scores have been computed for ECMWF. It clearly indicates that ECMWF precipitation forecast skill (correlation=0.35, bias= +3%) is better over the whole domain. The only main deficiency well knowed by African forecasters concerns the Sahel region where ECMWF has a negative bias of precipitation.

Figure 10a shows the seasonal evolution in 2006 of the daily rain rate averaged over the whole ALADIN-AMMA domain (dashed curve), and its 15 days average (thick curve). The mean rain seasonal cycle in 2006 is characterized by a minimum (2mm/day) beginning of July and a maximum (5mm/day) in August up to mid-September. Fig 10b illustrates the behavior of the different models. ALADIN clearly exhibits a positive bias ~2mm/day), whereas global models are closer to the CPC estimate. The mean seasonal cycle is well captured with the weak activity period end of June and beginning of July, except the mid-August maximum. A surprising feature is the decrease in precipitation rate noticed for all models mid-August. We have no explanation for this behavior shared by models having very different characteristics (resolution, parameterizations, assimilation systems). We nevertheless note that this period corresponds to the maximum of absolute number of available data assimilated in real time. Further studies (reanalysis and impacts) using the maximum of data collected during the whole SOP after the correction of humidity bias, are needed before concluding on the origin of  this behaviour.

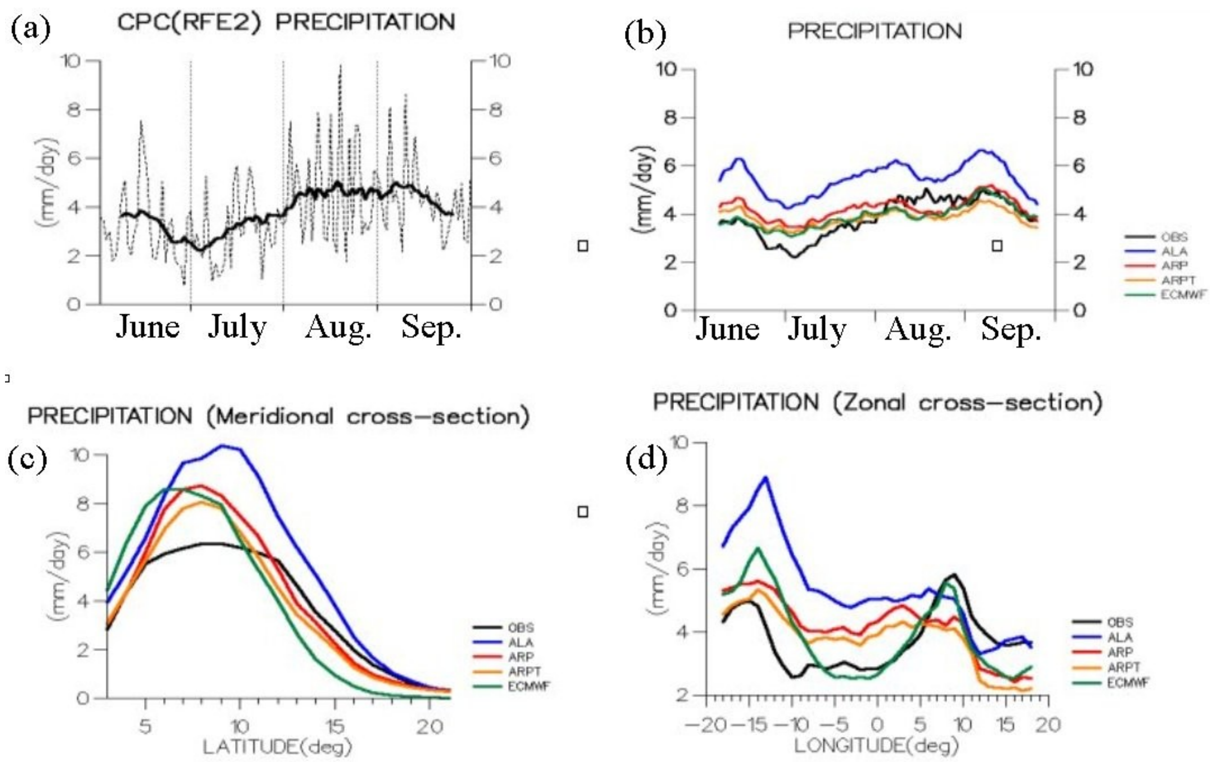


**Figure 10:** *(a) temporal evolution of the daily estimated rainfall (CPC/RFE2)(dashed black curve) and 15 day average (thick black curve); (b) temporal evolution of the 15 day average for the different forecasts and the estimate; (c) meridional and (d) zonal mean distributions.*

The mean meridional profiles (Fig.10c) allow analyzing the ITCZ position and the northward penetration of precipitation over the continent. All models produce more precipitation (8-10 mm/day) than the satellite estimate (6 mm/day). Whereas the satellite estimate exhibits a “plateau” shape between 5° and 12°N, all models forecast a “peak” shape ITCZ maximum. The ITCZ mean location provided by ARPEGE models agrees with satellite estimate (8°N), whereas it is shifted southward along the coast (6°N) by the ECMWF and northward (9°N) by ALADIN. This ECMWF southward shift of precipitation is true also for its penetration over the Sahel. For this point Météo-France models fit better with observations.

The mean zonal profiles (Fig.10d) of daily precipitation clearly describe the models behaviour. ECMWF performs very well for the mean zonal profile except some overestimation over Fouta-Djalloun. On the contrary all Meteo-France (MF) models have difficulties for the zonal distribution. Global models have not enough zonal variability (flat profiles). ALADIN LAM model increases this variability, but adds a strong positive westward trend. It corresponds to a strong positive bias localized close to the Fouta-Djalloun mountains (~15°W) and a weaker negative one on Mt Cameroon area (10°E). All MF models failed in predicting the region of weaker precipitation in the central part of the domain (10°W – 5°E). From Fig. 10d the positive precipitation bias of ALADIN previously noted, is clearly identified.

In short the skill of MF models in predicting precipitation is low and again the higher resolution (10 km) doesn’t improve and tends to increase the positive bias. ECMWF skill is better except its tendency to drift southward the ITCZ at short range (1-2 days).

### 4.8.5. GPS EVALUATION:

The available GPS network for the SOP (Bock et al.,2007) is composed of 6 stations localized on two south-north meridian transects. The first transect has been installed in June 2005. These stations are located at: Djougou (9.7°N), Niamey (13.5°N) and Gao (16.25°N). The second transect has been installed in April-May 2006. These stations are located at Tamale (9.6°N), Ouagadugu (12.4°N) and Timbuktu (16.7°N). The GPS data permit documenting the variability in total column water vapor (IWV hereafter) from sub-diurnal to intra-seasonal time scales. As these data were not assimilated, those represent an interesting independent dataset for validation.

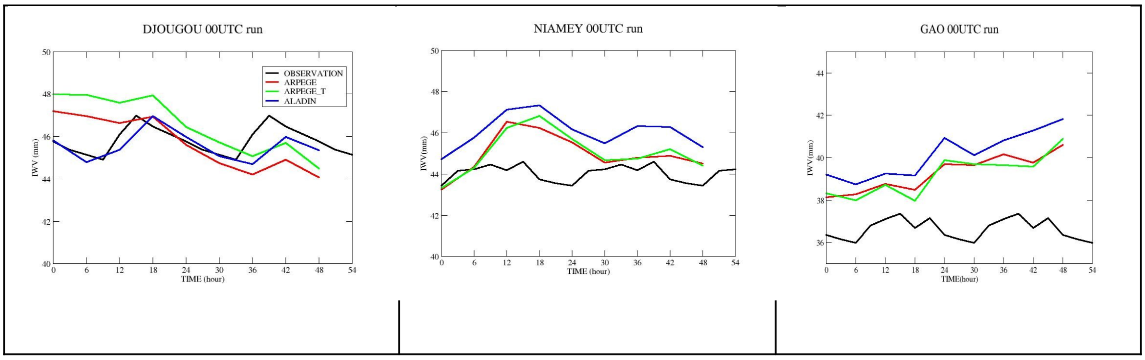


**Figure 11:** *Mean diurnal Integrated Water Vapour (IWV in mm) cycle over the 4 months SOP period (June to September 2006) computed from the GPS station of Djougou (left panel) Niamey (central panel) and Gao (right panel) in black. In colour, model IWV as a function of the forecast range at the GPS location (nearest grid point) (in red ARPEGE, in green ARPEGE_T, in blue ALADIN) . Runs initialized at 00UTC.*

Available GPS observations (3 hours sampling) have been averaged to get the mean daily cycle, which is plotted in, black on Fig 11. As expected the mean IWV decreases northward (~ 46mm at Djougou, ~ 44mm at Niamey, ~ 36.5mm at Gao). As described by Bock et al. (2007), the diurnal cycle is stronger in Djougou (2mm), and weaker if any, at Niamey and Gao (~1mm). The maximum IWV is generally observed at ~15UTC and the minimum in the morning around 06UTC (but 00UTC at Niamey). Except advection, the latent heat surface flux and the precipitation are the major source and sink of IWV respectively. The mean IWV diurnal cycle mainly results from the non-phasing of these processes: *i.e.* precipitation tend to occur after the latent heat fluxes diurnal maximum.

When comparing models with observations the elevation difference must be taken into account for the comparison of IWV; 100m elevation difference between observation and model corresponds to 1 to 2mm IWV difference (the lower elevation, the greater IWV).

- Djougou: observation elevation 436m (ARPEGE: 468m, ARPEGE_T: 440m, ALADIN: 421m). This is the location where a diurnal cycle of the IWV is clearly observed. A good fit is observed between GPS data and ALADIN model. The diurnal cycle (amplitude ~2 mm in the observation) is well captured by models. A clear negative trend (drying) in IWV with increasing forecast range is seen in ARPEGE and ARPEGE_T.
- Niamey: observation elevation 223m (ARPEGE: 248m, ARPEGE_T: 229m, ALADIN:229m). A strong positive bias in ALADIN (2 to 3 mm), almost no bias in ARPEGE and ARPEGE_T. Some diurnal cycle is noticeable in runs initialized at 00UTC, no diurnal cycle from 12UTC runs.
- Gao: observation elevation 260m (ARPEGE: 301m, ARPEGE_T: 317m, ALADIN: 233m). Models are positively biased (models too moist), and the bias is increasing with forecast range (moistening); for ALADIN the magnitude of the bias (3 to 4mm)

is meaningful since the elevation difference is close to 0m. No realistic diurnal cycle of the IWV is simulated in the models.

This comparison suggests that models have great difficulties in reproducing the weak observed IWV diurnal cycle in the Sahel region (Niamey, Gao). It could be related to the well-known failure of models to a get the good timing of the convection (too early) (Yang and Slingo, 2001). The drying and moistening trends noted to the South and to North respectively, may correspond to the northward drift of the ITCZ in the model with increasing forecast range as already noticed in section 4.

### 4.8.6. AROME evaluation (QPF):

The new AROME model has been run more or less regularly during the summer 2006 AMMA SOPs (on alert) up to 30 hr with initial conditions interpolated on to the 2.5km grid from the ALADIN-AMMA analysis (10km resolution). This domain (Fig. 1) is characterized by low elevation except over Nigeria with the Joss plateau (elevation reaching 800m).

The evaluation of this type of Cloud Resolving Models (CRM) is not a trivial task, for many reasons: difficulties to define relevant score at fine scales, lack of observation network at a fine scale, higher variability at smaller scale and decrease of the predictability. Here we thus want to present some attempts to evaluate this model and compare it with current operational models still using convection schemes.

First a subjective analysis of the forecasted precipitation patterns has been made by forecasters and scientists on the field. The main conclusions are: in most of the cases (~50%) AROME proposes a scenario similar to the one of its coupling model ALADIN with a weak to moderate improvement, the cases of degradation are rare (~10%), sometime the scenario is different (localization, timing) and better (~40%). The rain distribution appears more realistic with more areas without any precipitation, but a strong precipitation positive bias exits. The life cycle of rainy events is improved with a better propagation. This subjective appreciation will be confirmed by the following objective analysis based on scores.

In the following we will concentrate on the evaluation of the precipitation forecasted by AROME. All together 14 days from August 2006 can be used for precipitation validation (forecast reaching 30 hr range): 24 hr cumulated rainfall amount estimated by NOAA-CPC can be compared to the models value (F30-F06, runs starting at 00UTC) hence outside the spin-up period. The forecasted precipitation and satellite estimate are averaged on an inner 1°x1° latitude-longitude grid (7°N-16°N, 1°E-9°E) for the 14 days.

Statistics have been computed between the CPC estimation and the model values, all averaged on the 1°x1° grid; the size of the sample is fairly small (1260) but it seems that AROME exhibits a strong bias in term of precipitation (+77%) whereas the other models (ALADIN-AMMA, ARPEGE_T) are well balanced (see Table 1). For the correlation the scores are quite low but the best result is achieved by ARPEGE_T (standard deviation of the correlation coefficient is 0.02).

| | **CPC** | **ARPEGE_T** | **ALADIN-AMMA** | **AROME** |
|---|---|---|---|---|
| **Mean precipitation** | 6.0 mm/24hour | 5.6 mm/24hour | 5.6 mm/24hour | 10.6 mm/24hour |
| **Bias** | | -7% | -7% | +77% |
| **Correlation** | | 0.21 | 0.19 | 0.16 |

**Table 1:** *Mean precipitation, bias and correlation over the period (14 days of August 2006).*

The 24 hr cumulated rainfall distribution has been computed from the datasets at their raw resolution (2.5km for AROME, ~10km for ALADIN-AMMA, ~25km for ECMWF and ~50km for

ARPEGE_T) on the AROME domain and are shown. These distributions have also been computed from 1°x1° latitude-longitude averages of the same data (not shown). We also added the corresponding contribution distribution (Fig. 12).

Available SYNOP stations over AROME domain (4, sample size #500) and the CPC estimate indicate that it does not rain in ~50% of the time. When it rains, SYNOP and CPC data consistently show that as the 24 hr rainfall amount increases the frequency regularly decreases. Rain rate distributions can be analyzed by considering 3 regimes:

- No rain case: all models have difficulties in forecasting the absence of rain, but AROME (35%) and ECMWF (30%) perform much better than ARPEGE_T or ALADIN-AMMA (~10%).
- Weak-Moderate rain (< 10mm/24hr): ARPEGE_T and ALADIN-AMMA exhibit an unrealistic local frequency maximum around 4 mm/24hour, which is not found in the observations. ECMWF doesn't exhibit this maximum although such rates are too frequent as compared with observation. AROME clearly improves the rain distribution for weak-moderate rates. The contribution distribution (Fig. 13) confirms and quantifies better the above conclusions. Thus it is suggested that this unrealistic maximum found for ALADIN-AMMA or ARPEGE_T is linked to the convection scheme.
- Strong rain (>10mm/24hr): These events are rare and the sampling size is small so that the comparison with observation estimates must be carefully made. Nevertheless the contribution distribution (Fig. 13) allows drawing some conclusions. Models with a convection scheme (ARPEGE_Tropiques, ECMWF, ALADIN) exhibit a lack of strong rain events. Nevertheless up to 20mm/day ECMWF is closer from observation. On contrary AROME simulates too much strong rain events above 20 mm/day.

In short it appears that the rain rate distribution provides a clear signature of the models behavior. Globally models with a convective scheme forecast too frequently weak to moderate rainy events (<10mm/hr), and not enough both no-rain events and strong rainy events. A CRM model such as AROME improves drastically the weak to moderate rainy events frequency and a little the no-rain regime. But it increases too much the number of strong rainy events.

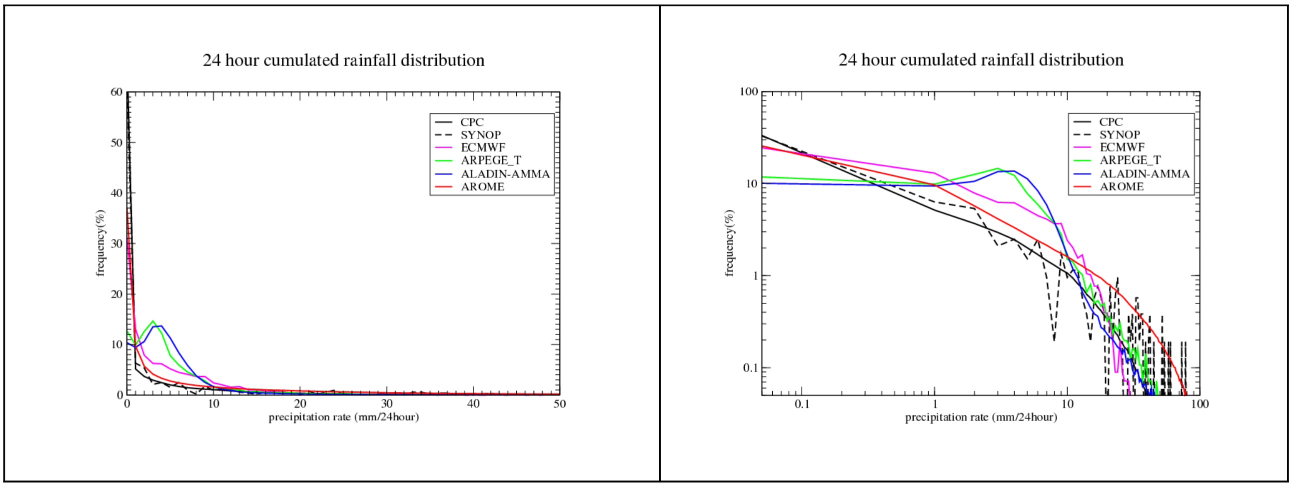


**Figure 12:** *distribution of 24 hr cumulated precipitation at raw geographical resolution for the 14 selected days of August 2006 (see fig. 23). CPC in black-10km resolution, SYNOP in dashed black, ECMWF in rose – 50km resolution, ARPEGE_T in green – 50 km resolution, ALADIN_AMMA in blue- 10km resolution and AROME in red- 10km resolution. Linear (left panel) and logarithmic (right panel) axis.*

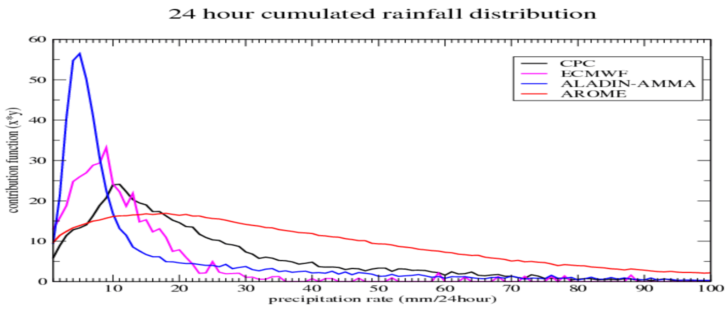


**Figure 13:** *Contribution function (precipitation rate x frequency), plotted from 1 to 100 mm/24hr (1°x1° grid).*

### 4.8.7. CONCLUSIONS:

a) In this note, we tried to evaluate the forecast skill of models run by Météo-France during the 4 months of the AMMA SOP in 2006 over West Africa. It concerns the operational global models ARPEGE and ARPEGE-Tropiques, the LAM ALADIN model and the CRM model AROME covering a wide range of resolution: ~50 km, 10 km and 2.5 km respectively. For comparison the ECMWF model (~25 km) is punctually considered. The main conclusions of this study are:

b) Owing to the huge AMMA effort the number of information entering the assimilation systems in real time for the West Africa have been significantly increased during the 4 months of the SOP in 2006 with a peak in August.

c) This study confirms that some soundings are affected by a dry bias of humidity.

d) For this region ARPEGE-Tropiques performed a little better than ARPEGE as often recognized by forecasters in the tropics, nevertheless we don't know if the longer cut-off is the only explanation.

e) ALADIN weakly improves the analysis but the gain is lost after 6hr.

f) All scores indicate that ARPEGE models perform better than ALADIN. Although ALADIN has not been specifically tuned for this tropical region, it appears that increase of resolution does not necessary improve the forecast.

g) Comparison with independent observations of IWV provided by 3 GPS available ground stations suggests that all models have great difficulties in reproducing the IWV diurnal cycle. It could be related to the well-known failure of models to get the good timing of the convection (too early).

h) The skill of MF models in predicting precipitation is low and again the higher resolution (10 km) doesn't improve and tends to increase the positive bias. The position of the monsoon and its associated south-north gradient of precipitation is well captured, but all the MF models have difficulty in simulating "suppressed convection" frequently observed during the monsoon period. Also too much precipitation are forecasted over Fouta-Djalloun.

i) ECMWF skill is better except its tendency to drift southward the ITCZ at short range (1-2 days).

j) The rain rate distribution provides a clear signature of the models behavior. Globally models with a convective scheme forecast too frequently weak to moderate rainy events (<10mm/hr), and not enough both no-rain events and strong rainy events. ECMWF exhibits the same behavior although less intense. A CRM model such as AROME improves drastically the weak to moderate rainy events frequency and a little the no-rain regime. But it increases too much the frequency of intense rain events (>20mm/day).

The above study is partial and prevents drawing definitive conclusions. After collection, checking and correction (humidity bias in particular) stages of all data, further studies will be needed to rerun NWP models and perform sensitivity experiments by using all the AMMA dataset. Nevertheless this study already points some weaknesses at least for MF models and will help in guiding further studies aimed at improving these models over the West Africa. The AMMA data set will be a powerful help to reach this challenging objective.

***Acknowledgments:*** *"Based on a French initiative, AMMA was built by an international scientific group and is currently funded by a large number of agencies, especially from France, UK, US and Africa. It has been the beneficiary of a major financial contribution from the European Community's Sixth Framework Research Programme. Details information on scientific coordination and funding is available on the AMMA international web site* http://www.amma-international.org*". The authors wish to thank all services at Météo-France that efficiently contributed to set up the forecasting operational NWP chain used during the SOP, in particular P. Labrot (CMS) for the satellite data collection and processing, B. Lacroix and his team to set up ALADIN and evaluation tools, Y Seity for the AROME runs, S. Croux and P. Chapelet for the post treatments. They are also grateful to JL Boichard and L. Mastrorillo from Medias-France for the AOC web site development and support. We also wish thank A. Agusti-Paraneda, A. Guelli and A. Beljaars from ECMWF for providing data and comments.*

**References:**

Agusti-Paraneda A. 2006: Report on sonde statistics at ECMWF.D4.1.1.d AMMA-EU deliverable.

Bock, O., M.-N. Bouin, A. Walpersdorf, J.-P. Lafore, S. Janicot, F. Guichard and A. agusti-Panareda, 2007: Comparison of ground-based GPS precipitable water vapour to independent observations and Numerical Weather Prediction model reanalyses over Africa. *Submitted to Q.J.R. Meteorol. Soc*.

Laws K. B., Janowiak, J. E. and G. Huffman, 2004: Verification of rainfall estimates over Africa using RFE, NASA MAPRT-RT and CMORPH. Combined preprints CD-ROM, 84$^{th}$ AMS annual meeting, Paper P2.2 in 18$^{th}$ Conf. On hydrology, 11-15 January 2004, Seattle, WA, 4pp.

Montmerle T., J.-P. Lafore, L. Berre and C. Fischer, 2006: Limited area model error statistics over Western Africa: comparisons with mid-latitude results. *Q. J. Roy. Meteorol. Soc.* vol. 18, n° 614, p. 213-230.

Yang, G.-Y. and Slingo, J. 2001: The diurnal cycle in the Tropics. *Mon. Weather Rev.*, 129: 784-81.

## 5. PhD Studies

**5.1. Tudor M.:** « Tests of numerical instabilities of the physics package. »

**5.2. Auligné Th.:** «Assimilation variationnelle des observations de sondeurs infrarouges hyperspectraux: Correction de biais et détection nuageuse.» thèse de doctorat de l’université Paul Sabatier. Soutenue le 08 juin 2007.

## 6. PUBLICATIONS

- L. Gerard, 2007: An integrated package for subgrid convection, clouds and precipitation compatible with the meso-gamma scales, *Quart. Jour.* Roy. *Meteor. Soc.,* **133**, pp.711-730.
- Brozkova R., M. Derkova, M. Bellus, A. Ferda, 2006: Atmospheric forcing by ALADIN/MFSTEP and MFSTEP oriented Atmospheric tunings , *Ocean Sci*., **2**, 113–121
- Descamps L. et O. Talagrand, 2007: On some aspects of the definition of initial conditions for ensemble prediction. *Mon. Wea. Rev.*,
- Illingworth et al 2007 "CLOUDNET..."
- Piriou, J-M, J.-L. Redelsperger, J.-F. Geleyn, J.-P. Lafore and F. Guichard: An approach for convective parameterization with memory, in separating microphysics and transport in grid-scale equations. *J. Atmos. Sci*.,
- Poli et al "...FORMOSAT-3/COSMIC.